ICES WGOH REPORT 2018

ECOSYSTEM PROCESSES AND DYNAMICS STEERING GROUP

ICES CM 2018/EPDSG:08

REF. SCICOM

Interim Report of the Working Group on Oceanic Hydrography (WGOH)

21–23 March 2018

Norwich, UK

ICES International Council for the Exploration of the Sea
CIEM Conseil International pour l'Exploration de la Mer

International Council for the Exploration of the Sea
Conseil International pour l'Exploration de la Mer

H. C. Andersens Boulevard 44–46
DK-1553 Copenhagen V
Denmark
Telephone (+45) 33 38 67 00
Telefax (+45) 33 93 42 15
www.ices.dk
info@ices.dk

Recommended format for purposes of citation:

ICES. 2018. Interim Report of the Working Group on Oceanic Hydrography (WGOH), 21–23 March 2018, Norwich, UK. ICES CM 2018/EPDSG:08. 131 pp. https://doi.org/10.17895/ices.pub.8094

Contents

Executive summary

The Working Group on Oceanic Hydrography (WGOH) meets yearly to review oceanographic conditions in the North Atlantic and Nordic Seas and to report on these in the ICES Report on Ocean Climate (IROC). The WGOH 2018 meeting was hosted by the Collaborative Centre for the Sustainable Use of the Seas, Norwich, United Kingdom, 21–23 March 2018. The joint analysis of the existing hydrographical time-series provided the following highlights for 2017.

Highlights of the North Atlantic for 2017

- Accelerated freshening in the upper ocean that was first observed in the eastern subpolar North Atlantic in 2016, persisted into 2017 and expanded to include the southern Norwegian Sea. Notably, the freshening is accompanied by above average temperatures.
- A cold anomaly observed in the surface and upper ocean of the central subpolar North Atlantic for the past 4 years weakened and shifted north-westward into the Irminger Sea.
- Sea surface temperature was higher than normal across most of the region, with the exception of the central subpolar North Atlantic and Baltic Sea.
- Following a five-year period of increasing heat content, the upper layer of the Norwegian Sea reached a new record-high value.
- Gradual freshening of upper waters (100–400 meters) in the northeast Subtropical Gyre is now widespread, reaching West Iberia and the Canaries.
- Ocean temperatures in the western North Atlantic were cooler than normal in the north (the Labrador and Newfoundland Shelves) and warmer than normal in the south, along the Northeast U.S. Shelf.
- Ice cover in the Barents Sea remained very low.

Highlights of the North Atlantic atmosphere in winter 2016/2017

- The winter North Atlantic Oscillation (NAO) index was positive (+1.47) for the fourth consecutive winter, the first such positive run since 1992–1995.
- The anomaly in Sea Level Pressure (SLP) did not resemble a typical NAO pattern. Instead, the high-pressure anomaly was shifted east, centered over the North Sea, and the low-pressure anomaly over the Arctic was split to the southeast and southwest of Iceland and the Nordic Seas.
- Winds were more northerly over the Labrador Sea and southerly from the north-eastern Atlantic and into the Nordic Seas.
- Winter air temperatures were near average (1981–2010) over the Subpolar Gyre and central North Atlantic, whereas temperatures were generally higher than normal elsewhere around the margins and particularly so over the northern Barents Sea.

Beyond 2017: initial assessment of the north Atlantic atmosphere in winter 2017/2018

- An initial assessment of the North Atlantic atmosphere at the end of the IROC year is included. Atmospheric conditions during winter are a determining factor of oceanic conditions for the following year; therefore, this outlook offers some predictive capability for spring-autumn 2018.
- The sea level pressure pattern for December 2017–February 2018 suggest that this will have been a positive NAO index winter but probably weaker than those preceding it. More negative conditions experienced in March may mean the overall NAO winter is close to neutral. As expected for a weak NAO index the SLP anomaly pattern is not a clear NAO pattern with a low pressure trough between Greenland and Greece separating anticyclonic anomalies centered over the western North Atlantic and Russia.
- Air temperatures were cold over Iberia, Norway and the Subpolar Gyre, including over the Irminger Sea and Iceland Basin. Warmer-than-average conditions were evident southwest and northeast of the Subpolar Gyre. Experimental forecasts from the US (over seasonal periods) and the UK (over 1–5 years) suggest a warmer outlook for the Subpolar Gyre region more typical of the long-term average (1981–2010).

1 Administrative details

Working Group name

Working Group on Oceanic Hydrography (WGOH)

Year of Appointment within current cycle

2018

Reporting year within current cycle (1, 2 or 3)

1

Chair(s)

Cesar Gonzalez-Pola, Spain

Paula Fratantoni, United States

Meeting dates

21–23 March 2018

Meeting venue

Norwich, United Kingdom

2 Terms of Reference a) – z)

a) Examine the hydrographic variability of the North Atlantic and its subpolar seas. Identify events, trends and drivers in the region;

b) Standard Sections and Stations summarized into the production of the IROC report and submitted to IROC data portal;

c) Report on developments within international climate monitoring, multi decadal reanalyses & prediction programmes relevant to ICES;

d-f) Support for ICES processes on hydrographic data and ocean scale marine climate variability. Including Data Centre, other EGs, and advice programmes where and when requested;

g) Contribute to objectives, activities of the Ecosystems Processes and Dynamics SG;

h) Prepare a new decadal symposium in 2021;

i) Ongoing self-evaluation of the EGs work.

3 Summary of Work plan

Year 1	a) IROC 2017 production & recommendations for modifications to IROC format and content, including discussion on potential for reanalyses, forecast products to be included and addition of ICES Regional Ecosystem area focussed component, also potential move to purely web based product. b) WG Activities progress report including highlights of North Atlantic hydrographic conditions and any significant events synthesized from the national reports and IROC findings. c) Initial identification of climate monitoring, reanalysis and forecasting programmes d) develop plans for Decadal Symposium.
Year 2	a) IROC 2018 production including first implementation of recommended changes. b) WG Activities progress report including highlights of North Atlantic hydrographic conditions and any significant events synthesized from the national reports and IROC findings. c) Map marine climate reanalysis and forecast parameters to ICES interests. e) Prepare for for Decadal Symposium
Year 3	a) IROC 2019 production and review of content and requirement to continue IROC process. b) WG Final report c) Participation and delivery of Decadal Symposium

4 List of Outcomes and Achievements of the WG in this delivery period

- Streamline production and improve quality of IROC through use of LATEX editing tool, standardizing formats, including author attributions, inventorying included time-series, and revising chapter organization;
- Improving IROC delivery and expanding access/awareness of IROC, adding an online archive of historical reports;
- New editorial team established for preparation of IROC;
- Delivery of IROC 2016 (CRR339);
- IROC 2017 on target and new developments in progress.

5 Progress report on ToRs and workplan

Report on the work done in connection to the meeting in 2018: The meeting was opened with introductions for the benefit of new members and a review of the agenda. A significant amount of time was spent discussing the production workflow for the IROC, prompted by a discussion of the unusual circumstances that led to delays in the release of the 2016 IROC. Time was spent developing a production timeline and prioritized list of improvements to be implemented with future reports.

A mini- symposium was held in conjunction with the WGOH meeting on the afternoon of the first meeting day. As is typical, the symposium included a combination of talks from the host institution and invited WGOH members. The entire second day was spent reporting findings from the various ICES areas, work which addresses ToRs a) and b).

The remainder of the meeting was spent working through the other ToRs (c–h) and the last couple of hours were spent working on the upcoming IROC.

ToR a): Update and review results from Standard Sections and Stations

Area Reports were presented to the WGOH and additional scientific work reviewed during a mini-symposium. WGOH were grateful to members whom, although unable to attend the meeting, were still able to offer an area report as this is incredibly useful to the group when preparing the IROC.

Some groups support their presentation with a formal report and these offer valuable comprehensive reviews of the different sea areas within the North Atlantic as covered by members of the WGOH. These reports contain much more detailed information than the ICES Report on Ocean Climate which can only summarise the general conditions. Table 1 below lists the area reports presented at the meeting.

Table 1. List of Area reports Presented to ICES WGOH in 2017.

Region of Report	Presenter	Country	Presentation/Report
Atmosphere	Stephen Dye	UK	Presentation
Greenland	Boris	Germany	Presentation
Newfoundland/ Labrador Shelf	Eugene Colbourne	Canada	Report
Northeast U.S. Shelf	Paula Fratantoni	USA	Presentation
Bay of Biscay	Almudena Fontan	Spain	Presentation
Iberian Coast & Canaries	Cesar Gonzalez-Pola	Spain	Presentation
Western English Channels	Kieran Lyons	Ireland	Presentation
Rockall Trough and Extended Ellet Line	Penny Holliday	UK	Presentation
Faroese Waters	Karin Margaretha H. Larsen	Faroe, Denmark	Presentation
Scottish Waters	Jenny Hindson	Scottland, UK	Report
North Sea	Holger Klein	Germany	Report
Baltic	Johanna Linder, Tycjan Wodzinowski	Sweden, Poland	Presentation
Norwegian Sea	Kjell Arne Mork	Norway	Presentation
Barents Sea	Alexander Trofimov	Russia	Presentation
Fram Strait	Ilona Goszczko	Poland	Presentation

ToR b): Standard Sections and Stations summarized into the production of the IROC report and submitted to IROC data portal

A significant portion of the morning of the first meeting day was spent discussing improvements to the production and delivery of the IROC. The 2016 IROC production was delayed for a variety of reasons, including the unanticipated departure of a key member of the editorial team and illness in the editorial staff at ICES. The WGOH agreed on new deadlines for the submission of data and descriptive text as well as editorial deadlines to ensure timely release of following reports. It was agreed that: subsequent reports should be published during summer before the ICES Annual Science Conference; summary highlights will be posted immediately following the annual WGOH meeting each spring; and a preliminary internally edited draft of the IROC would be made available on the IROC website prior to final release by ICES editorial staff. Later interaction with SCICOMM raised concerns about the convenience of two version of the IROC circulating, having the draft less quality control and lack of DOI. After some discussion within the editorial group it was decided not to provide an early-release of the IROC in 2018 and analyze the option further in the future, involving ICES SCICOM and Secretariat in the discussion

A decision was made last year to begin using LATEX document typesetting tool for production of the IROC. This tool is designed specifically for preparing technical and scientific documents and allows for maximum flexibility in the organization and content of the report (e.g. adding time-series figures and rearranging sections/chapters). The working group reviewed the production workflow and considered improvements proposed by the editorial staff. The proposed improvements include standardization of maps, coherence in figure colors, some reorganization of content within existing chapters, and inclusion of author attributions within chapters. The working group reviewed the definition of ecosystem areas used in the report, agreeing that editorial staff would seek feedback from other expert groups to determine what is most useful to end-users.

The working group inventoried the list of IROC time-series data received so far and confirmed any changes in data contributors, making corrections and providing status updates where necessary. Finally, the working group reviewed methods used to compute anomalies, in order to determine the feasibility of automating this process for all submitted data. This is a long term goal of the IROC editorial team.

ToR c): Report on developments within international climate monitoring, multi decadal reanalyses & prediction programmes relevant to ICES

An abstract entitled "The ICES Working Group on Oceanic Hydrography: A bridge from in-situ sampling to the remote autonomous observation era" was prepared and submitted by WGOH to OceanObs19 call for Community White papers. The intention is to explore where WGOH and the IROC fit into the world of global ocean observations at a time when large consortiums such as Copernicus are being established. A response is expected by late April. If the abstract is accepted, a white paper for further peer review will be requested by 30 September.

Some key points raised during discussions were:

- Time-series reported in the IROC are the longest in the world and become more valuable to climate science the longer they are sampled;
- There will always be a need for local environmental monitoring for ecosystem management purposes; A global ocean observing system cannot fulfil that need, but these high resolution region-specific surveys can enhance a global observing system if data are made available;
- The strength of the WGOH-IROC is the science-based analysis done at regional level by local specialists.

ToRs d–f): Support for ICES processes on hydrographic data and ocean scale marine climate variability. Including Data Centre, other EGs, and advice programmes where and when requested

There are strong benefits to establishing closer involvement with the GOOS community. We should aim to become more integrated with GOOS for mutual benefit.

The WGOH meeting in 2018 was preceded by a General meeting of WG Chairs that took place at ICES Headquarters on 23–25 January. The purpose of such meeting was to "facilitate communication between Expert Groups, Steering Groups, the Advisory Committee (ACOM), and the Science Committee (SCICOM)", adding up to 50 participants. The WGOH co-chair César Gonzalez-Pola attended the meeting, gathering valuable background on the general functioning of ICES. Within the meeting there was a side meeting under the topic "Integrating ocean data" that directly addressed the issue of low feedback between different EG and in particular how the work carried out by the WGOH could benefit other ICES EGs. This discussion triggered suggested changes in the IROC production and WGOH web that were addressed later in the WGOH meeting. The session also motivated further interaction with Silvana Birchenough, Chair of our parent Steering Group (Ecosystems Processes and Dynamics SG) within the WGOH meeting (see next ToR).

Within the WG meeting it was discussed in depth what is or should be the role of the WGOH/IROC in relationship with the GOOS community (specifically addressed when reviewing possible contribution to the OceanObs19 Conference). A set of enquires/responses was established with JCOMMPS through Penny Holliday, aimig to engage those repeat hydrography programmes as those feeding the WGOH work into the GOOS partnership and getting metadata into these Databases. Further discussion within the ICES Data Center regarding EMODNET portal are also in progress.

ToR g): Contribute to objectives, activities of the Ecosystems Processes and Dynamics SG

Dr Silvana Birchenough, Chair of the Ecosystems Processes and Dynamics Steering Group, joined the WGOH meeting on the final day. Discussion centred around how WGOH might better support the work of other expert working groups within ICES. The group requested feedback from other expert groups on the IROC, including who is aware of and using the product, which elements are useful, and how the product might be improved. Members expressed a desire to receive feedback on the usefulness of information

and/or expert advice provided in response to requests from within ICES in order to improve WGOH service to ICES.

ToR h): Prepare a new decadal symposium in 2021

WGOH has begun to gather information on the logistics surrounding the planning for the next decadal symposium (2021). A tentative venue has been identified and a 5-member working sub-committee has been established. The sub-committee is reviewing guidance from chairs and committee members who planned the last symposium and will begin to prepare an ICES resolution for consideration.

ToR i): Ongoing self-evaluation of the EGs work

The work of WGOH contributes substantively to all four of the science priorities recently proposed by SCICOM. We assesses the physical state of regional seas and describe changes in the predominant climatic and hydrological processes important for regional ecosystems. We contribute vital information, which can be used by others who wish to understand the impacts of climate variability and change on marine ecosystems.

The primary work product of the WGOH is its annual ICES Report on Ocean Climate (IROC), which provides expert analysis of time-series observations of ocean hydrography collected at long-standing stations throughout the North Atlantic. The Ocean and Atmosphere Highlights from the IROC represent our summary of oceanographic conditions in the latest year and should be used in the Advisory process together with the national reports. Outputs from this working group also feed into assessments for NAFO and regional and national assessments of climate variability.

It is recognized that the utility of the IROC rests on its timely publication. Steps are being taken to identify the users of the IROC and improve it based on feedback from a growing community of users. Plans are underway to provide immediate release of annual highlights following the WGOH meeting and to distribute an early internally edited draft in advance of the final publication. The WGOH is continually evaluating how it might better identify and respond to stakeholder needs and will focus energy in the next year on exploring ways it can contribute to global ocean observing systems.

The information WGOH prepares is incredibly valuable to ICES and the wider community and we therefore seek to continue with this work. We aim to continue to develop the IROC website and to publish the annual ICES Report on Ocean Climate.

6 Revisions to the work plan and justification

Not required.

7 Next meetings

It was proposed that the 2019 WGOH meeting will be held in Bergen, Norway, either 2–4 April 2019 or 19–21 March 2019. It was suggested out-year meetings may be held in the USA and Ireland.

Annex 1: List of participants

Name	Institute	Country (of institute)	Email
Paula Fratantoni	NOAA Northeast Fisheries Science Center	USA	Paula.fratantoni@noaa.gov
Cesar Gonzalez-Pola	Centro Oceanografico de Gijon	Spain	cesar.pola@ieo.es
Karin Margretha Larsin	Faroe Marine Research Institute	Faroe Islands, Denmark	karinl@hav.fo
Stephen Dye	Centre for Environment Fisheries and Aquaculture Science (Cefas)	UK	stephen.dye@cefas.co.uk
Penny Holliday	National Oceanography Centre Southampton	UK	penny.holliday@noc.ac.uk
Tycjan Wodzinowski	National Marine Fisheries Research Institute	Poland	tycjan@mir.gdynia.pl
Boris Cisewski	Thünen Institute	Germany	boris.cisewski@thuenen.de
Kieran Lyons	Marine Institute	Ireland	kieran.lyons@marine.ie
Caroline Cusak	Marine Institute	Ireland	caroline.cusack@marine.ie
Almudena Fontan	AZTI-Tecnalia	Spain	afontan@azti.es
Johanna Linders	Swedish Meteorological and Hydrological Institute	Sweden	johanna.linders@smhi.se
Alexander Trofimov	Knipovich Polar Research Institute of Marine Fisheries and Oceanography(PINRO)	Russia	trofimov@pinro.ru
Kjell Arne Mork	Institute of Marine Research	Norway	kjell.arne.mork@imr.no
Ilona Goszczko	Institute of Oceanology, PAS	Poland	ilona_g@iopan.gda.pl

Annex 2: Recommendations

RECOMMENDATION	ADRESSED TO
1. The WGOH continuously tries to improve the IROC and its outreach. An important part of the background material is the national reports from WGOH members. To improve the visibility of these underlying national reports the group recommends linking them directly on the website rather than embedding them into the WGOH report.	ICES Secretariat
2. The WGOH recommends providing a link to all historical copies of the ICES Report on Climate (IROC) in addition to linking the recent report on the WGOH IROC website.	ICES Secretariat

Annex 3: Agenda WGOH

University of East Anglia , Norwich, UK School of Environmental Sciences March 20, 2017 0900-1730			
Time	**Topic/Purpose**	**Lead/ Facilitator**	**Term of Reference (ToR)**
0900-	General Information, Membership Introductions, Agenda Review	Paula/Cesar	
	IROC-2016 – overview of delays/causes IROC 2017 – process and proposed improvements; overview of contributions received	Cesar	ToR(b): Standard Sections and Stations summarized into the production of the IROC report and submitted to IROC data portal.
	2017 Atmospheric Conditions, including update on community reanalyses/prediction programs	Stephen Dye	ToR(c): Report on developments within international climate monitoring, multi decadal reanalyses & prediction programmes relevant to ICES
Time permitting	2017 Area Reports: latest results from standard sections and stations	Attending Members	ToR(a): Examine the hydrographic variability of the North Atlantic and its subpolar seas. Identify events, trends and drivers in the region.
1230-1330	Lunch		
1400-1700	**Observing northern seas – CCSUS-WGOH Pop-up Symposium**, *Keith Clayton Seminar Room Sci01.38* ***Stephen Dye(Cefas/UEA) –*** *Introducing an ocean of acronyms Cefas-CCSUS-COAS in ENV, UEA and ICES -WGOH* ***Tiago Silva (Cefas):*** *Use of earth observation to monitor water quality in coastal areas.*	Stephen Dye	ToR(c)

	***Boris Cisewski (Thünen Institute of Marine Fisheries, Bremerhaven/Hamburg)**: COSYNA underwater node systems and recent developments* ***Carolyn Graves(Cefas):** Methane in shallow subsurface sediments western Svalbard.* ***Peter Sheehan(COAS, UEA - Marine Scotland Science):** Inflows to the north-western North Sea: forcing and variability.*		
1515-1540	**Coffee Break**		
1540-	**CCSUS-WGOH Pop-up Symposium cont.** *Keith Clayton Seminar Room Sci01.38* ***Marcos Cobas-Garcia(COAS, UEA)**: The UEA glider group facility* ***Karin Margretha Larsen (Havstovan - Faroe Marine Research Institute)**: On the Overflow through the Western Valley of the Iceland- Faroe Ridge* ***Rob Hall (COAS, UEA):** Investigating internal tides in Whittard Canyon & the Faroe Shetland Channel with gliders* ***Penny Holliday(NOC)**: Recent rapid freshening in the eastern subpolar gyre*	Stephen Dye	ToR(c)

University of East Anglia , Norwich, UK March 21, 2017 0900-1700			
Time	**Topic/Purpose/Process**	**Lead**	**Term of Reference (ToR)**
0900-	2017 Area Reports: latest results from standard sections and stations	Attending Members	ToR(a): Examine the hydrographic variability of the North Atlantic and its subpolar seas. Identify events, trends and drivers in the region
1230-1330	Lunch		
1330-	Group Photo		
1345-	Continue 2017 Area Reports	Attending Members	ToR(a)
-1700	Begin drafting IROC Highlights from Nation Reports	Chairs	ToR(a,b)
TBD	Group dinner	Stephen Dye	

University of East Anglia , Norwich, UK March 22, 2017 0900-1200			
Time	**Topic/Purpose/Process**	**Lead**	**Term of Reference (ToR)**
0900	Finalize IROC Highlights	Chairs	ToR(a,b)
0930	Overview of WGOH steering group: Ecosystem Processes and Dynamics Steering Group	Silvana Birchenoug, Steering Group Chair	
1000	Discuss other ocean status reporting efforts (e.g. CLIVAR, Copernicus, etc.); review status of community reanalyses/prediction programs; OceanObs Abstract on the IROC	Chairs	ToR's (c-f): Support for ICES processes on hydrographic data and ocean scale marine climate variability. Including Data Centre, other EGs, and advice programmes where and when requested
1100	2021 Decadal Symposium Planning	Chairs	ToR(h): Prepare a new decadal symposium in 2021
1200	Adjourn Meeting		

Regional report on West Greenland 2017

Boris Cisewski, Thünen Institute of Sea Fisheries, Germany

The water mass circulation off Greenland comprises three main currents: Irminger Current, West Greenland and East Greenland Currents (Figure 1). The East Greenland Current (EGC) transports ice and cold low-salinity Surface Polar Water (SPW) to the south along the eastern coast of Greenland. On the inner shelf the East Greenland Coastal Current (EGCC), predominantly a bifurcated branch of the EGC, transports cold fresh Polar Water southward near the shelf break (Sutherland and Pickart, 2008). The Irminger Current is a branch of the North Atlantic Current. Figure 2 reveals warm and salty Atlantic Waters flowing northward along the Reykjanes Ridge. South of the Denmark Strait (DS) the current bifurcates. While a smaller branch continues northward through the DS to form the Icelandic Irminger Current, the bulk of the current recirculates to the south and transports salty and warm Irminger Sea Water (ISW) southward along the eastern continental slope of Greenland. It makes a cyclonic loop in the Irminger Sea. South of Greenland both currents bifurcate and spread northward as a single jet of the West Greenland Current (WGC). The WGC carries the water northward and consists of two components: a cold and fresh inshore component, which is a mixture of the SPW and melt water, and a saltier and warmer Irminger Sea Water (ISW) offshore component. The WGC transports water into the Labrador Sea, and hence is important for Labrador Sea Water formation, which is an essential element of the Atlantic Meridional Overturning Circulation. The dynamics of the current is monitored yearly in autumn at two standard ICES/NAFO oceanographic sections across the slope off West Greenland (Figure 3). The German groundfish survey off Greenland is conducted since 1981, aiming at monitoring

groundfish stocks in particular of cod and redfish. The monitoring is carried out by the Thünen-Institute of Sea Fisheries (TI-SF) from board of R/V 'Walter Herwig III' and reveals significant interannual and long-term variability of both components of the WGC.

Atmospheric conditions

The variability of the atmospheric conditions over Greenland and the Labrador Sea is driven by the large scale atmospheric circulation over the North Atlantic, which is normally described in terms of the North Atlantic Oscillation (NAO). During a positive NAO strong northwest winds bring cold air from the North American continent and cause negative anomalies of the air temperatures over Greenland, Labrador Sea and Baffin Bay (Hurrell and Deser, 2010). During a negative NAO the westerlies slacken and the weather is normally milder over the whole region. According to ICES standards, the Hurrell winter (DJFM) NAO index is used for this study, which is available at *https://climatedataguide.ucar.edu/climate-data/hurrell-north-atlantic-oscillation-nao-index-station-based*.

In winter 2016/2017, the NAO index was positive (1.47) for the fourth consecutive year (Figure 4). Figure 5a shows the winter sea level pressure (SLP) averaged over 30 years (1981-2010), mainly dominated by the Iceland Low and the Azores High. Both, the Icelandic Low and the Azores High were strengthening resulting in an increased pressure difference over the North Atlantic sector than normal during winter 2016/2017 (Figure 5b). The anomaly in sea level pressure reveals not a typical NAO pattern with the high pressure anomaly shifted east and centred over the North Sea. (Figure 5c). Air temperature at Nuuk was used to characterize the atmospheric conditions in 2017. Annual and monthly mean values were obtained from the Danish Meteorological Institute

(Figures 6 and 7). The resulting annual mean temperature at Nuuk was 0.4°C in 2017, which was 1.0°C above the long-term mean (1981-2010) (Figure 7).

Hydrographic Conditions

The core properties of the water masses of the WGC are formed in the western Irminger Basin where the EGC meets the Irminger current (IC). The EGC transports fresh and cold PSW of Arctic origin. The IC is a northern branch of the Gulf Stream, which makes a cyclonic loop in the Irminger Sea and carries warm and saline ISW. After the currents converge, they turn around the southern tip of Greenland, form the WGC and propagate northward along the western coast of Greenland. During this propagation considerable mixing between two water masses takes place and ISW gradually deepens (Clarke and Gascard, 1983; Myers et al., 2009). The annual sea surface temperature (NOAA OI SST) anomalies for 2017 indicate positive anomalies in the Northwestern Atlantic with highest values occurring northeast of Iceland and along the coast of East Greenland (Figure 8), whereas negative anomalies were observed in the central area of the North Atlantic.

CTD profiles were conducted with a Sea-Bird 911plus sonde attached to a 12-bottle water sampler. The hydrographic database consisted of 35 hydrographic stations sampled between October 21 and November 09, 2017, from R/V ‘Walther Herwig III’. Study area and station locations are shown in Figure 3. However, the Cape Desolation and Fyllas Bank Sections had to be abandoned due to severe weather conditions.

Tables

Table 1. Details on the times series, analysed in this study.

Name	Lat (°N)	Lon (°W)	Type	Source
Nuuk (4250)[1]	64.17	51.75	Weather station	DMI
Nuuk airport (4254)[1]	64.20	51.68	Weather station	DMI
Cape Desolation Station 3	60.47	50.00	Oceanographic station	TI-SF
Fyllas Bank Station 4	63.88	53.37	Oceanographic station	TI-SF

Table 2. Water mass characteristics in the study area.

The water masses in the area	Potential temperature (θ)	Salinity (S)
Surface Polar Water (SPW)	$\theta \leq 0$	$S \leq 34.4$
Irminger Sea water (ISW)	$\theta \geq 4.5$	$S \geq 34.95$

[1] In recent years, Nuuk air temperature was taken from the Nuuk airport synop station 04254 due to a failure on Nuuk synop station 04250 (Cappelen, 2013).

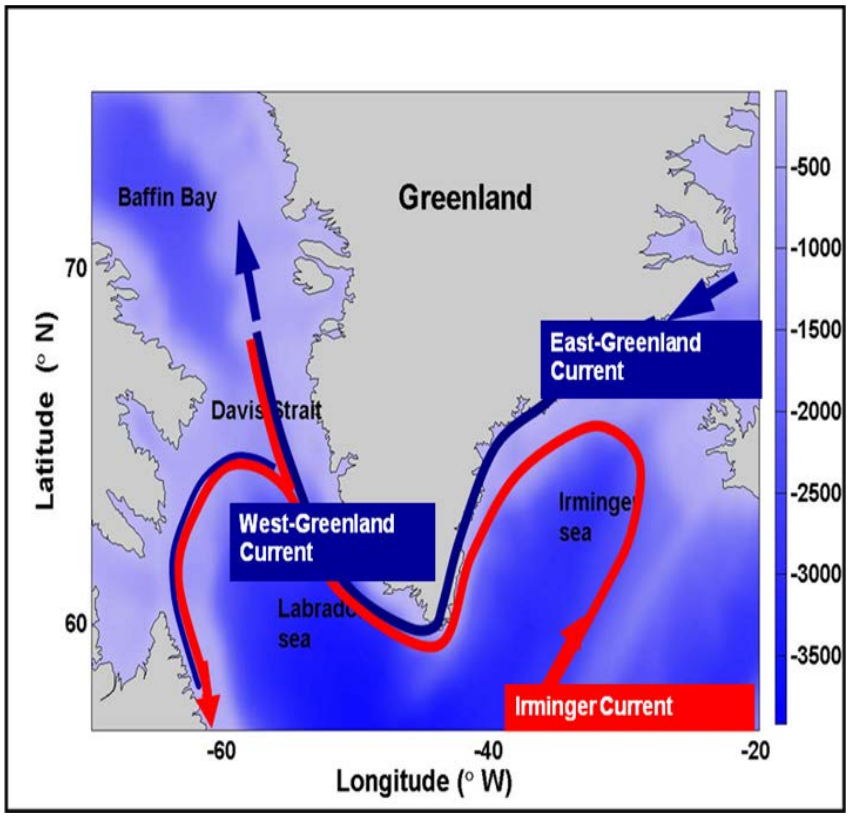

Figure 1. Scheme of the upper ocean circulation in the study area. Red and blue curves show the trajectories of warm Irminger Sea Water and cold Surface Polar Water, respectively.

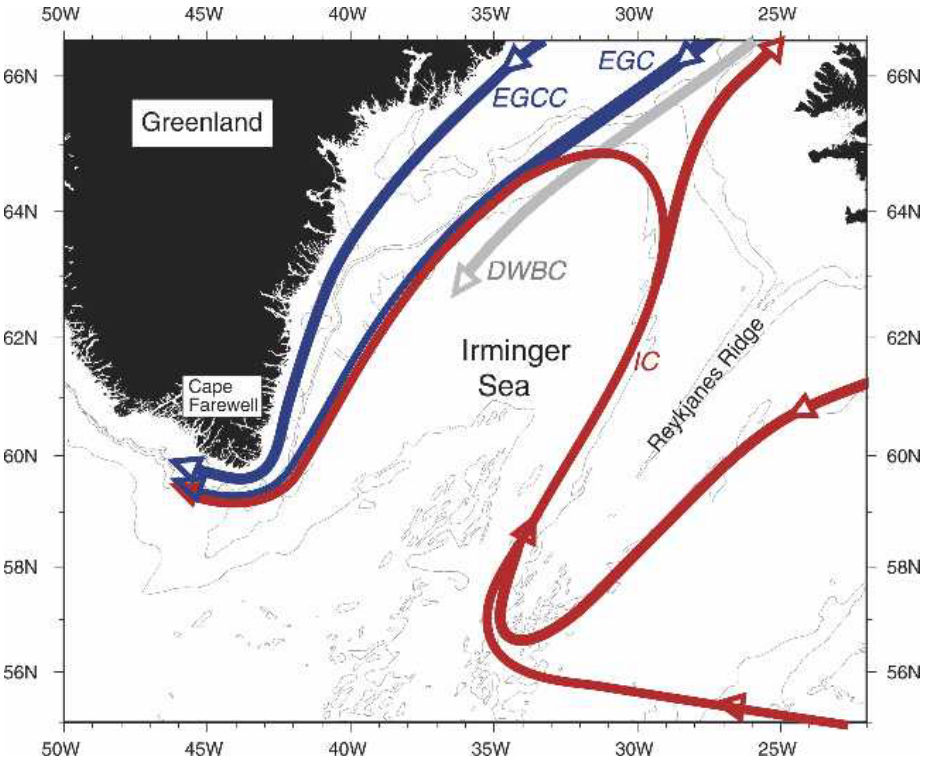

Figure 2. Schematic of the boundary currents of the Irminger Sea (depicted from Pickart et al., 2005)

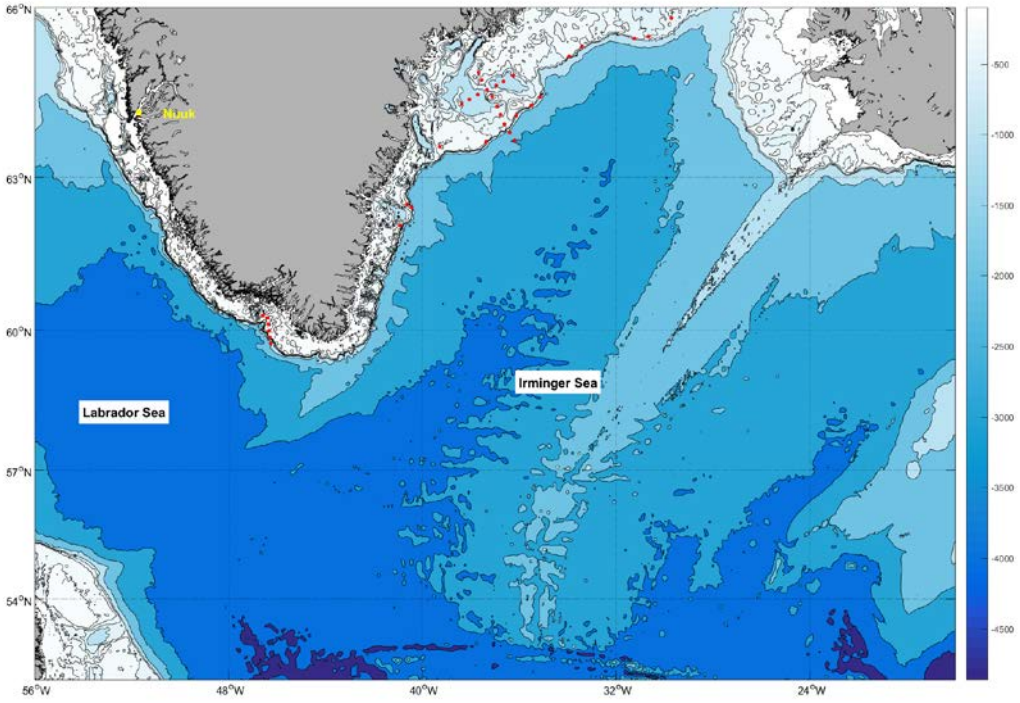

Figure 3. Map and bathymetry of the study region. Meteorological station location is shown in yellow. Red dots show the location of the hydrographic stations, conducted during the survey in 2017. The Fyllas Bank and Cape Desolation sections had to be abandoned due to severe weather conditions.

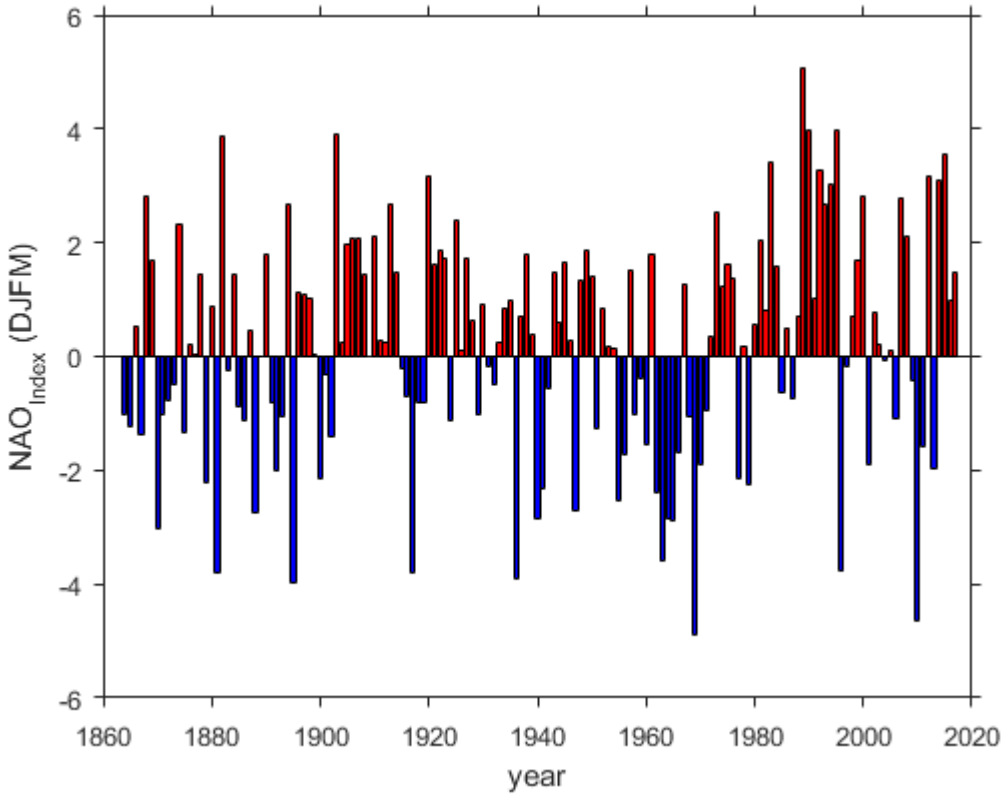

Figure 4. The Hurrell winter (DJFM) NAO index.

Data source: https://climatedataguide.ucar.edu/climate-data/hurrell-north-atlantic-oscillation-nao-index-station-based

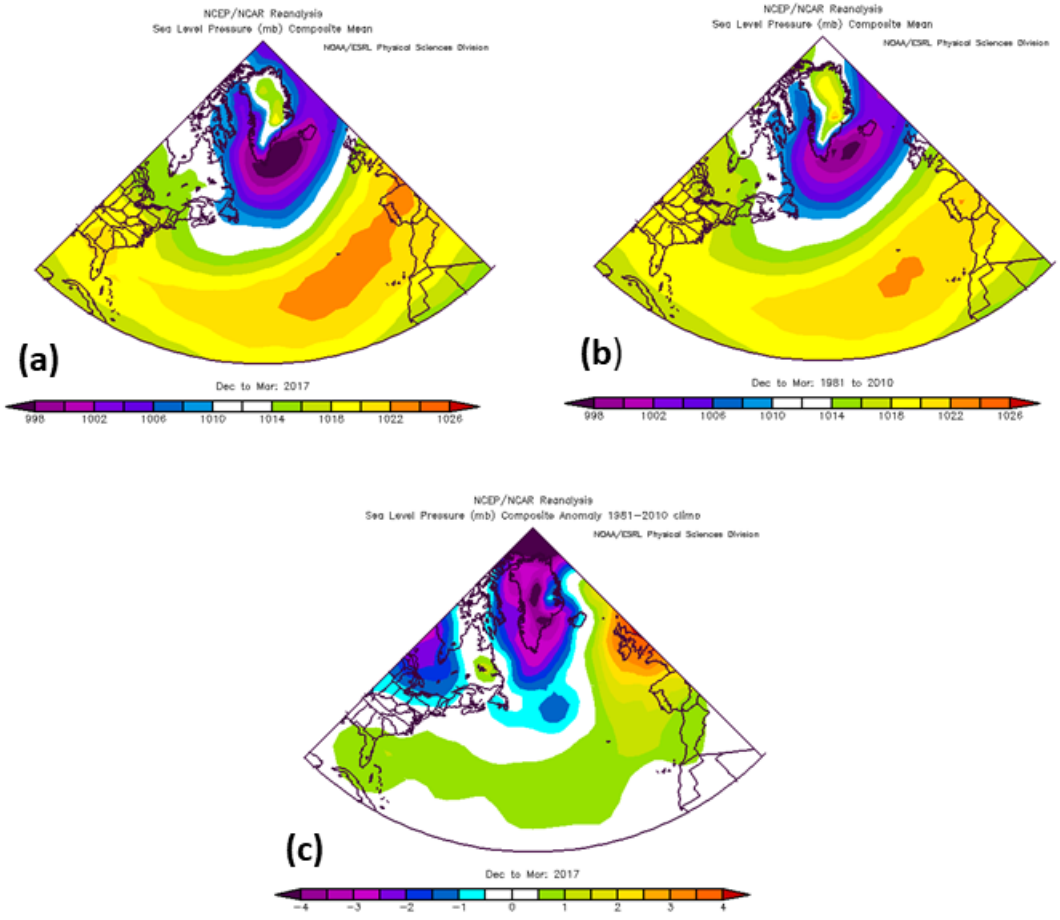

Figure 5. Maps of winter 1981-2010 (DJFM) mean sea level pressure (SLP) **(a)**, winter 2017 SLP **(b)**, and resulting SLP anomaly **(c)** over the North Atlantic. *Images are provided by the NOAA/ESRL Physical Science Division, Boulder, Colorado*

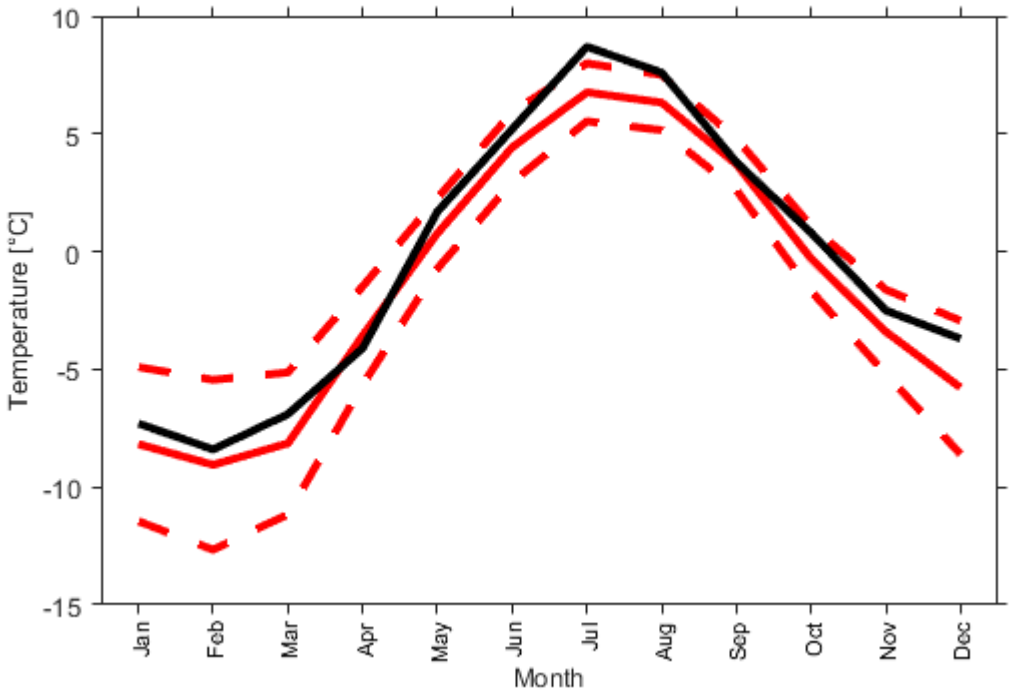

Figure 6. Monthly mean air temperature at Nuuk station in 2017 (black line), long-term monthly mean temperature (red solid line) and one standard deviation (red dashed lines) are shown. Reference period is 1981 to 2010. Data source: Danish Meteorological Institute (DMI), Cappelen (2018)

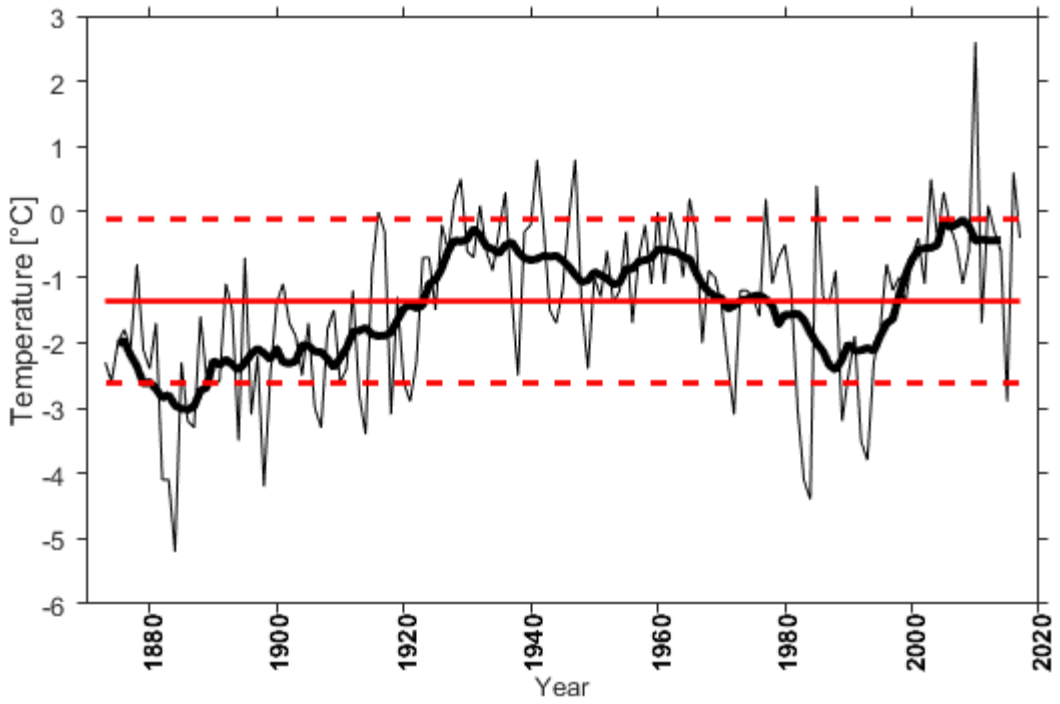

Figure 7. Annual mean air temperature at Nuuk station. Thick black line shows the 5-year smoothed data. Red solid line indicates the long-term mean temperature, referenced to 1981-2010. Dashed red lines mark corresponding standard deviations. Data source: Danish Meteorological Institute (DMI)

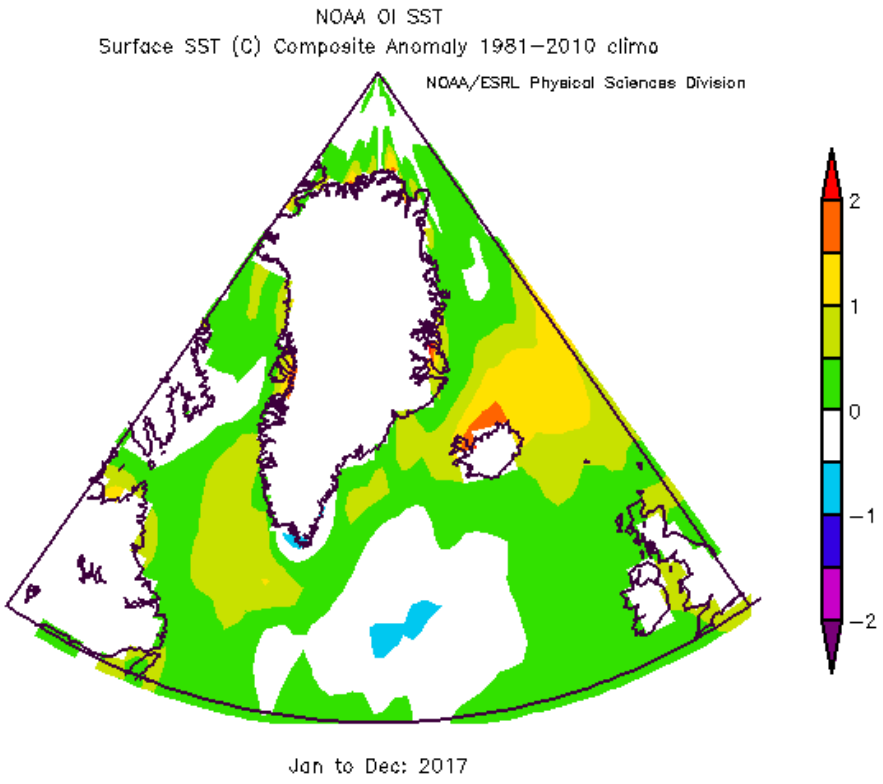

Figure 8. Map of 2017 annual sea surface temperature (NOAA OI SST) anomalies in the study region. The long-term mean corresponds to 1981-2010. *Image is provided by the NOAA/ESRL Physical Science Division, Boulder, Colorado*

References:

Cappelen, J. (ed.) (2013), Greenland - DMI Historical Climate Data Collection 1873-2012 – with Danish Abstracts, *DMI Technical Report 13-04*, Copenhagen.

Cappelen, J. (ed.) (2018), Weather observations from Greenland 1958-2017 - Observation data with description, *DMI Report 18-08*, Copenhagen.

Clarke, R. A., and J. C. Gascard (1983), The Formation of Labrador Sea Water. Part I: Large-Scale Processes, *Journal of Physical Oceanography*, *13*, 1764–1778.

Hurrell, J. W., and C. Deser (2010), North Atlantic climate variability: The role of the North Atlantic Oscillation, *Journal of Marine Systems*, *79*(3-4), 231-244.

Myers, P. G., D. Chris, and M. H. Ribergaard (2009), Structure and variability of the West Greenland Current in Summer derived from 6 repeat standard sections, *Progress in Oceanography*, *80*(1-2), 93-112.

Pickart, R. S., D. J. Torres, and P. Fratantoni (2005), The East Greenland Spill Jet, *Journal of Physical Oceanography*, *35*, 1037-1053.

Schmidt, S., and U. Send (2007), Origin and Composition of Seasonal Labrador Sea Freshwater, *Journal of Physical Oceanograpphy*, *37*, 1445–1454.

Stein, M. (2005), North Atlantic subpolar gyre warming –impacts on Greenland offshore waters, *Journal of Northwest Atlantic Fishery Science*, *36*, 43 –54.

Stein, M. (2010), The oceanographic work of the Institute of Sea Fisheries in Greenland Waters, 1952-2008, *Journal of Applied Ichthyology*, *26*(C1), 19-31.

Sutherland, D. A., R. S. Pickart (2008), The East Greenland Coastal Current: structure, variablility, and forcing, *Progress in Oceanography*, 78, 58-77.

Area 2c: Hydrographic Conditions on the Northeast United States Continental Shelf in 2017

Paula Fratantoni
NOAA National Marine Fisheries Service
Northeast Fisheries Science Center
166 Water Street, Woods Hole, MA, 02543 USA

Background

The Northeast United States (NEUS) Continental Shelf extends from the southern tip of Nova Scotia, Canada, southwestward through the Gulf of Maine and the Middle Atlantic Bight, to Cape Hatteras, North Carolina (Fig. 1). Contrasting water masses from the subtropical and subpolar gyres influence the hydrography in this region. Located at the downstream end of an extensive interconnected coastal boundary current system, the NEUS shelf is the direct recipient of cold/fresh arctic-origin water, accumulated coastal discharge and ice melt that has been advected thousands of kilometers around the boundary of the subpolar North Atlantic. Likewise, subtropical water masses, advected by the Gulf Stream, slope currents and associated eddies, also influence the composition of water masses within the NEUS shelf region. The western boundary currents of the subpolar and subtropical gyres respond to variations in basin-scale forcing through changes in position, volume transport and/or water mass composition and it is partly through these changes that basin-scale climate variability is communicated to the local NEUS shelf.

To first order, hydrographic conditions along the NEUS shelf are determined by the relative proportion of two main sources of water entering the region: cold/fresh arctic-origin water advected by the coastal boundary current from the north and warmer, more saline slope waters residing offshore of the shelf break. The source waters first enter the NEUS shelf region through the Gulf of Maine, a semi-enclosed shelf sea that is partially isolated from the open Northwest Atlantic by two shallow banks, Browns and Georges Banks. Below 100 meters, exchange between the Gulf of Maine and the deeper North Atlantic is restricted to a single deep channel, the Northeast Channel, which bisects the shelf between the two banks. This deep channel interrupts the continued flow of cold, fresh arctic-origin water along the coast, redirecting the majority of this flow into the Gulf of Maine. In the meantime, denser slope waters enter the basin through the same channel at depth, gradually spreading into a network of deep basins within the Gulf of Maine (Fig. 1b). In the upper layers of the Gulf of Maine, the shelf waters circulate counter-clockwise around the basin before continuing southwestward through the Middle-Atlantic Bight (Fig. 1b). The shelf water is progressively modified by atmospheric fluxes of heat and salt and through mixing with both deeper slope waters and the discharge of several local rivers. In this way, the Gulf of Maine represents the gateway to the NEUS shelf region, responsible for setting the initial hydrographic conditions for water masses entering the Middle Atlantic Bight further downstream.

The pronounced seasonal cycle of heating and cooling over the region drives seasonal variations in water mass composition that are typically larger than interannual variations. During fall and winter, intense cooling at the surface removes buoyancy, resulting in overturning and vertical homogenization of a significant portion of the water column. During spring and summer, surface heating re-stratifies the surface layer, isolating a remnant of the previous winter's cold/fresh mixed water at depth. Variations in these seasonal processes (e.g. less intense cooling in the winter or shifts in the timing of springtime warming) can result in interannual variations in the composition and distribution of water masses. In addition, fluctuations in the composition and volume of source waters entering the Gulf of Maine may also drive interannual variations in water properties relative to this seasonal mean picture.

The slope water that enters the Gulf of Maine is a mixture of two water masses: warm, saline, relatively nutrient-rich Warm Slope Water (WSLW) originating in the subtropics and cold, fresh, relatively nutrient-poor Labrador Slope Water (LSLW) originating in the subpolar region. Seaward of the Gulf of Maine, the relative proportion of these two water masses varies over time. However, in general, the volume of each decreases with increasing along-slope distance from their respective sources; LSLW (WSLW) volume decreases from north to south (south to north). Decadal shifts in the position of the Gulf Stream appear to be closely tied to changes in slope water temperature offshore of the NEUS shelf and to the composition of slope water entering the Gulf of Maine (Pers. Comm. T. Joyce and Y-O. Kwon.) Cooling in the slope water offshore is accompanied by a southward shift in the Gulf Stream and a predominance of northern source water (LSLW) in the deep layers of the Northeast Channel.

Basin-Scale Conditions in 2017

Surface air temperatures were warmer than average (1981-2010) over the western North Atlantic basin during winter and fall. (Fig. 2). A series of late-winter storms resulted in anomalously cold air temperatures over the NEUS Shelf in March, ending a 10-month streak of warm anomalies. Air temperatures were weakly negative between May and August, while anomalously warm conditions returned in autumn. Sea surface temperature mirrored these patterns, with warmer than average SST over the NEUS Shelf during winter and fall (Fig. 3). Annually, the magnitude of the warming was comparable to that observed in the 1950s (Fig 4).

Hydrographic Conditions in 2017

The U.S. National Oceanic and Atmospheric Administration's Northeast Fisheries Science Center (NEFSC) conducts multiple shelf-wide surveys every year in support of its mission to monitor the NEUS ecosystem. Monitoring efforts have been ongoing since 1977. Typically, the NEFSC completes six full-shelf hydrographic surveys per year, in addition to several more regionally focused surveys – the minimum required to resolve the dominant seasonal cycle in this region. However, ship maintenance issues in 2017 led to the elimination of the summer Ecosystem Monitoring (EcoMon) Survey and truncation of the fall ground fish and EcoMon surveys. While reinstatement of the winter EcoMon survey saw a return to winter sampling for the first time in 4 years, overall roughly half as many stations were occupied, leading to a loss of seasonal resolution.

Relative to historical values, regional ocean temperatures across the NEUS shelf were warm during 2017 (Fig. 5). Annually, waters in the upper 30 meters were between 0.9-1.2°C warmer than normal everywhere. Of the seasons sampled, warming was most pronounced during fall in the Middle Atlantic Bight and Gulf of Maine, where regional temperature anomalies approached 2°C (Fig. 6a). Extremely warm conditions were also observed near the bottom across the entire region, with anomalies exceeding those at the surface in most seasons (Fig. 6b). During fall, the bottom temperature measured more than one standard deviation above normal across the entire NEUS Shelf, while similarly large anomalies were observed near bottom in the eastern Gulf of Maine year round. The exception was during March and April in the northern Middle Atlantic Bight, where cold anomalies were observed near the bottom. The details of the seasonal differences are revealed in synoptic maps compiled from the spring and fall ground fish surveys (Fig 7). Warm anomalies were pervasive across the Gulf of Maine at the surface and bottom during fall. Whereas, in spring, a mix of warm and cold anomalies were observed at the surface across the NEUS while notably cold anomalies were observed in the Middle Atlantic Bight near the bottom at the shelf edge during March and April (Fig 7). Time series observations of near-surface temperature from NDBC buoy 44008, located south of Nantucket Shoals, observed near normal conditions during spring (April-June), followed by highly variable conditions during

summer (July-September), and finally persistent warming from October to November (Fig. 8). In general, this is consistent with the time history of atmospheric warming observed in Fig 2.

Annually, surface waters in the upper 30 meters were saltier than normal in 2017, particularly in the northern Middle Atlantic Bight (Fig. 9). Seasonally, large positive anomalies were observed during February and March in the southern and northern Middle Atlantic Bight, where anomalies exceeded 0.6 psu, and in the eastern Gulf of Maine during fall, where anomalies exceeded 0.8 psu (Fig. 10a). Bottom waters in the eastern Gulf of Maine were saltier than average year round, while freshening was observed in the western Gulf of Maine (Fig. 9 and 10b). Bottom water conditions were more seasonally variable in the southern Middle Atlantic Bight. Synoptically, saline conditions were pervasive during spring throughout the Middle Atlantic Bight (Fig 11). Extremely fresh anomalies were also observed near the bottom at the shelf edge, coincident with cold anomalies observed along the shelf edge during spring (Fig 7). Satellite derived observations of sea surface temperature suggest offshore forcing is responsible for this cold fresh shelfbreak anomaly. Satellite images reveal a prominent filament of cold shelf water protruding offshore in the region, likely having been advected offshore by the circulation of a large warm core ring impinging on the shelf (Fig 12).

Deep inflow through the Northeast Channel continues to be dominated by Warm Slope Water, except in June when cool very fresh water was observed (Fig. 13). Springtime temperature-salinity and temperature-depth profiles indicate the presence of a warmer, thinner Cold Intermediate layer in the western Gulf of Maine, a mid-depth water mass formed seasonally as a product of convective mixing driven by winter cooling (Fig. 14 & 15). The remnant winter water in the Cold Intermediate Layer was over 0.5°C warmer than average in 2017, suggesting that convective mixing was suppressed in the preceding winter (Fig. 14). In Wilkinson Basin, the entire water column below 50 meters was warmer than average, with anomalies increasing toward the bottom (Fig. 15 & 16). It is expected that extremely warm air temperatures over the North American continent during January and February suppressed wintertime convective mixing in the western Gulf of Maine, and the mild spring / summer to follow led to weaker than normal seasonal stratification (Fig 2). Vertical mixing during winter is an important process in the Western Gulf of Maine. Deeper mixing has greater potential to tap into nutrient rich slope water at depth resulting in a thicker intermediate layer during spring, both potentially having an impact on the timing or intensity of spring phytoplankton blooms.

Fisheries Implications

Our observations suggest that the Northeast U.S. Continental Shelf has been warming at a rate of ~.03-.05 °C/year since 1977, with significant interannual variations in temperature and salinity superimposed on this trend. As a result, the habitats of fish and invertebrate species in this region have experienced change on a variety of temporal and spatial scales, driving changes in distribution and abundance. Observations suggest that the NEUS Continental Shelf is being influenced more frequently by the Gulf Stream (Gawarkiewicz et al., 2018) and that the increased interactions may be related to changes in the meandering character of the current (Andres, 2016). Extreme diversions and meanders in the Gulf Stream's path (e.g. Gawarkiewicz et al., 2012) and detached Gulf Stream Warm Core Rings (e.g. Zhang and Gawarkiewicz, 2015) directly and indirectly influence the hydrography on the shelf, often leading to intrusions of comparatively warm and salty water onto the shelf. These episodic intrusions have the potential to cause significant changes in the ecosystem, for instance leading to significant changes in nutrient loading on the shelf, the seasonal elimination of critical habitats such as the cold pool and shelf-slope front, disruption of seasonal migration cues, and an increase in the concentration of offshore larval fish on the shelf.

Andres, M. (2016), On the recent destabilization of the Gulf Stream path downstream of Cape Hatteras, Geophys. Res. Lett., 43, doi:10.1002/2016GL069966.

Gawarkiewicz, G.G., R.E. Todd, W. Zhang, J. Partida, A. Gangopadhyay, M.-U.-H. Monim, P. Fratantoni, A. Malek Mercer, and M. Dent (2018), The changing nature of shelfbreak exchange revealed by the OOI Pioneer Array. *Oceanography* 31(1):60–70, https://doi.org/10.5670/oceanog.2018.110.

Gawarkiewicz, G. G., R. E. Todd, A. J. Plueddemann, M. Andres, and J. P. Manning (2012), Direct interaction between the Gulf Stream and the shelf break south of New England, Sci. Rep., 2, 553, doi:10.1038/srep00553.

Zhang, W. G., and G. G. Gawarkiewicz (2015), Dynamics of the direct intrusion of Gulf Stream ring water onto the Mid-Atlantic Bight shelf, Geophys. Res. Lett., 42, 7687–7695, doi:10.1002/2015GL065530.

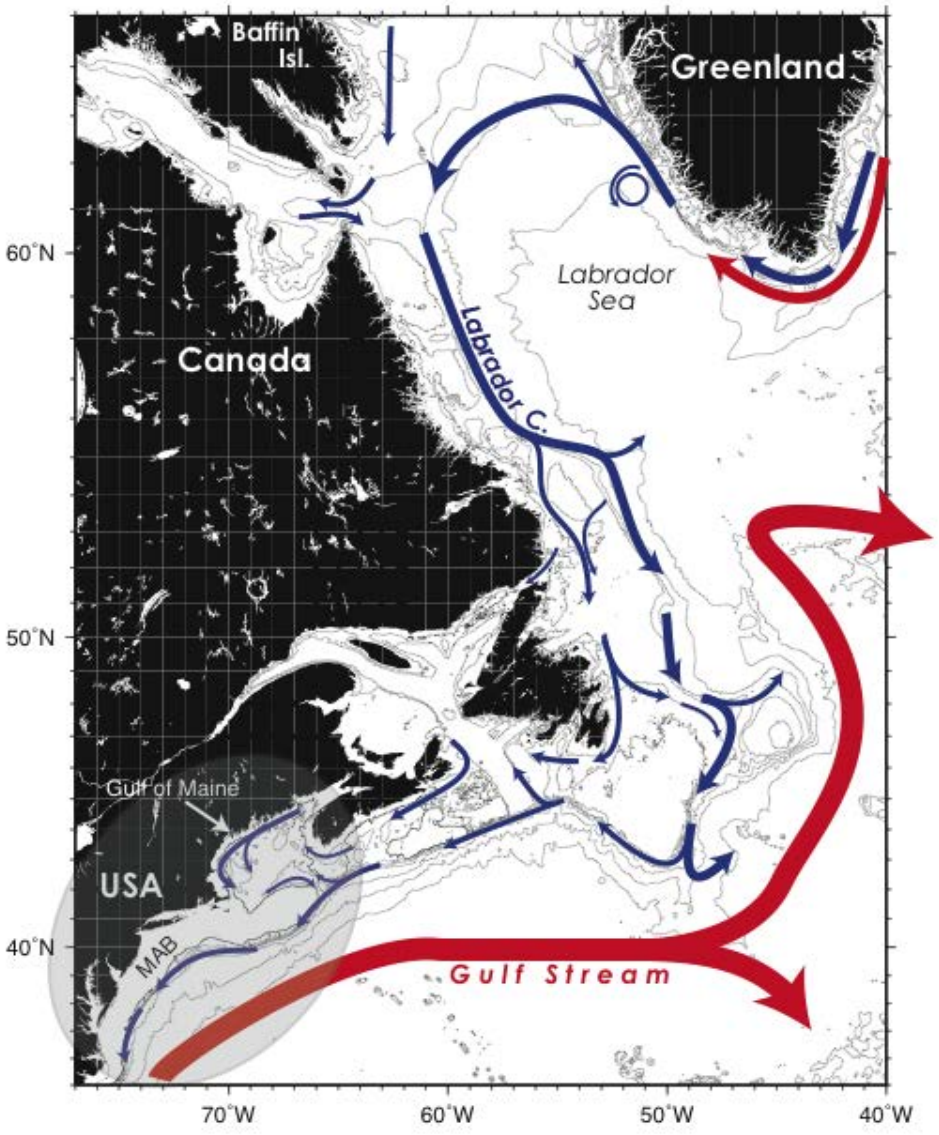

Figure 1a: Circulation schematic of the western North Atlantic. The Northeast U.S. Shelf region is identified by the shaded oval. The 100, 200, 500, 1000, 2000, 3000 and 4000 meter isobaths are shown.

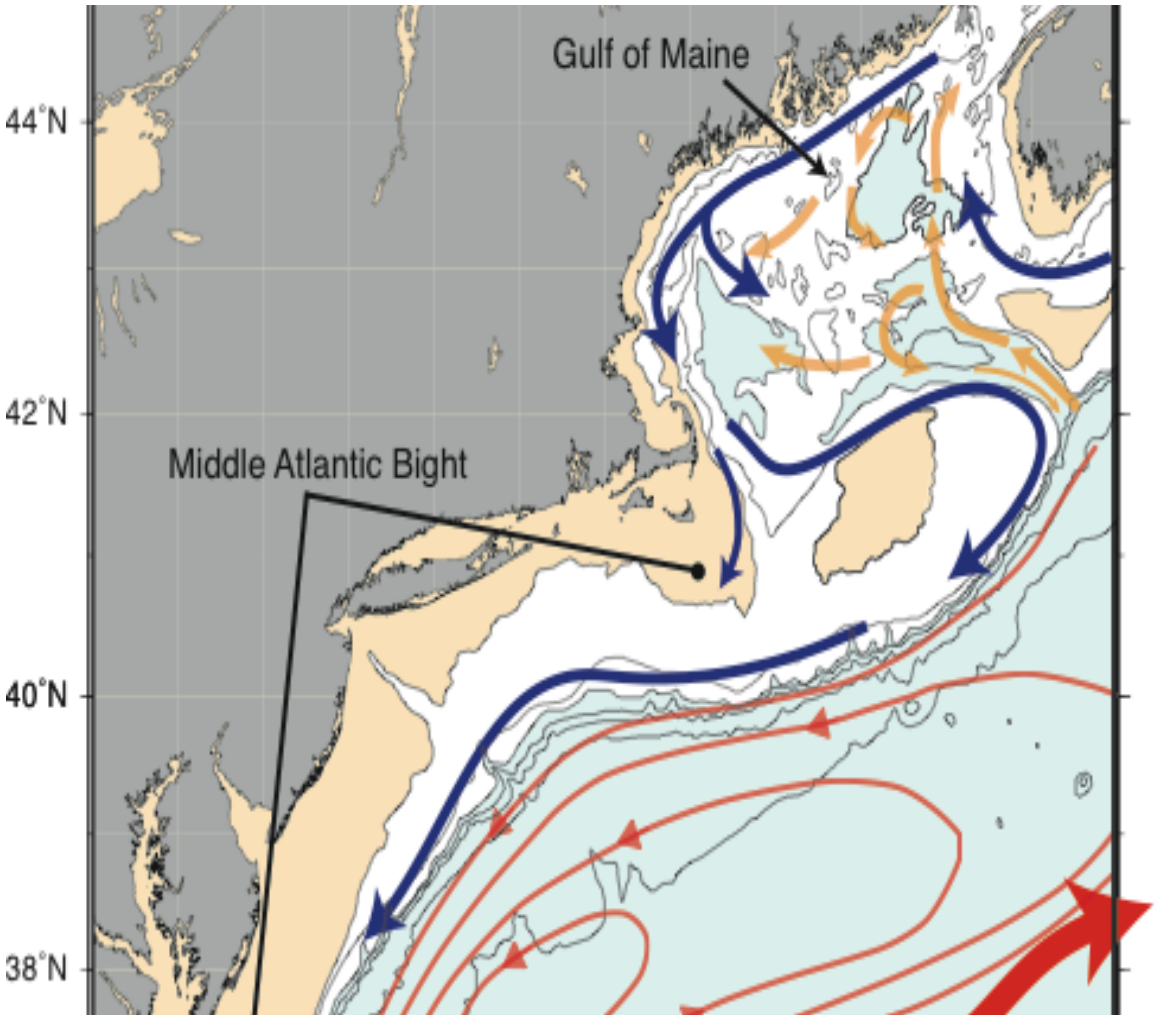

Figure 1b: Circulation schematic for the Northeast U.S. Shelf region, where blue arrows represent shelf water circulation and orange arrows represent deeper slope water circulation pathways. Water depths deeper than 200 meters are shaded blue. Water depths shallower than 50 meters are shaded tan.

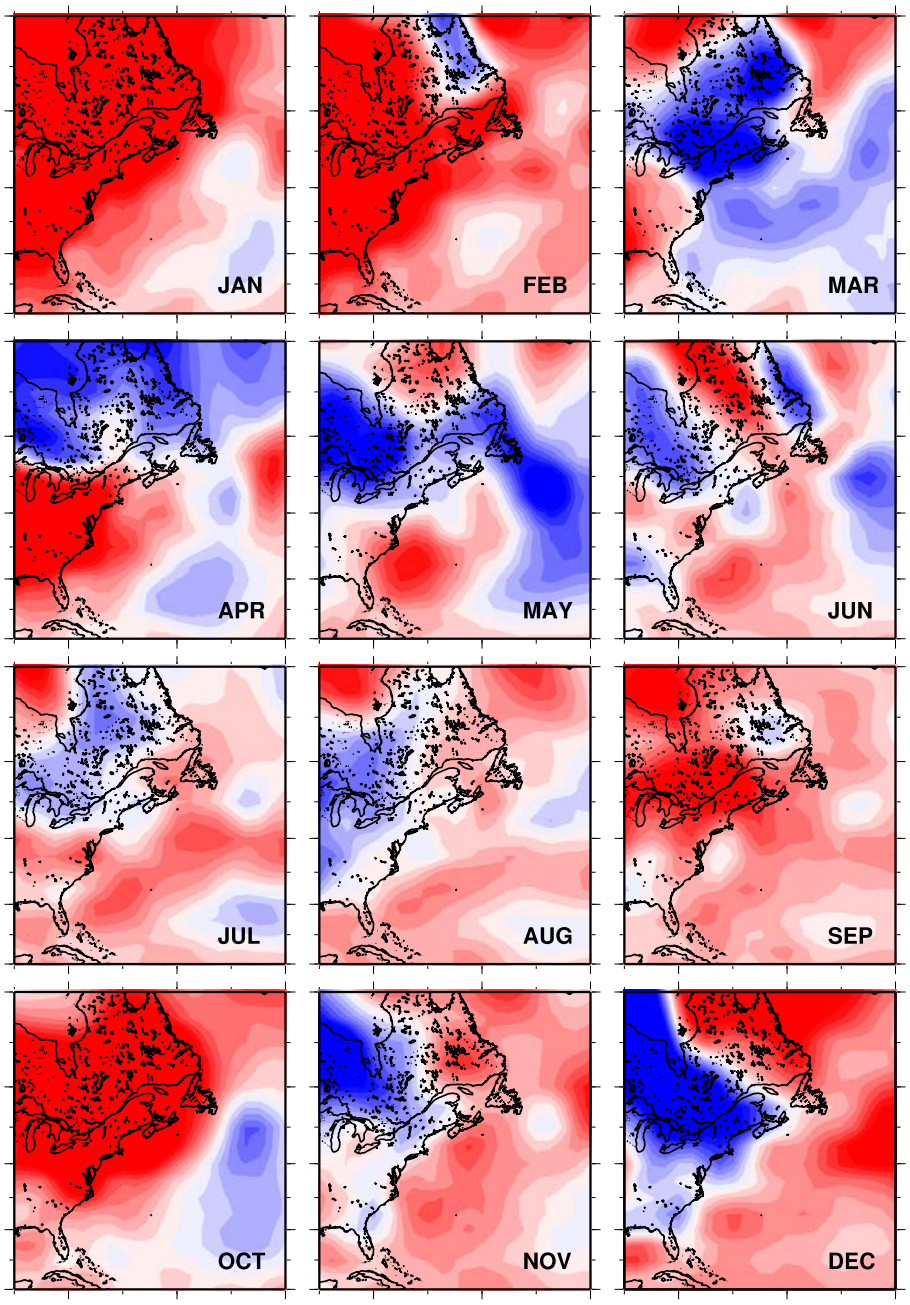

Figure 2: Surface air temperature anomaly derived from the NCEP/NCAR Reanalysis product (http://www.esrl.noaa.gov/psd/data/composites/day/). Positive anomalies correspond to warming in 2017 relative to the reference period (1981-2010).

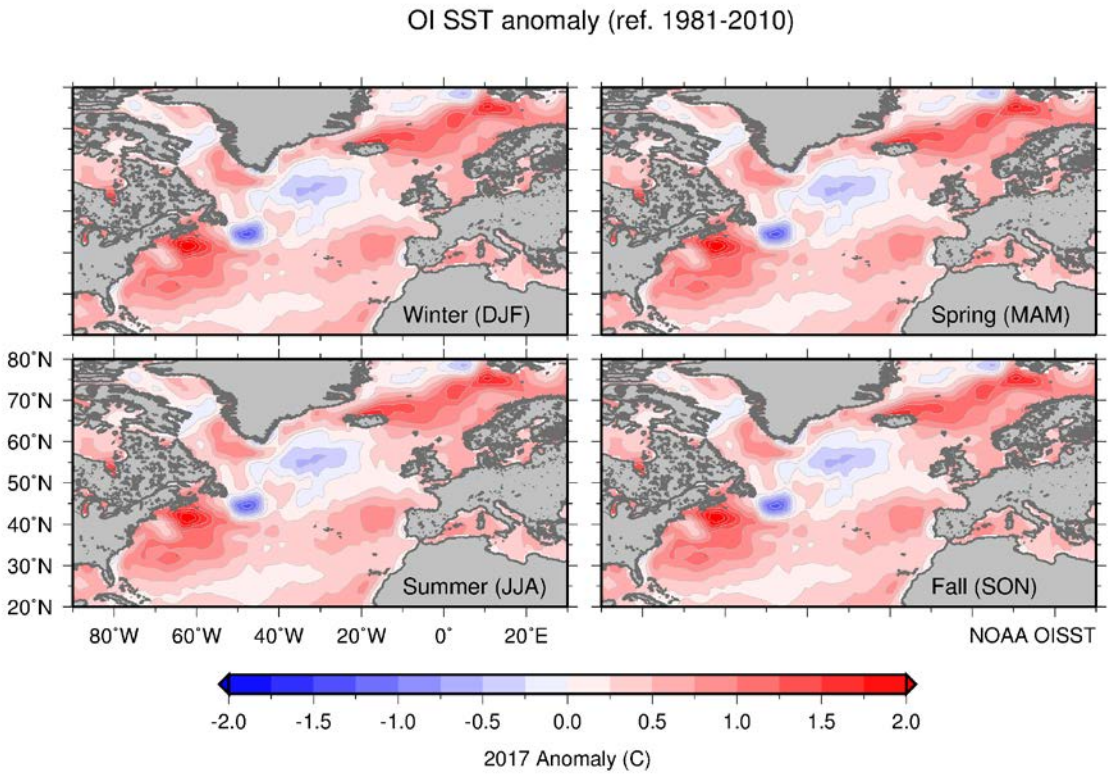

Figure 3: Sea surface temperature anomaly derived from the NOAA's Optimum Interpolation (OI) SST product (http://www.esrl.noaa.gov/psd/data/gridded/data.noaa.oisst.v2.html). Seasons are made up of 3-month periods where winter spans December-February. Positive anomalies correspond to warming in 2017 relative to the reference period (1981-2010).

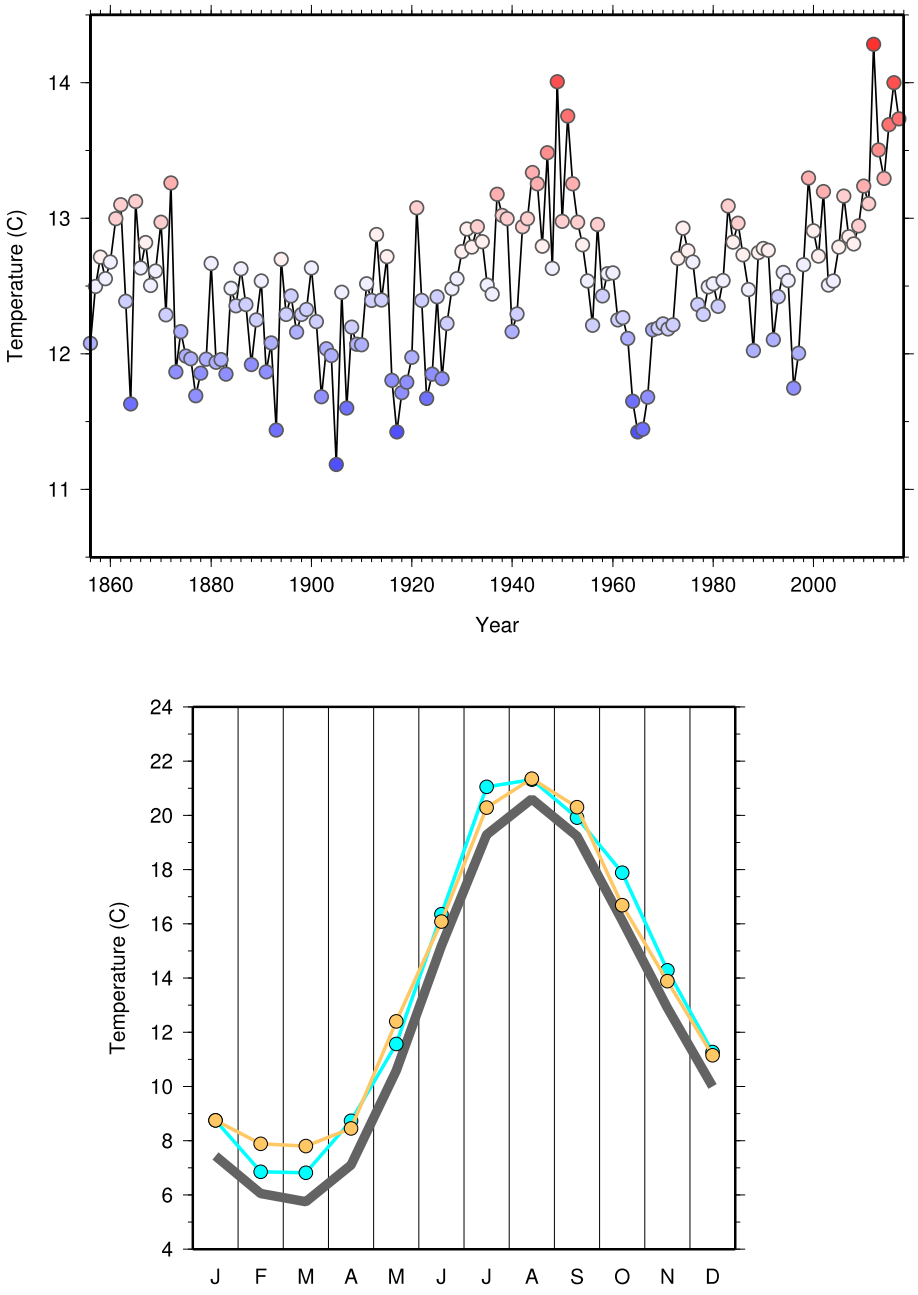

Figure 4: Top: Regional average annual sea surface temperature for the NEUS shelf region calculated from NOAA's extended reconstructed sea surface temperature product (http://www.esrl.noaa.gov/psd/data/gridded/data.noaa.ersst.html). Colors correspond with the anomaly scale in Figure 3. Bottom: Regional average monthly mean SST for the NEUS shelf for 2017 (cyan), 1950 (orange) and 1981-2010 (gray).

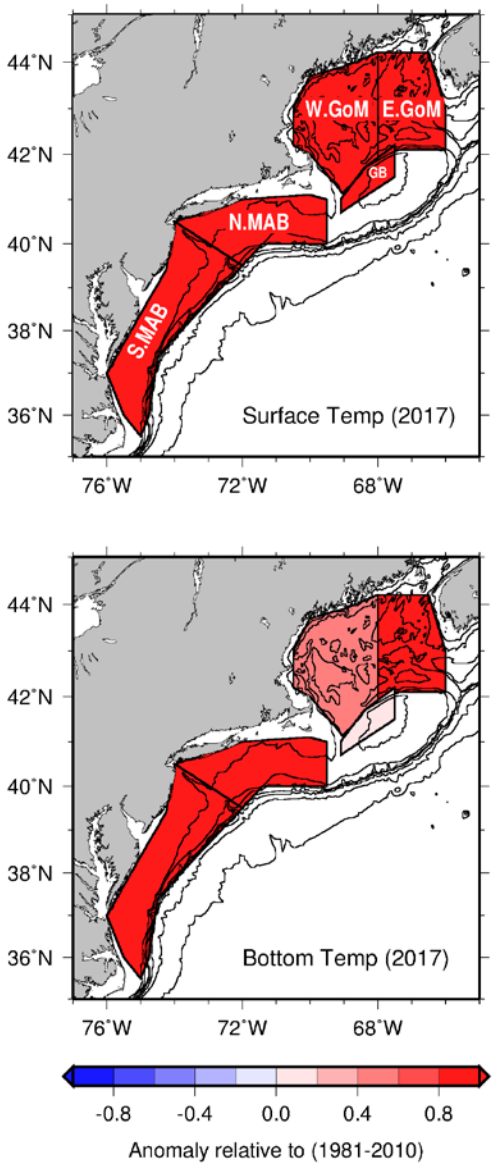

Figure 5: Surface (upper panel) and bottom (lower panel) regional annual temperature anomaly (°C). Positive anomalies correspond to warming in 2017 relative to the reference period (1981-2010). The region labels correspond to the panels in Figure 6.

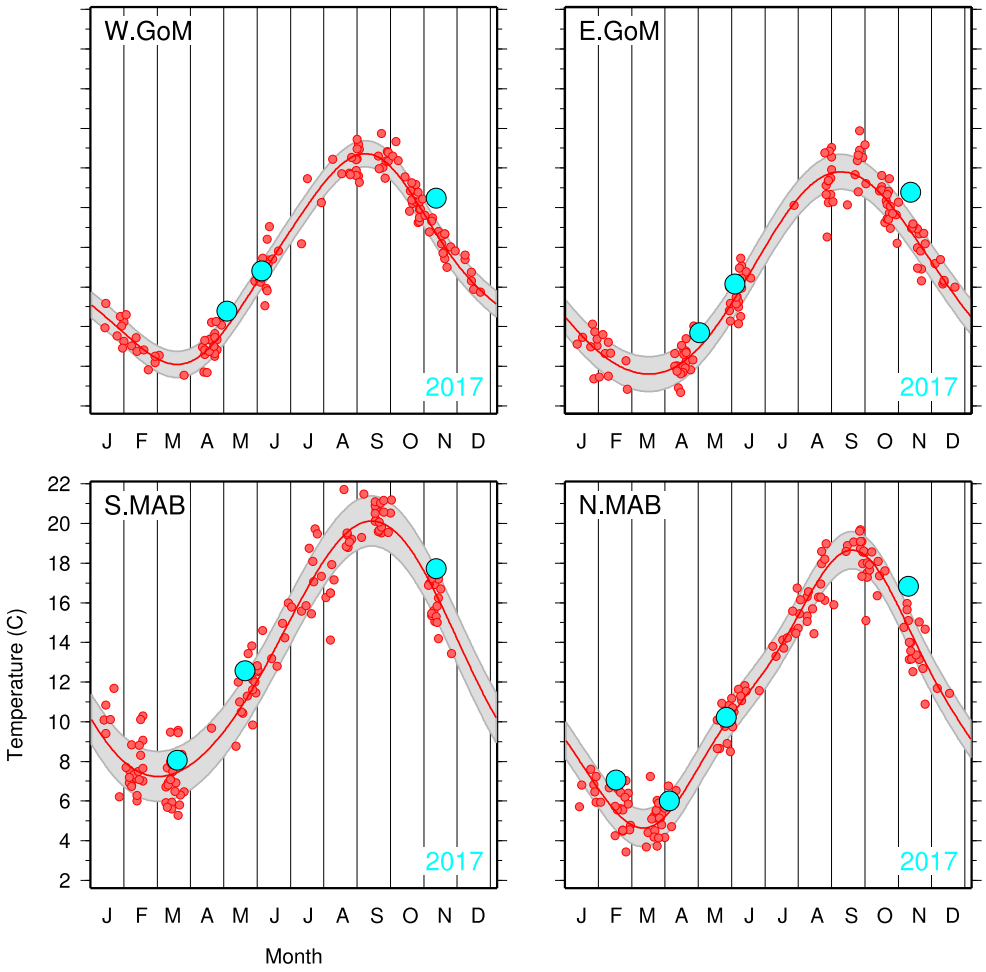

Figure 6a: Regional average 0-30 meter temperature (°C) as a function of calendar day. Each dot represents a volume-weighted average of all observations from a single survey falling within the regions delineated in Fig. 5. An annual harmonic fit to the regional average temperatures from 1981-2010 is shown by the red curve with the points contributing to the fit also shown in red. The gray shading depicts one standard deviation around this fit. The regional average temperatures from 2017 surveys are shown in cyan.

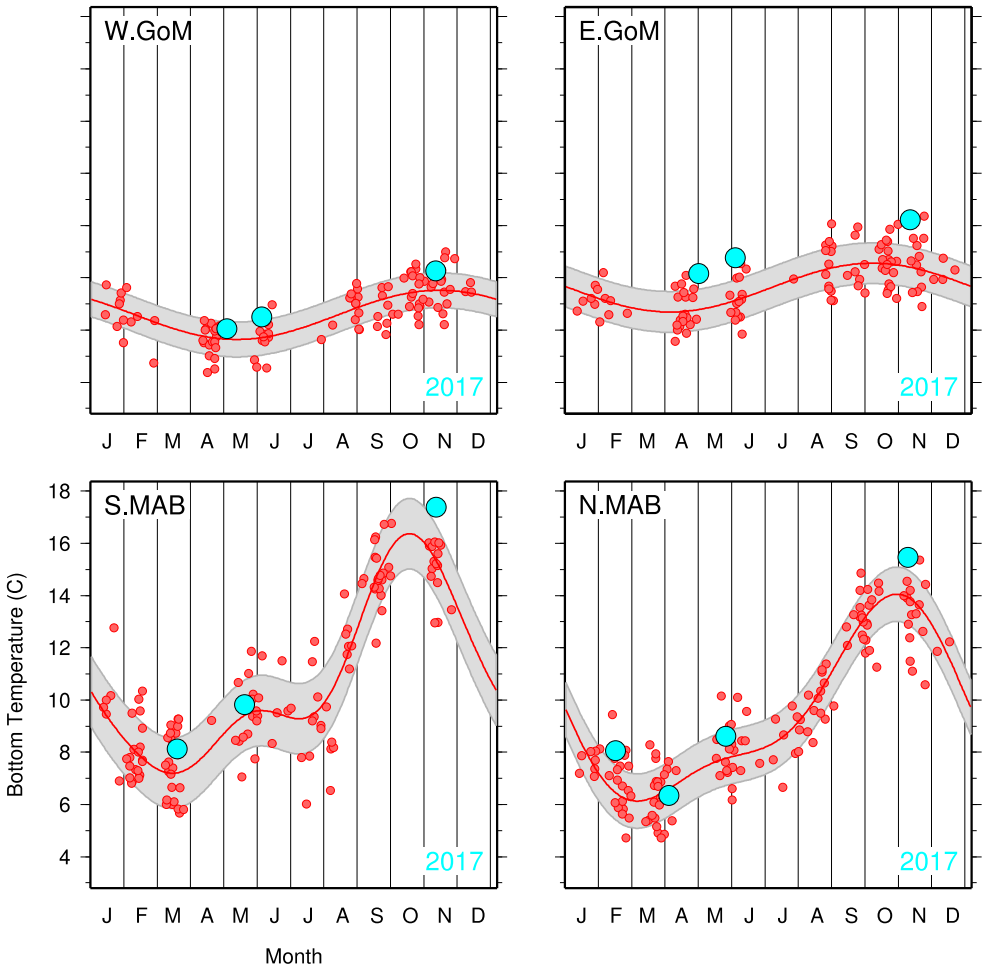

Figure 6b: As in Fig. 6a, but for bottom temperatures.

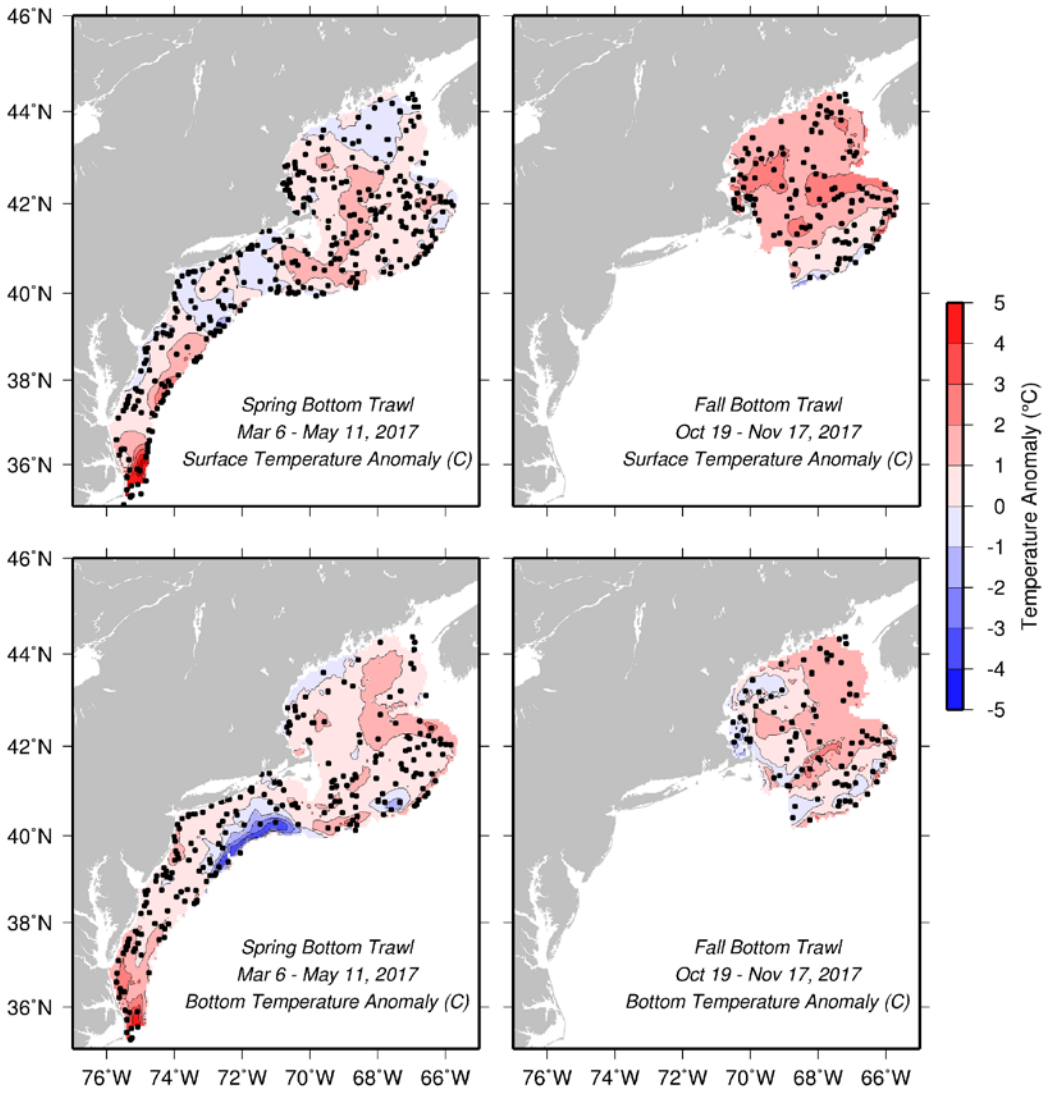

Figure 7: Surface (upper panels) and bottom (lower panels) temperature anomaly from the spring (left) and fall 2017 (right) ground fish surveys. Positive anomalies correspond to warming in 2017 relative to the reference period (1977-1987).

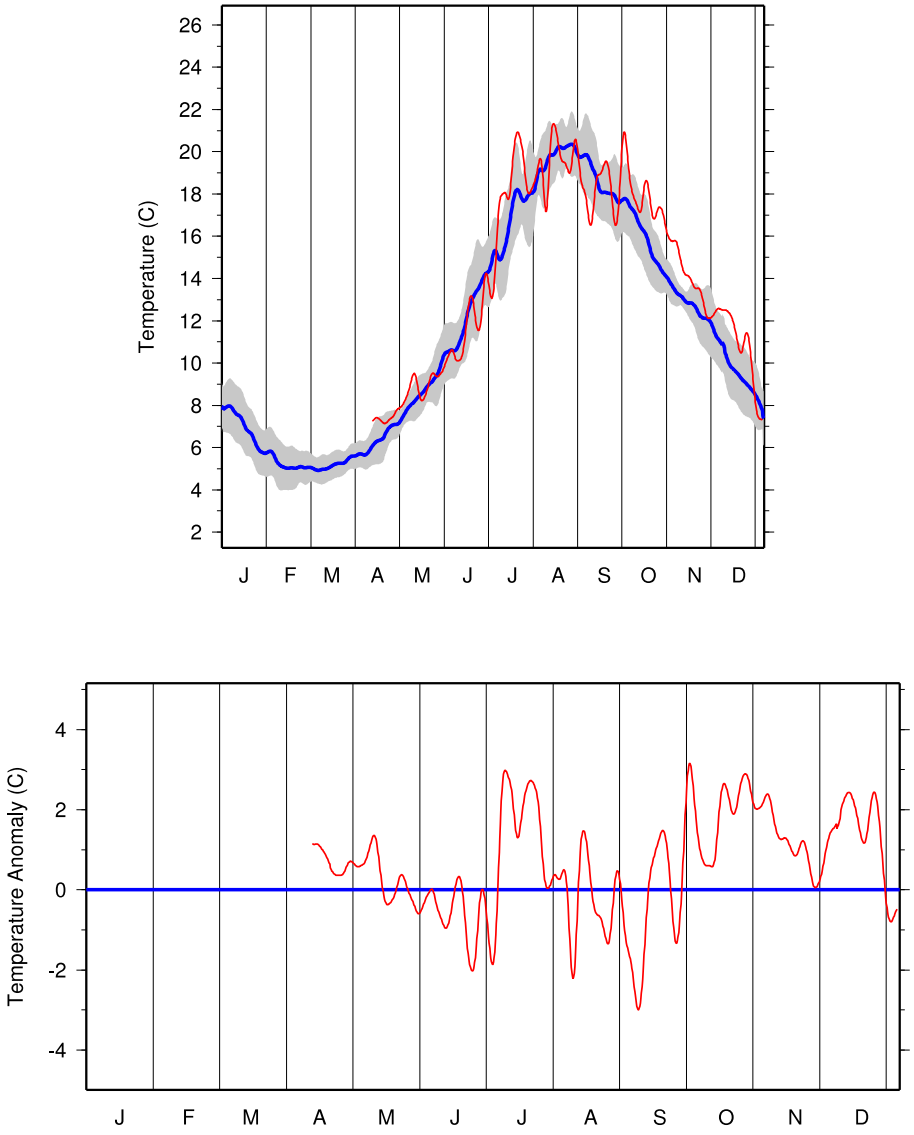

Figure 8: (top) Time series of surface ocean temperature from NDBC buoy 44008 located south of Nantucket Shoals in the northern Middle Atlantic Bight. Temperatures observed in 2017 (red) are compared with average temperatures (2000-2010, blue) in the top panel. The gray shading indicates one standard deviation about the long-term mean. The lower panel shows the difference between 2017 and the long-term mean temperature, where positive values indicate warmer conditions in 2017.

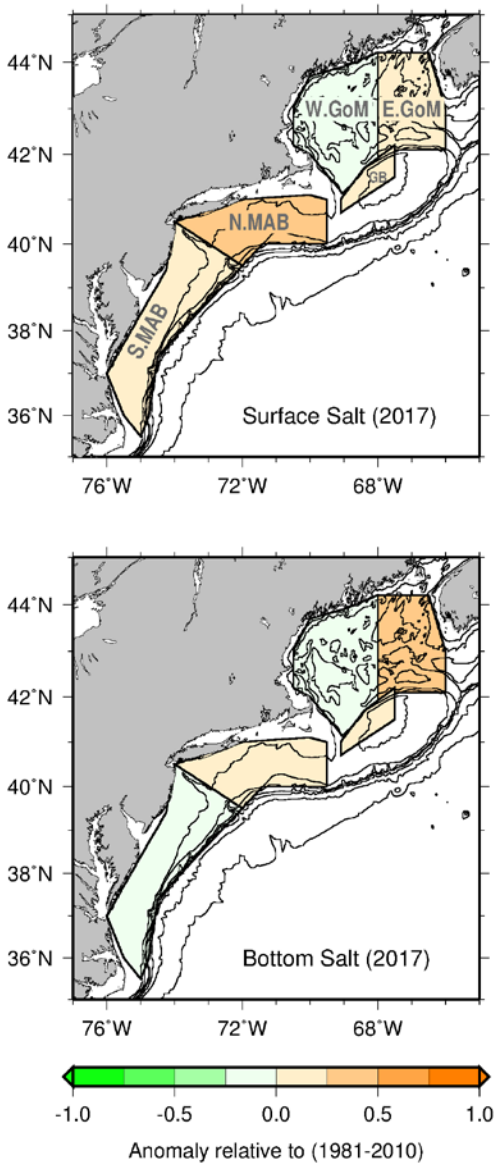

Figure 9: Surface (upper panel) and bottom (lower panel) regional annual salinity anomaly. Positive anomalies correspond to more saline conditions in 2017 relative to the reference period (1981-2010). The region labels correspond to the panels in Figure 10.

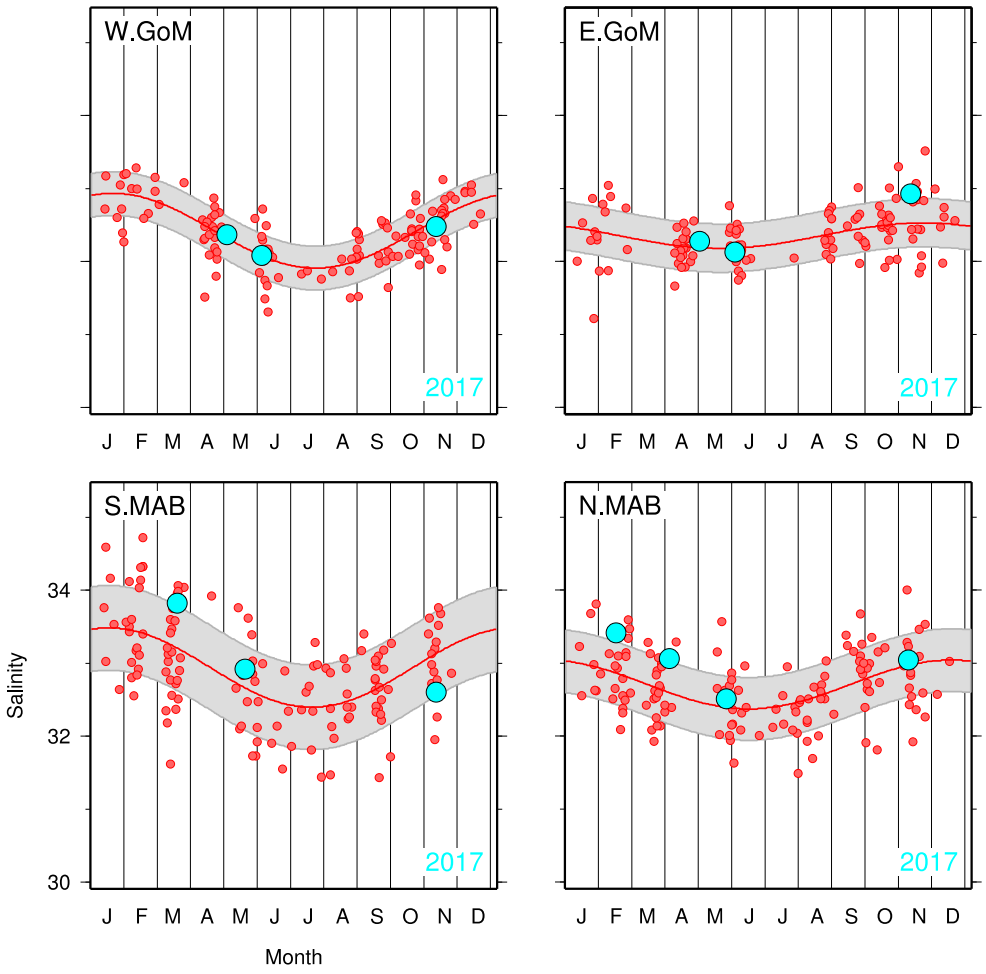

Figure 10a: Regional average 0-30 meter salinity as a function of calendar day. Each dot represents a volume-weighted average of all observations from a single survey falling within the regions delineated in Fig. 9. An annual harmonic fit to the regional average salinities from 1981-2010 is shown by the red curve with the points contributing to the fit also shown in red. The gray shading depicts one standard deviation around this fit. The regional average salinities from 2017 surveys are shown in cyan.

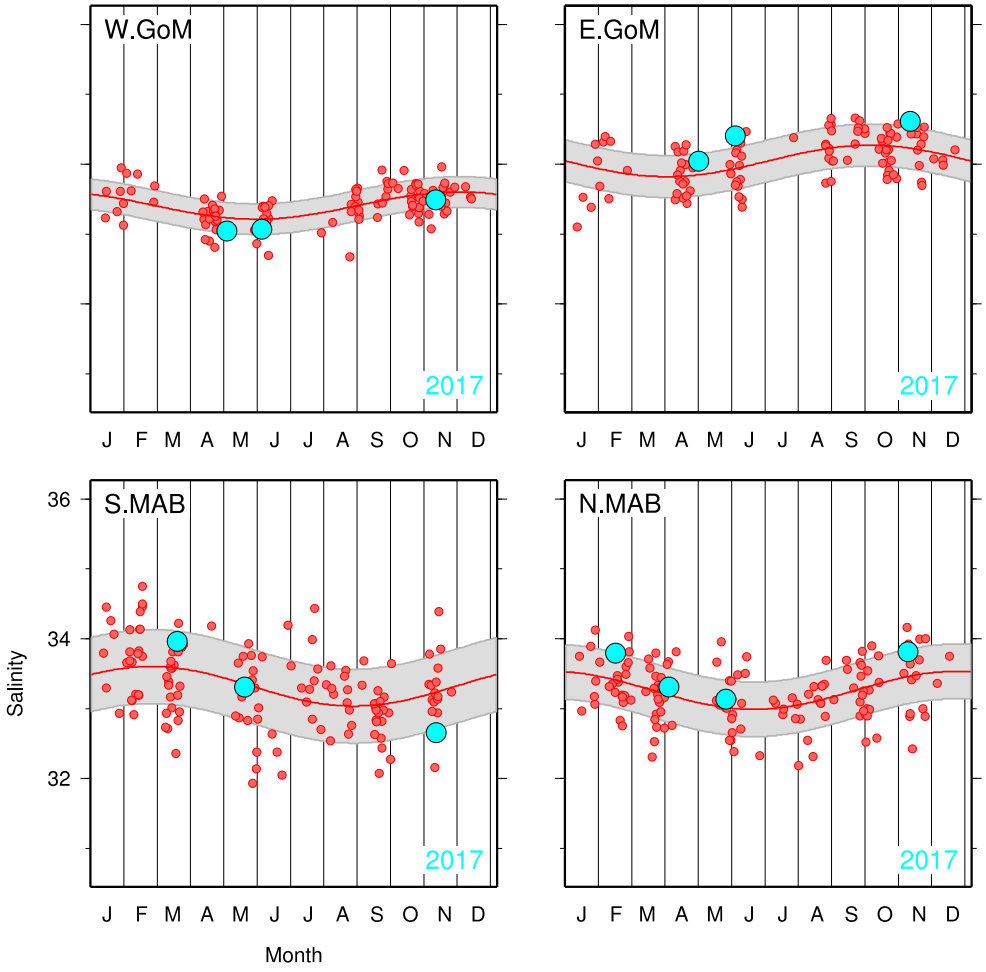

Figure 10b: As in Fig. 10a, but for bottom salinity.

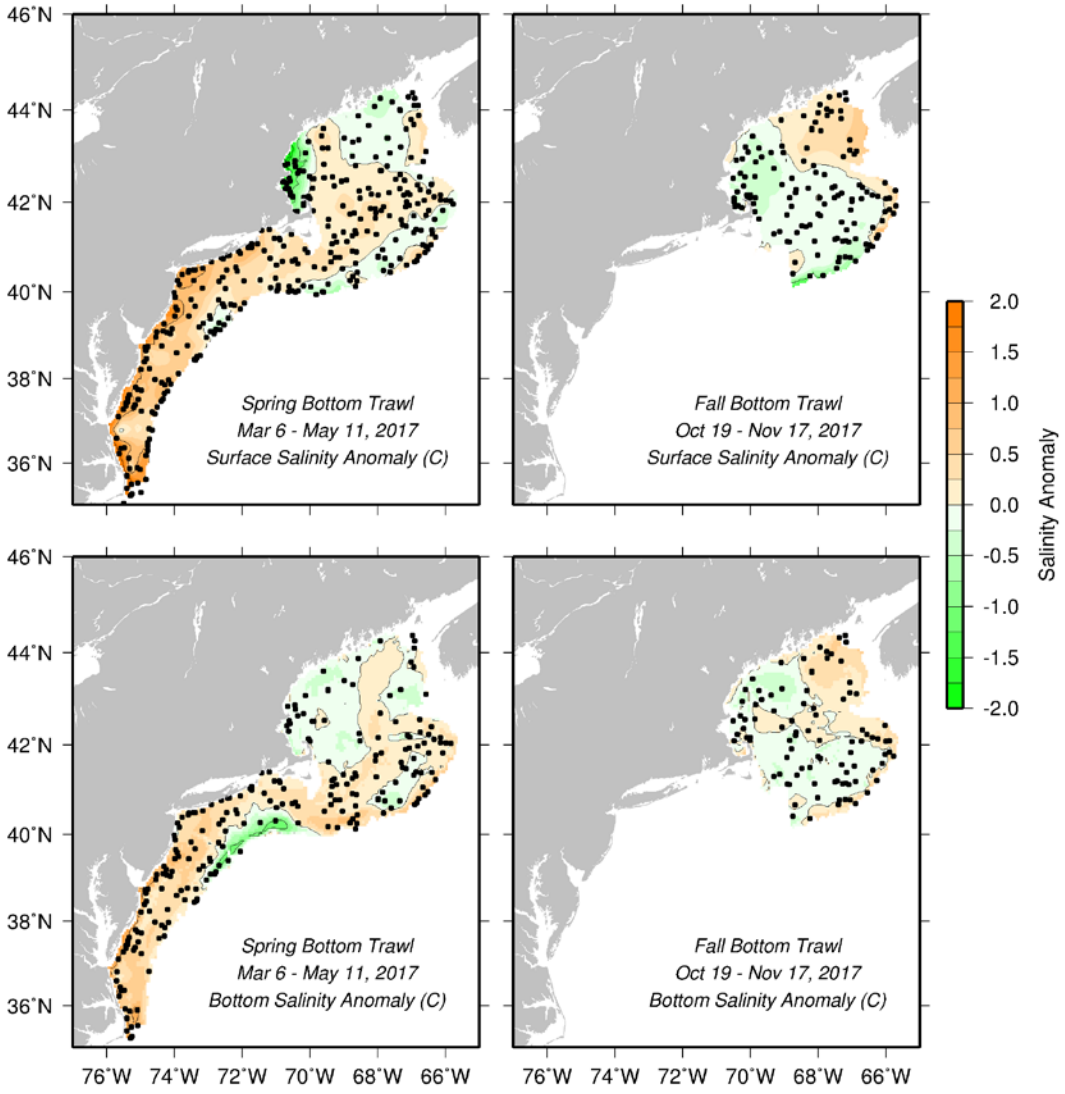

Figure 11: Surface (upper panels) and bottom (lower panels) salinity anomaly from the spring (left) and fall 2017 (right) ground fish surveys. Positive anomalies correspond to more saline conditions in 2017 relative to the reference period (1977-1987).

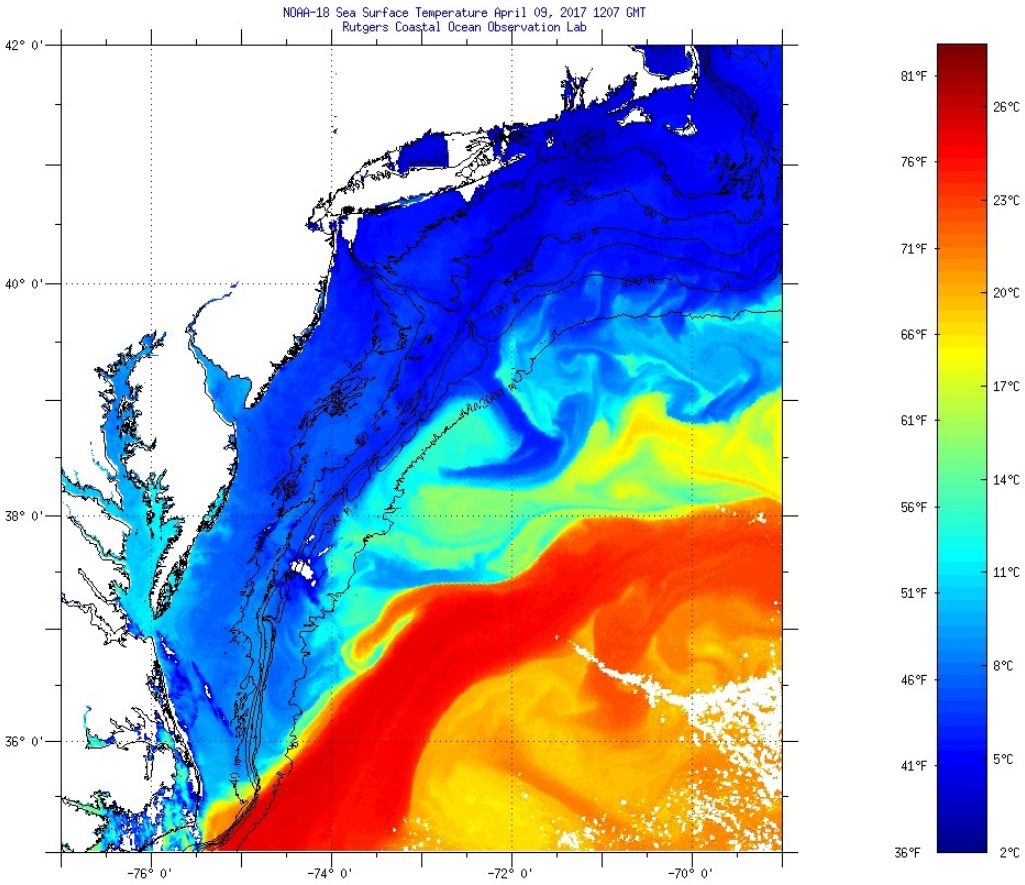

Figure 12: Daily composite sea surface temperature derived by the Coastal Ocean Observations Lab, Rutgers University, from data collected by the Advanced Very High Resolution Radiometer on April 9, 2017.

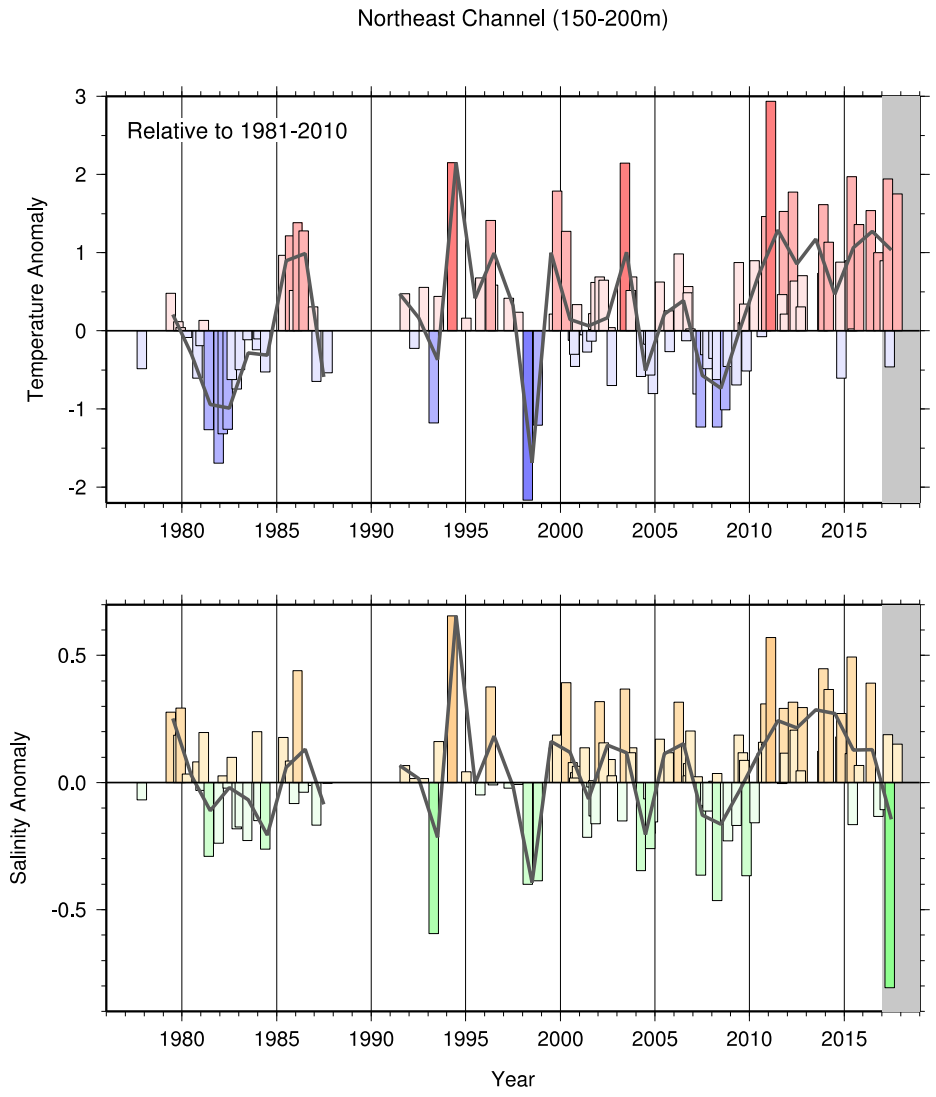

Figure 13: Time series of temperature and salinity anomaly in the deep Northeast Channel. Each bar represents a volume-weighted average of all observations from a single survey collected between 150-200 meters in the Northeast Channel. The grey curve shows the annual average anomaly time series. Positive values are warmer and saltier than the long-term mean calculated for 1981-2010. The gray shading highlights observations made in 2017.

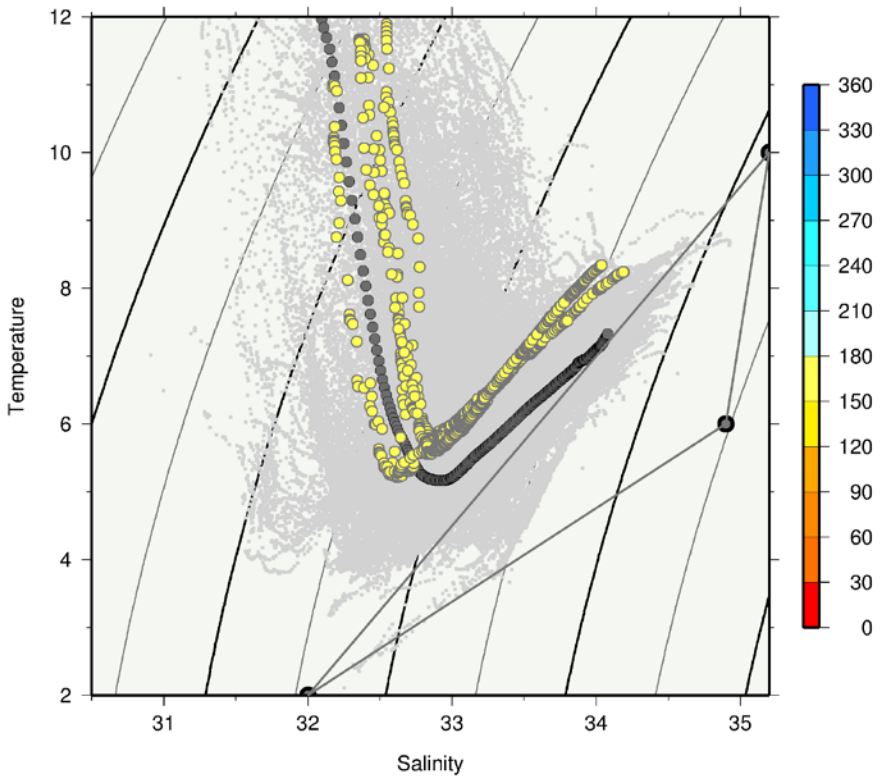

Figure 14: Temperature-salinity diagram showing water properties in Wilkinson Basin in the western Gulf of Maine. All observations from June (yellow) 2017 are shown along with the spring climatological average profile (1981-2010, dark gray). The lightest gray dots show the historical range encompassed by observations from the reference period, 1981-2010. Temperature and salinity properties representative of source waters entering the Gulf of Maine are shown by the mixing triangle.

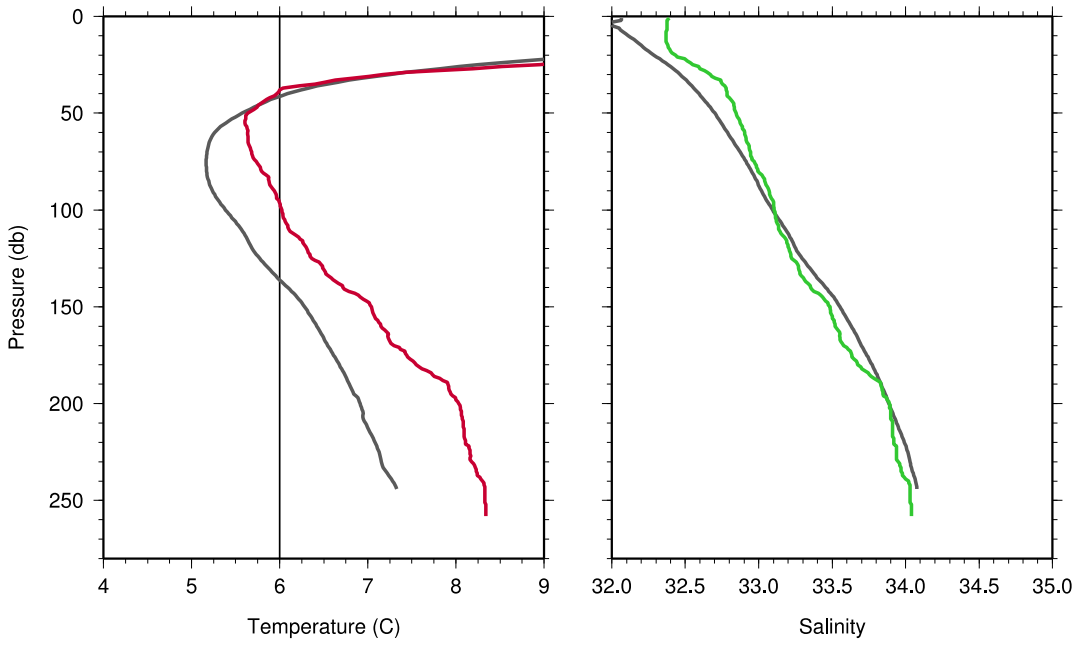

Figure 15: Average profiles of temperature (left) and salinity (right) from repeated observations collected during June in Wilkinson Basin in the western Gulf of Maine. All observations from June 2017 (red and green) are shown along with the climatological average profile for the same month (1981-2010, dark gray). Waters in the Cold Intermediate Layer in the western Gulf of Maine are typically colder than 6°C, denoted by the vertical line.

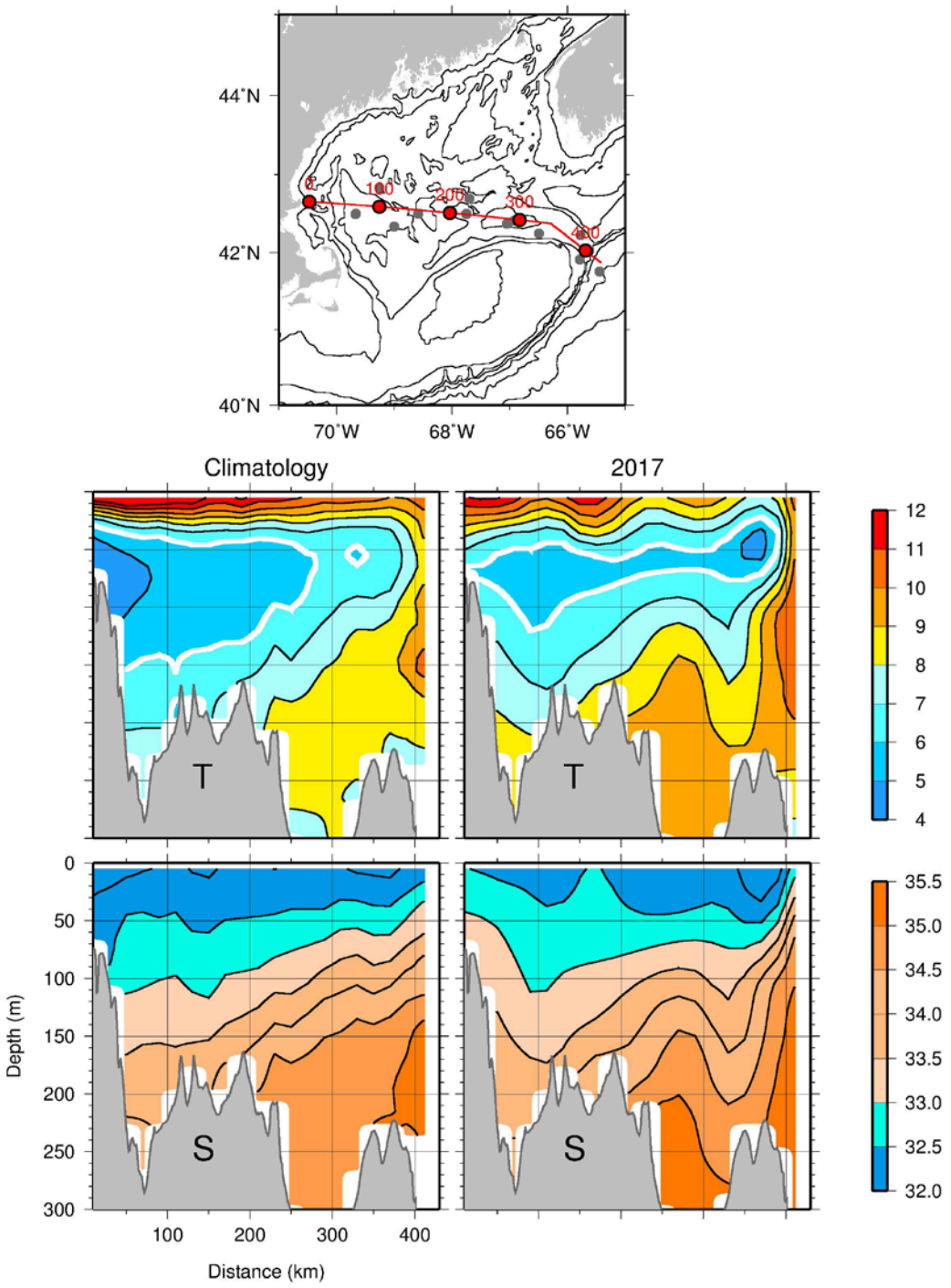

Figure 16: Vertical sections of temperature (top) and salinity (bottom) crossing the Gulf of Maine along a zonal transect shown in the map. The left panels show the climatological average for June spanning the years 1981-2010. The right panels show the synoptic mean section for June 2017. The heavy white contour highlights the 6°C isotherm as an indicator of the boundary of the cold intermediate layer. Along-transect distances and the June 2017 station distribution are shown on the map for reference.

Hydrographic Status Report 2017: Bay of Biscay and West Iberia

C. González-Pola

Spanish Institute of Oceanography. *Coastal Centre of Gijón, Avda Príncipe de Asturias 70Bis, 33212, Gijón Spain. cesar.pola@gi.ieo.es

V. Valencia, A. Fontán, N. Goikoetxea, M. Chifflet

AZTI-Tecnalia. Unidad de Investigación Marina. Muelle de la Herrera s/n, 20110 Pasaia (Gipuzkoa) Spain

1 INTRODUCTION

The Spanish Standard Sections cover the area of the shelf, shelf-break and oceanic basins around the Iberian Peninsula (Biscay, West Iberia and Gulf of Cadiz) and Canaries. The north and northwest Spanish shelves are sampled monthly by the Spanish Institute of Oceanography and by AZTI Foundation under the long-term hydrographic monitoring programs RADIALES (www.seriestemporales-ieo.com, Valdés et. al. 2004) and VARIACIONES (Valencia et al., 2004). Western Iberia is covered annually since early 2000's program RADPROF (Prieto et al. 2013). The Gulf of Cádiz and the Canaries are covered in subsequent Annexes.

Main circulation patterns within the region are depicted for different levels in Figure 1. Roughly, central waters (200-700 m) and Labrador Seawater (c.a. 2000 m) flows from the northwest, while Mediterranean waters spreads from it is origin at Gibraltar. Deep waters describe slow cyclonic flow.

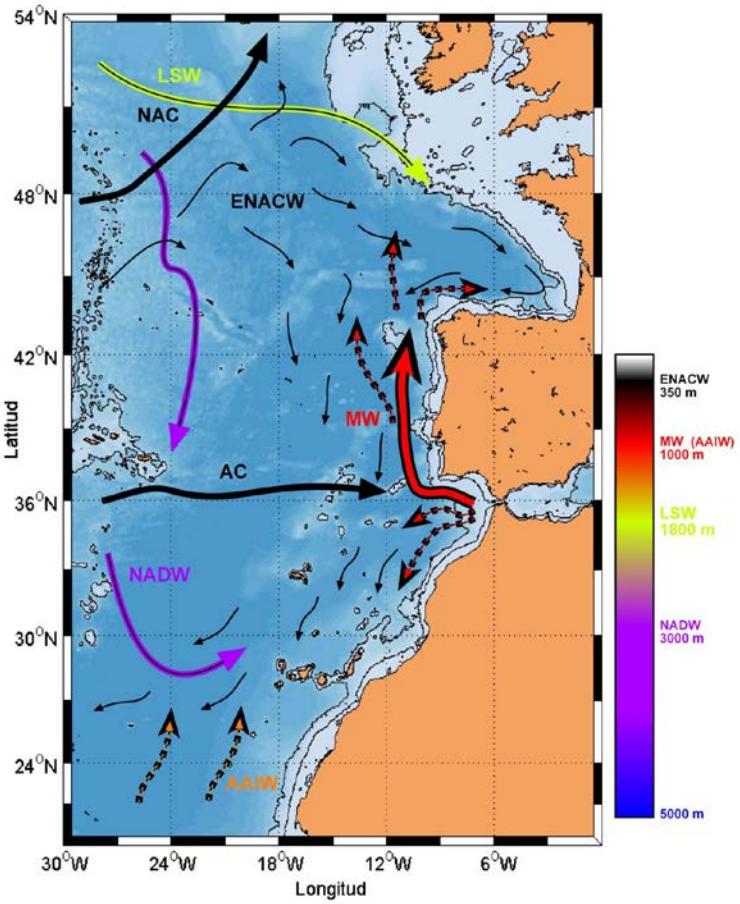

Figure 1.Main circulation patterns at different levels in the temperate NE Atlantic

2 ATMOSPHERIC CONDITIONS AND CONTINENTAL RUNOFF

2.1 Atmospheric temperature

Meteorological conditions at the Iberian Peninsula and the Canary Islands in 2017 indicate that it was a very warm or extremely warm year, with few exceptions in some areas of the Cantabrian coast, Ebro Valley and the Balearic Islands where 2017 was just warm (AEMET, 2018). Annual air temperature anomalies were between +0.5 °C and +1.5 °C relative to 1981-2010 for most of the region and negative anomalies were not recorded in any location (Figure 2).

Regarding the seasonal cycle of air temperature (Figure 3), the spatial distribution of thermal anomalies was very irregular over the area, especially in winter and autumn. The spatial distribution of thermal anomalies in winter was characterised by alternating positive and negative anomalies though the positive anomalies prevailed. Overall, the winter was warm at the Iberian Peninsula and slightly cold at the Canary Islands (Figure 3c). Conversely, the spring and summer were characterised by the prevalence of very warm to extremely warm conditions for most of the locations with very few exceptions. Finally, the autumn was again spatially irregular: from very warm to extremely warm in the southwestern Peninsula and the Canary Islands, from normal to slightly cold towards the northeastern Peninsula, mostly warm in the rest of the Peninsula and from cold to very cold in the Balearics.

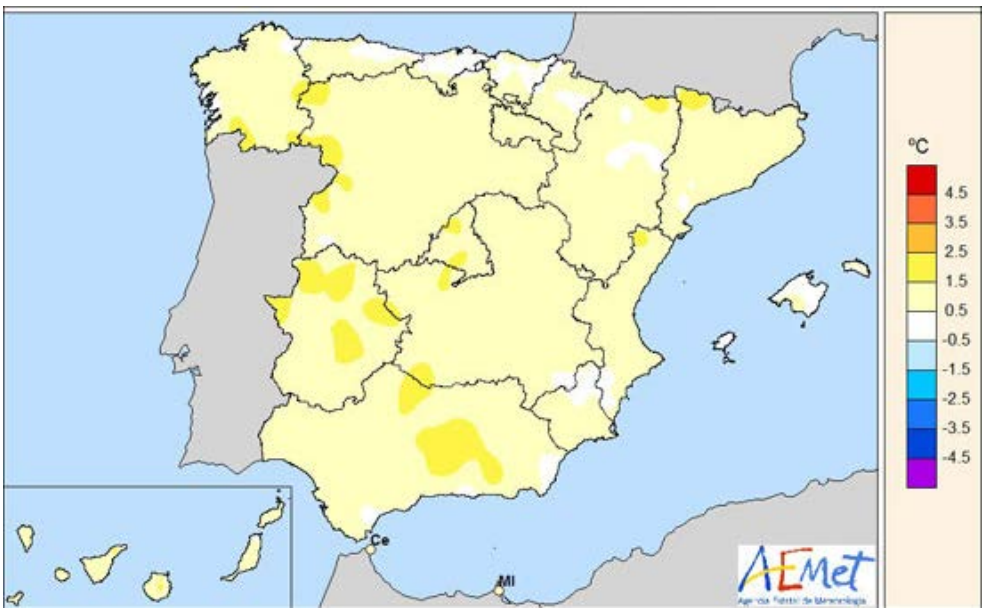

Figure 2. Annual air temperature anomalies at the Iberian Peninsula and the Canaries (AEMET, 2018).

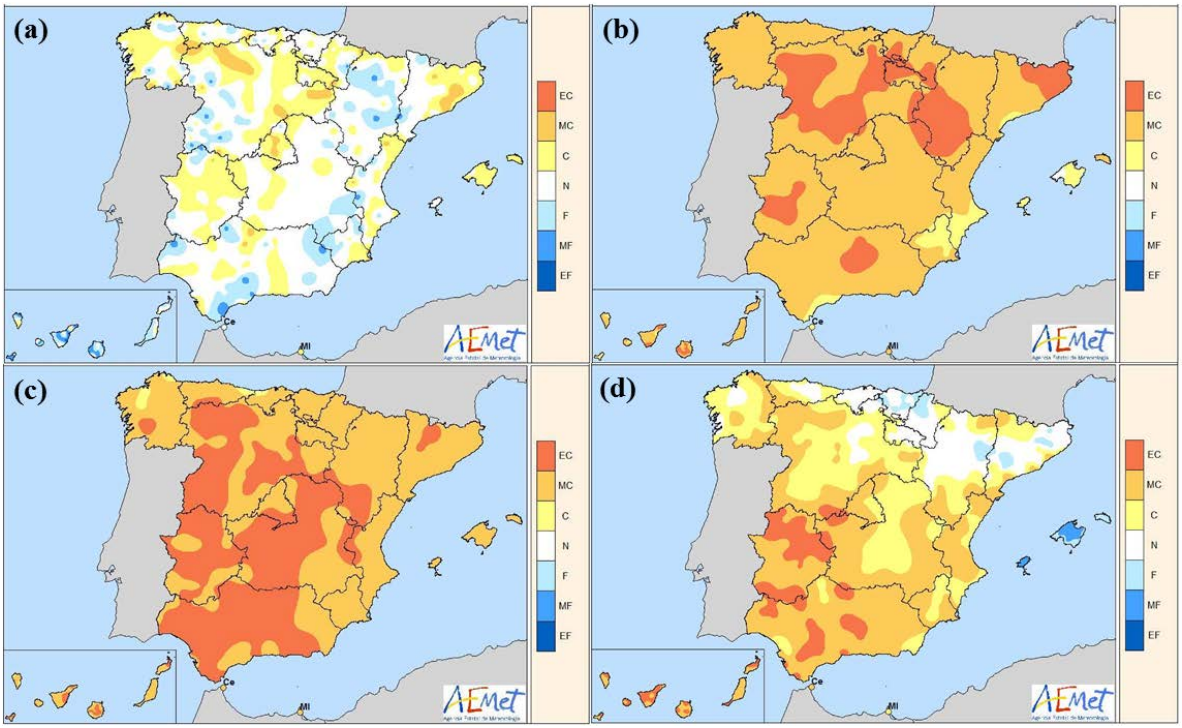

Figure 3. Seasonal weather classification according to air temperature at the Iberian Peninsula and Canaries. Note that EC is extremely warm, MC very warm, C warm, N normal, F cold, MF very cold and EF extremely cold (for additional information, see AEMET [2018]). The seasons are defined as (a) winter (December, January, February), (b) spring (March, April, May), (c) summer (June, July, August) and (d) autumn (September, October, November).

2.2 Precipitation

Globally, 2017 can be defined as very dry year concerning the precipitation regime. In particular, the year was extremely dry in extensive areas of the northwestern Peninsula and northern Extremadura, wet or very wet in the sourtheastern Peninsula and Mallorca and from dry to very dry in the rest of the Peninsula and the Canaries (Figure 4).

Concerning the seasonal cycle of precipitation in 2017, it was spatially very irregular as shown in Figure 5. On average, the winter was slightly dry although it was very wet or extremely wet in the southeastern Peninsula and Balearics whilst it was dry or very dry in extensive areas of the Peninsula and in the Canaries (Figure 5a). The spring was dry or very dry for most of the Peninsular territory and Canary and Balearic Islands with a few exceptions (Figure 5b). Conversely, the summer was wet or very wet for the whole region excluding few locations (Figure 5c). Finally, the winter can be classified as dry to extremely dry (Figure 5d).

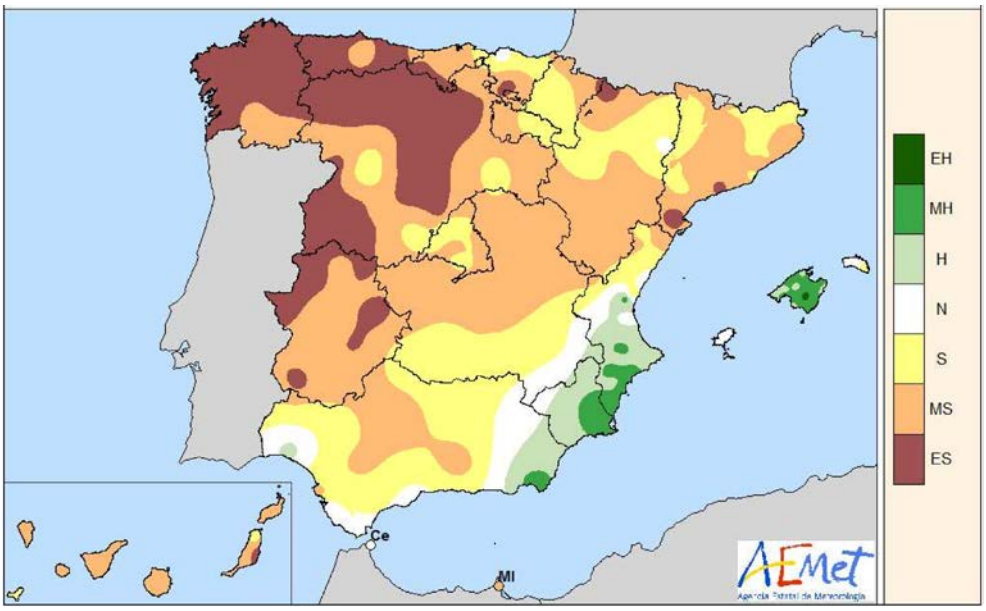

Figure 4. Annual weather classification according to precipitation at the Iberian Peninsula and the Canaries. Note that EH is extremely wet, MH very wet, H wet, N normal, S dry, MS very dry and ES extremely dry (for additional information, see AEMET [2018]).

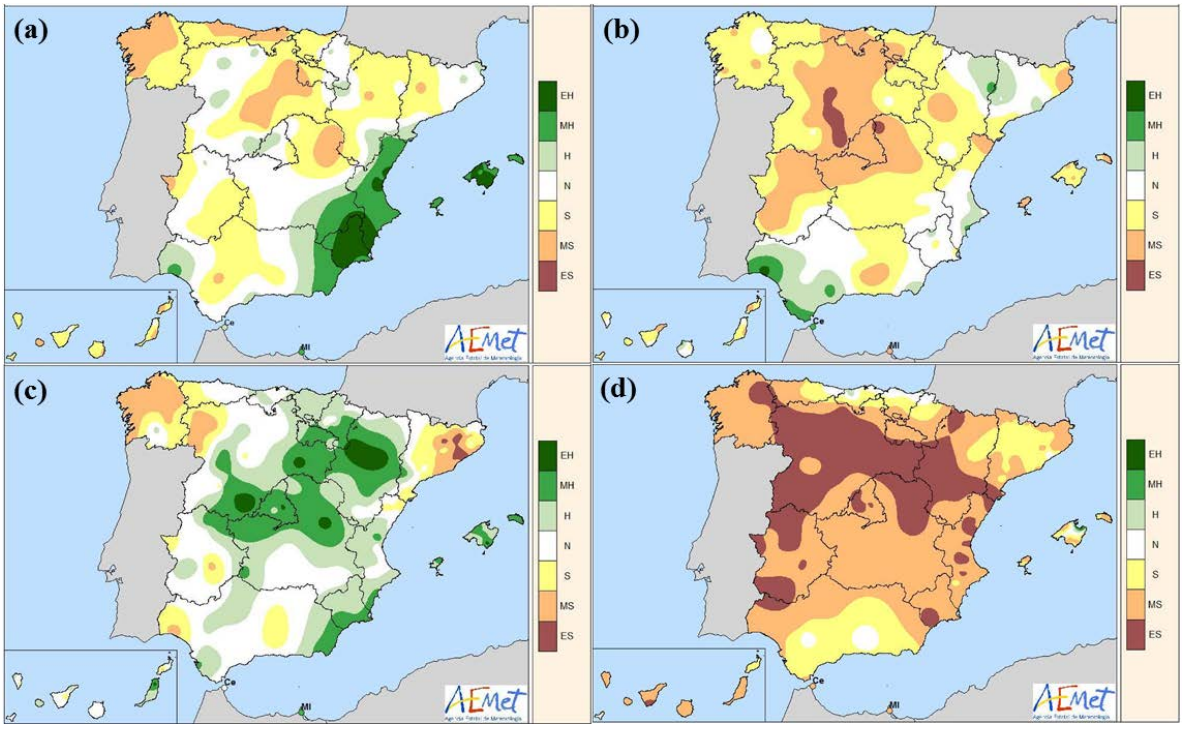

Figure 5. Seasonal weather classification according to precipitation at the Iberian Peninsula and Canaries. Note that EH is extremely wet, MH very wet, H wet, N normal, S dry, MS very dry and ES extremely dry (for additional information, see AEMET [2018]). The seasons are defined as (a) winter (December, January, February), (b) spring (March, April, May), (c) summer (June, July, August) and (d) autumn (September, October, November).

2.3 Continental runoff

The Gironde river can be considered representative of the freshwater inputs into the SE Bay of Biscay (Valencia et al., 2004). In a quarterly basis, the Gironde River flow correlates significantly with the precipitation in San Sebastián as well as with the flow of the other small Cantabrian Rivers incoming into the SE Bay of Biscay (Table 1).

Table 1. *Correlation matrix for the Gironde river flow, precipitation in San Sebastián (PP) and precipitation minus evaporation balance (PP-EV) in San Sebastián in a quarterly basis, for the period 1986-2017. NS: not significant; *P=0.05; **P=0.01 ***P=0.005.*

	FLOW WINTER	**FLOW SPRING**	**FLOW SUMMER**	**FLOW AUTUMN**
PP WINTER	0.64***			
PP-EV WINTER	0.60***			
PP SPRING		NS		
PP-EV SPRING		NS		
PP SUMMER			0.40*	
PP-EV SUMMER			0.47**	
PP AUTUMN				0.49***
PP-EV AUTUMN				0.54***

The Gironde River flow in 2017, 571 $m^3 \cdot s^{-1}$, was 284 $m^3 \cdot s^{-1}$ below the 1981-2010 average. On a monthly basis, the flow was around the average minus one standard deviation for the period 1981-2010, with the exception of February, March and December (Figure 6). In 2017, the seasonal cycle of the Gironde River flow was not consistent with that of the precipitation in San Sebastián (Figure 10).

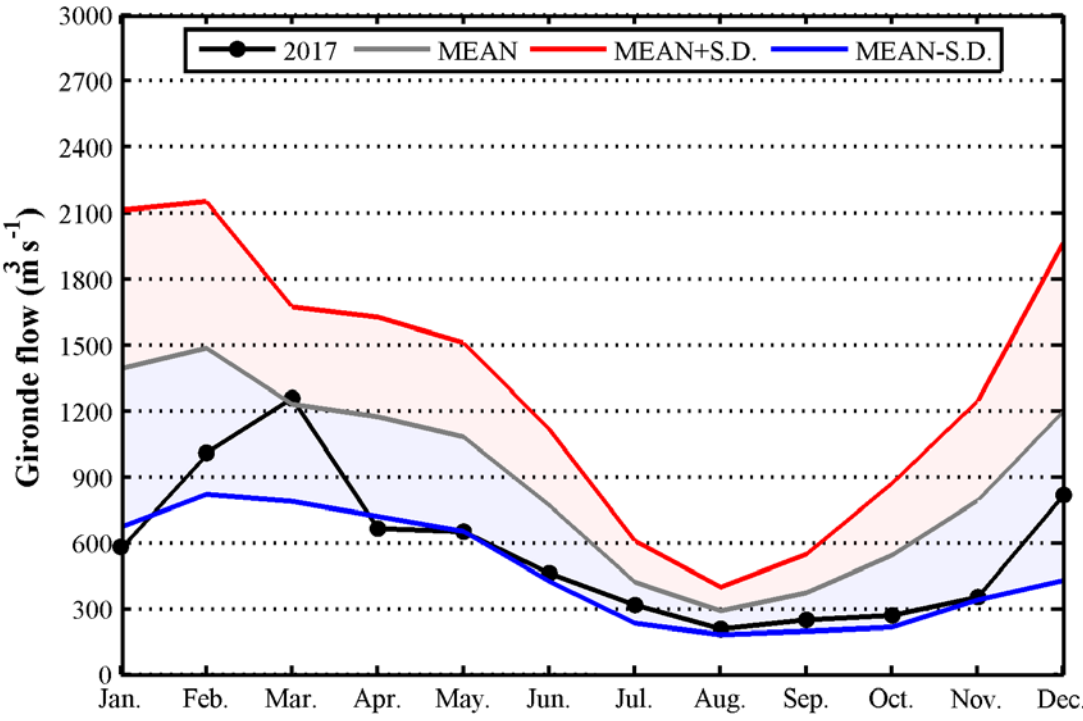

Figure 6. Monthly mean flow (m^3 s^{-1}) of the Gironde River in 2017 compared with the mean ± standard deviation (S.D.) for the period 1981-2010. Data Courtesy of the 'Bordeaux Harbour Authority'.

3 HYDROGRAPHY

3.1 Bay of Biscay and West Iberia

The Bay of Biscay, located in the eastern North Atlantic at the NE edge of the subtropical anticyclonic gyre, is almost an adjacent sea with weak anticyclonic circulation (1-2 $cm \cdot s^{-1}$). Shelf and slope currents are important in the system, characterized by coastal upwelling events in spring-summer and the dominance of a geostrophic balanced poleward flow (known as the IPC) in autumn and winter (Figure 7). Upper water properties are modulated by the combination of local air-sea forcing, the development shelf currents and the river runoff. All these processes have a strong seasonal character with regional differences:

- Seasonal warming/cooling cycle is enhanced towards the southeastern Bay of Biscay due to the continental effect.
- The effect of shelf-slope currents is enhanced at the western Iberian margin (Galician area). This happens for both the upwelling in summertime and the IPC in wintertime.
- Precipitation peaks during autumn-winter periods in the whole area. However, river runoff at the main French rivers (influencing the eastern Cantabrian Sea) is dominated by spring snowmelt at the Pyrenees, while there is no significant snow accumulation in northern Spanish mountains. Therefore, the salinity surface minimum is delayed as we move towards the east.

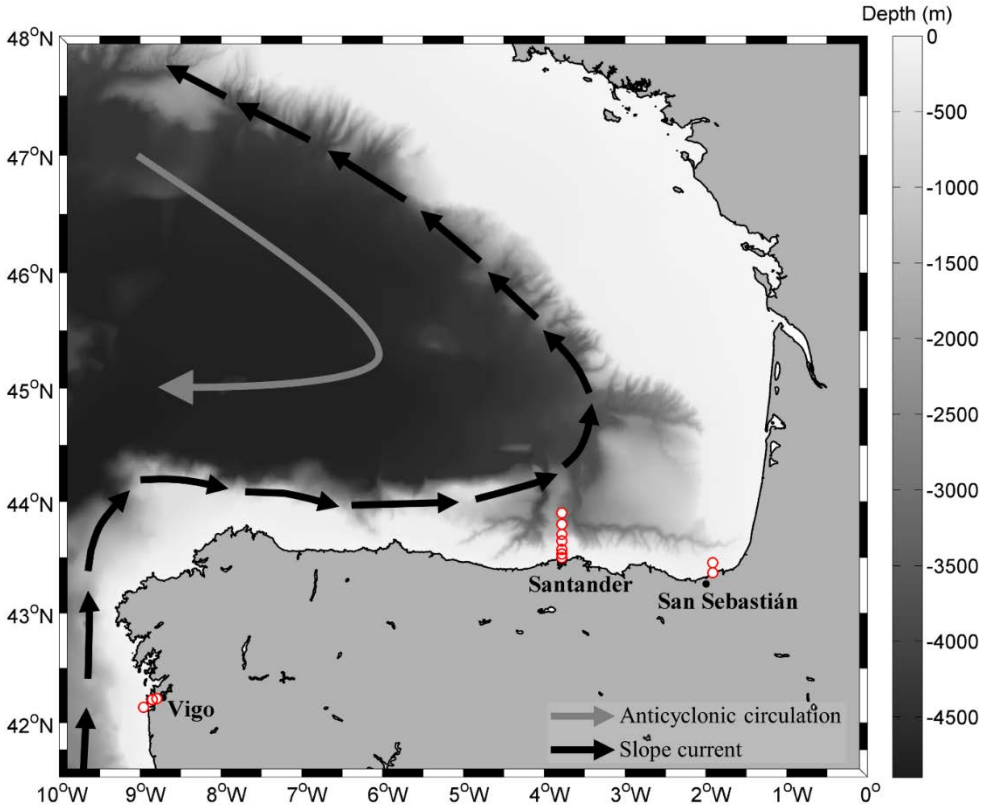

Figure 7. Spanish Standard Sections in the Northern and Western Iberian Peninsula from the Spanish Oceanographic Institution (Vigo and Santander) and from AZTI (San Sebastián) together with a schematic illustration of the circulation.

3.1.1 Upper Waters

The sea surface temperature (SST) in a coastal station in San Sebastián (from the Aquarium of the Oceanographic Society of Gipuzkoa) represents well the evolution of surface waters in 2017 at the southeastern Bay of Biscay (Figure 8). Starting from a relatively low value in January, late winter and spring were very warm, around the average plus one standard deviation for the period 1981-2010. Summer was normal in terms of SST and autumn again was warm with the exception of December. The pattern is consistent with the atmospheric conditions in San Sebastián (Figure 9). Annual mean SST in 2017 was 16.72 °C, 0.56 °C above the 1981-2010 average.

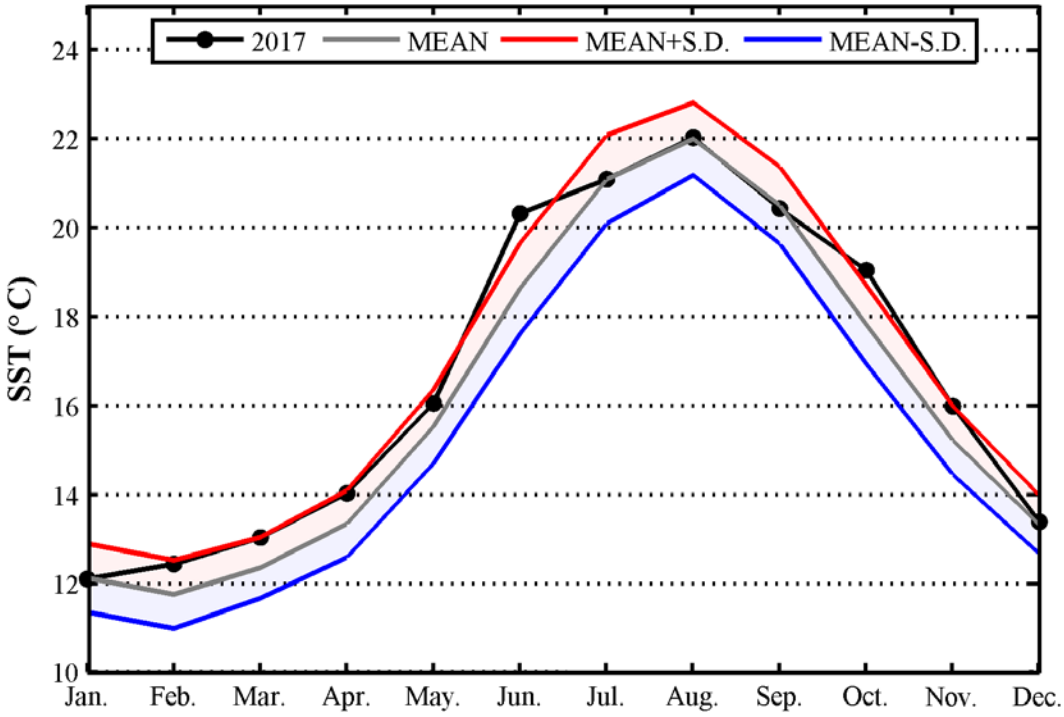

Figure 8. Monthly averaged sea surface temperature (°C) in San Sebastián in 2017 in comparison with the mean ± standard deviation for the period 1981-2010 period. Data Courtesy of the 'Sociedad Oceanográfica de Gipuzkoa'.

A detailed view of hydrographic conditions in 2017 at the southeasternmost Bay of Biscay can be summarised from TS diagram representing waters over the continental shelf (0-100 m) as shown in Figure 9. In February, the TS diagram is characterised by haline stratification. Despite the warm atmospheric conditions in late winter and early summer, the thermal stratification remains moderate until May, with more or less extended haline stratification depending on the precipitation regime. Thermal stratification prevails between June and October, in relation to the progression of the summertime warming. Due to the warm atmospheric conditions in May and June, strong thermal stratification and warmer than usual waters are observed for June. In July, the heat accumulated in the previous months is distributed through the water column due to unusual events of high turbulence at the end of June. Again, unusual high turbulence in September favours the mixing of the water column causing warmer than usual conditions in the transition between summer and autumn. In November, a reduction of the vertical gradients of temperature and salinity is observed due to vertical mixing and cooling. Finally, in December, the TS diagram is characterised by homogeneity of the water column, due to the prevalence of vertical mixing and convergence. The water column is warmer than usual, which is consistent with the prevalence of warmer than usual conditions in that period.

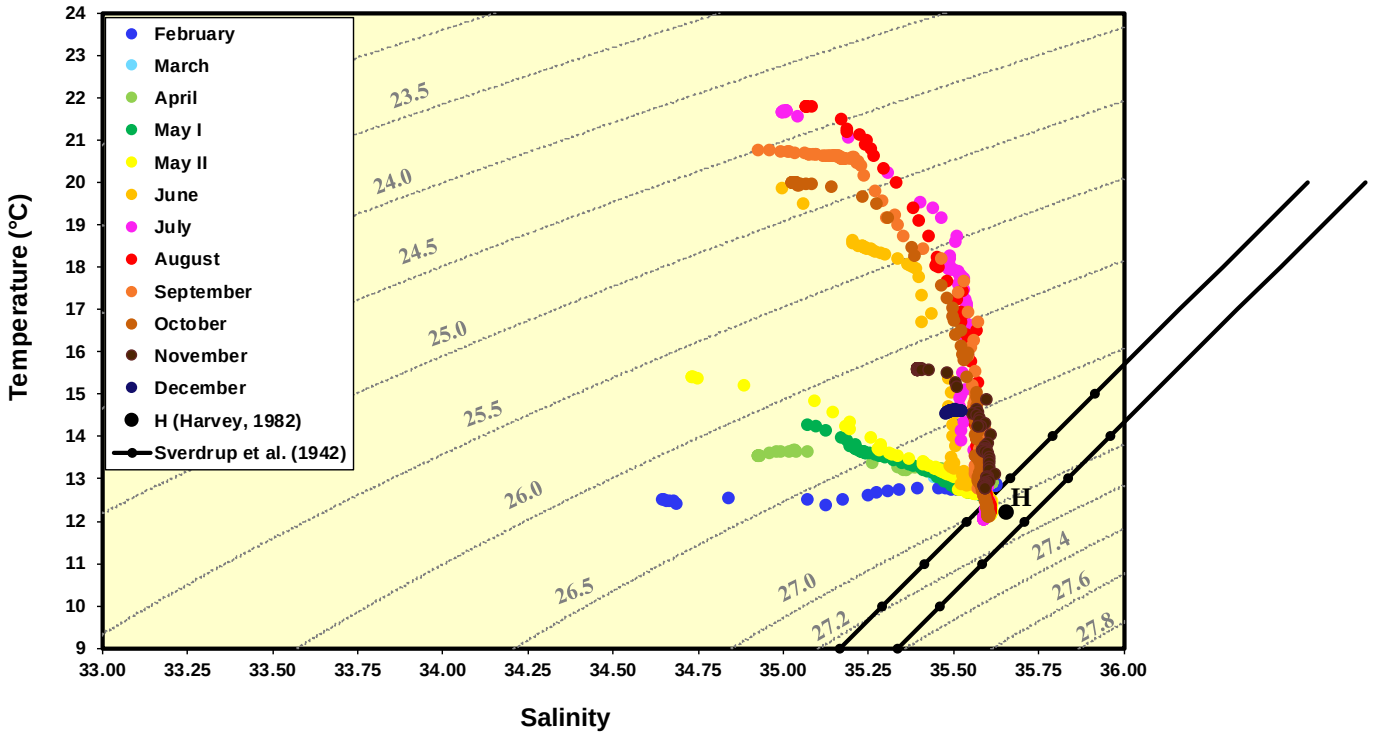

Figure 9. TS diagram of the waters (0-100 m) over the continental shelf of the SE Bay of Biscay in 2017.

Contour maps of temperature and salinity (over the shelf, 100 m depth) in the Santander section are shown in Figure 10. The main characteristic of 2017 is that the subsurface structure recovered respect to the minimum values achieved in the preceding years, being now about average. Temperature at the shelf was high due to atmospheric warm conditions, weak upwelling and lack of a strong signature of the Iberian Poleward Current. The overall combination of these features results, for the upper-ocean influenced by the mixed layer development (0-300dbar), in a warm and slightly fresh year (Figure 10 and 11).

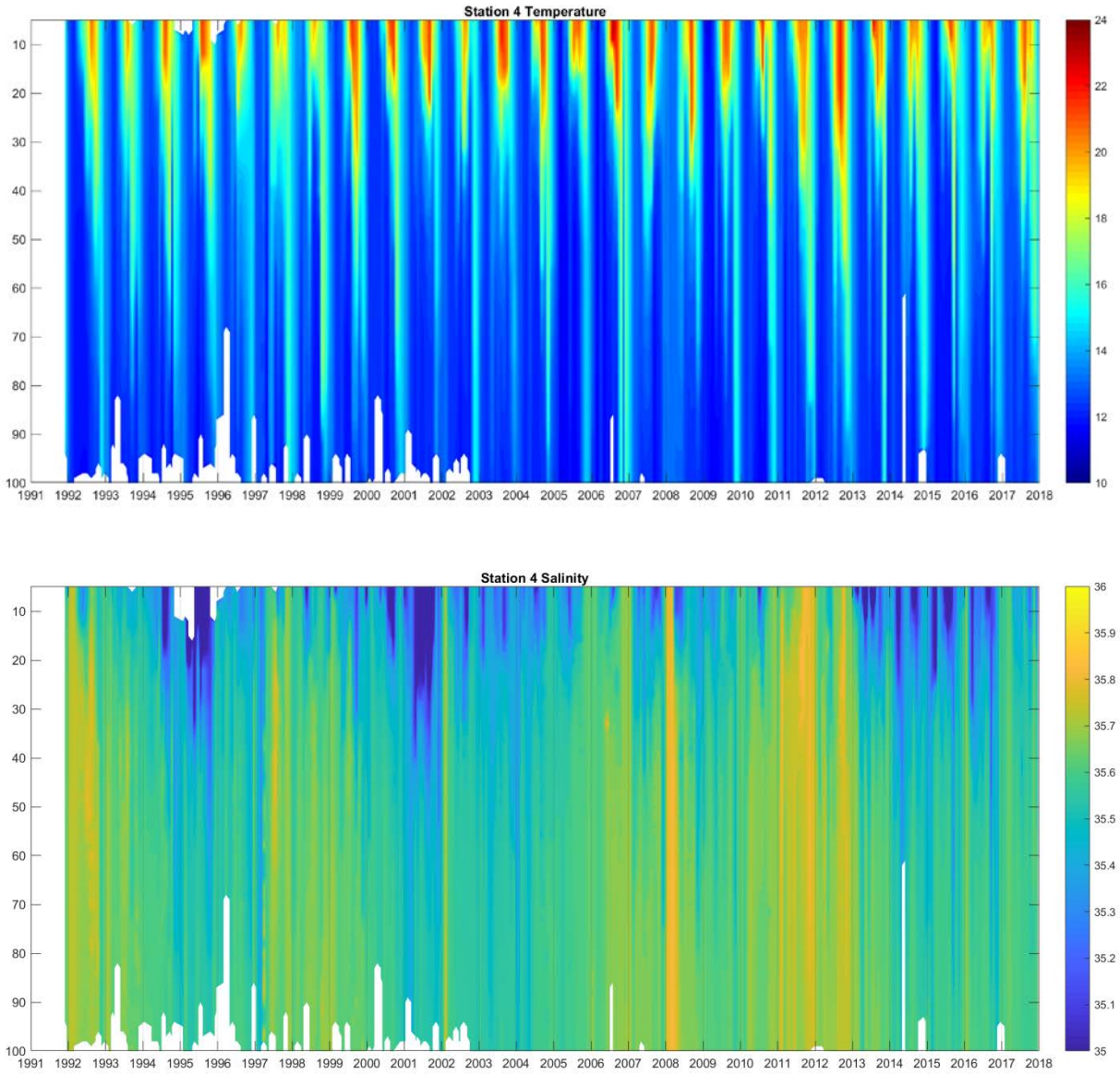

Figure 10. *Timeseries of temperature (upper) and salinity (lower) at the shelf at Santander (43º35'N,3º47'W).*

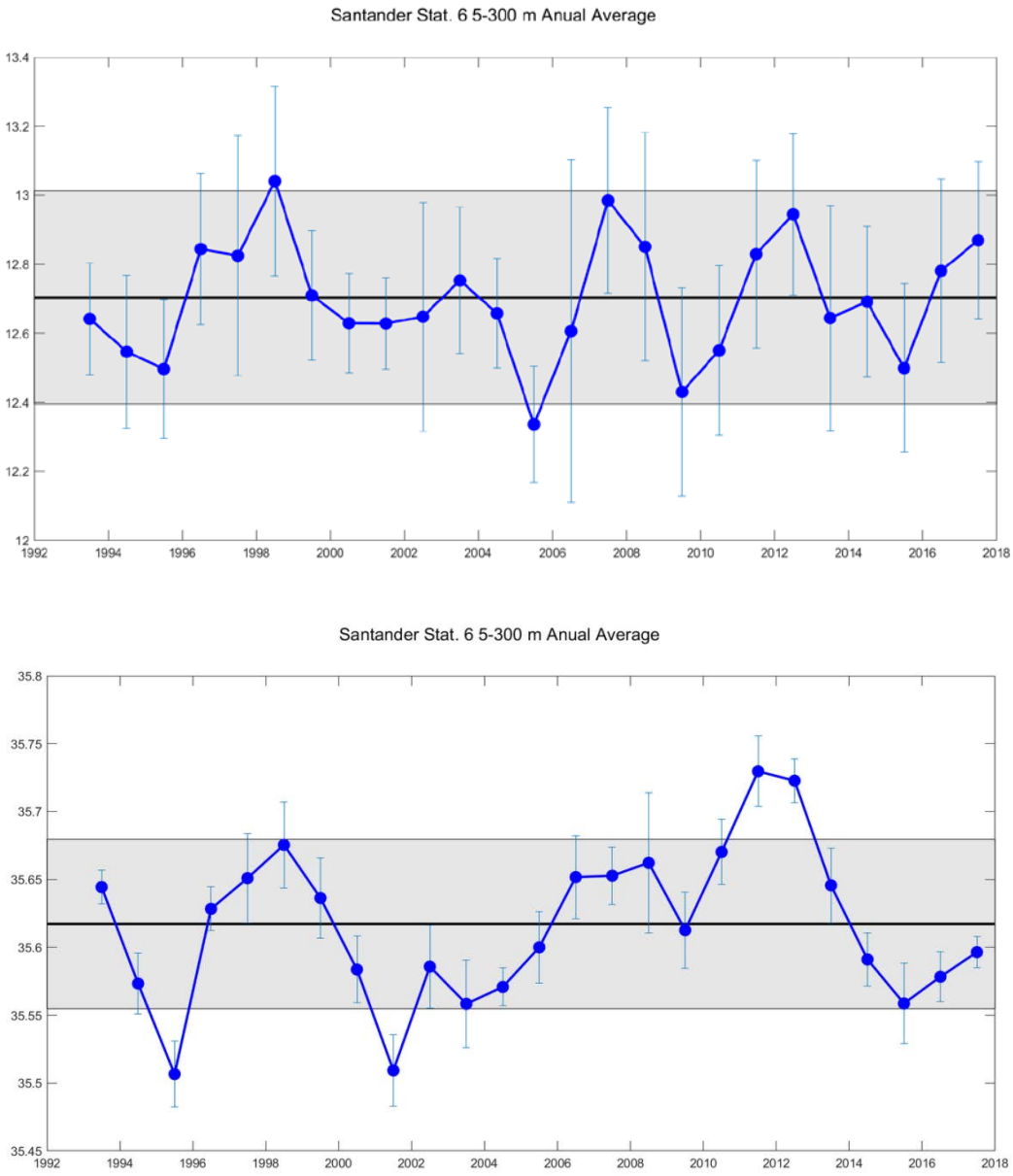

Figure 11. *Temperature (up.) and salinity (low) averages for the upper 300 m at the slope at Santander* (43º42'N,3º47'W).

Contours of temperature and salinity over the shelf-break (600 m depth) in the Santander section are presented in Figure 12. Modal waters stabilized after two years of progressive freshening progressively.

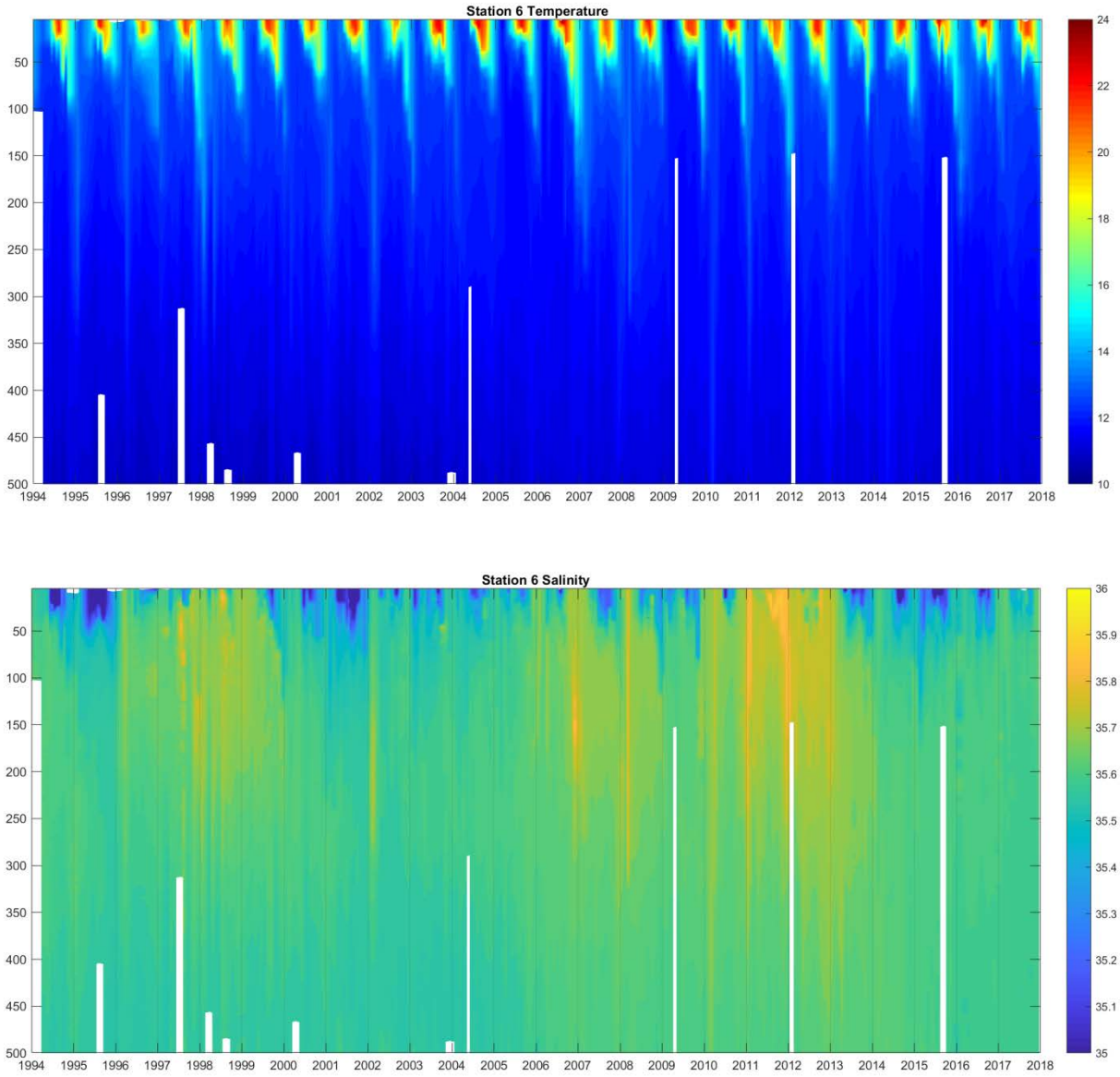

Figure 12. *Timeseries of temperature (up.) and salinity (low) at the slope at Santander (43º42'N,3º47'W).*

3.1.2 Intermediate and Deep Waters

Figures 13-15 show the TS diagram and hydrographic series at isobaric levels from 200 to 1000 m depth over the slope in Santander (St 7). Overall warming trends are evident at most layers, corresponding to the East North Atlantic Central Water (ENACW) (200-600) and upper Mediterranean Water (600-1000). Salinity shows variability along the series with overall increase.

The water masses evolution is strongly influenced by a strong shift in salinity at lower ENACW (~400 m) in 2005 after the occurrence of very strong winter mixing. After years of high salinity stable conditions, 2014 showed freshening and cooling for the first time in about a decade. In 2015 salinity

values fell continuously along the year being by the end of 2015 about 0.05 units lower than in mid 2014. During 2016 and 2017 hydrographical conditions kept stable. Deeper at the level of the MW the water masses continues pretty stable since mid-00`s getting progressively fresher at its core since the maximum reached around 2007-2009.

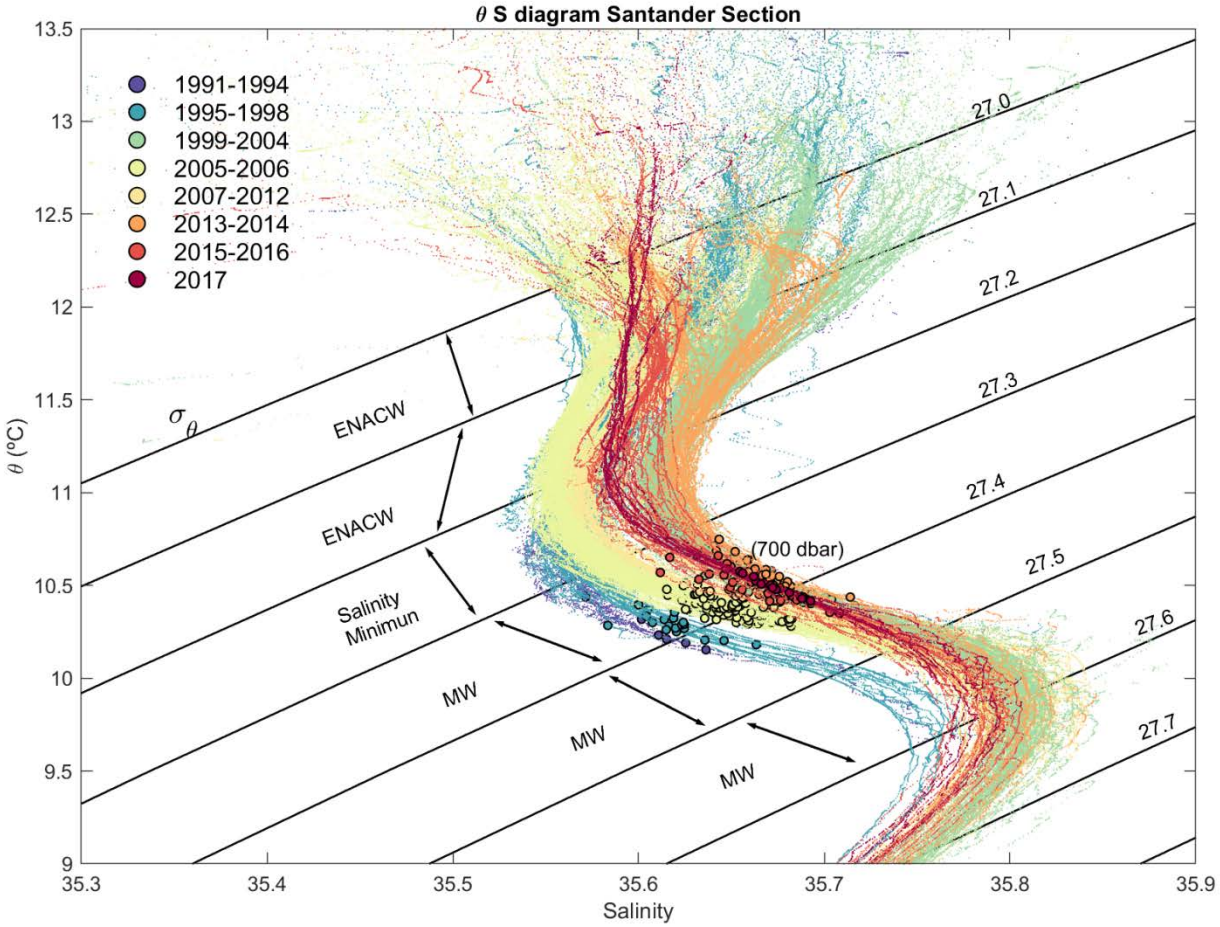

Figure 13. *TS diagram of water mass properties at Santander station 7(43º 48'N, 3º 47'W) (outer slope).*

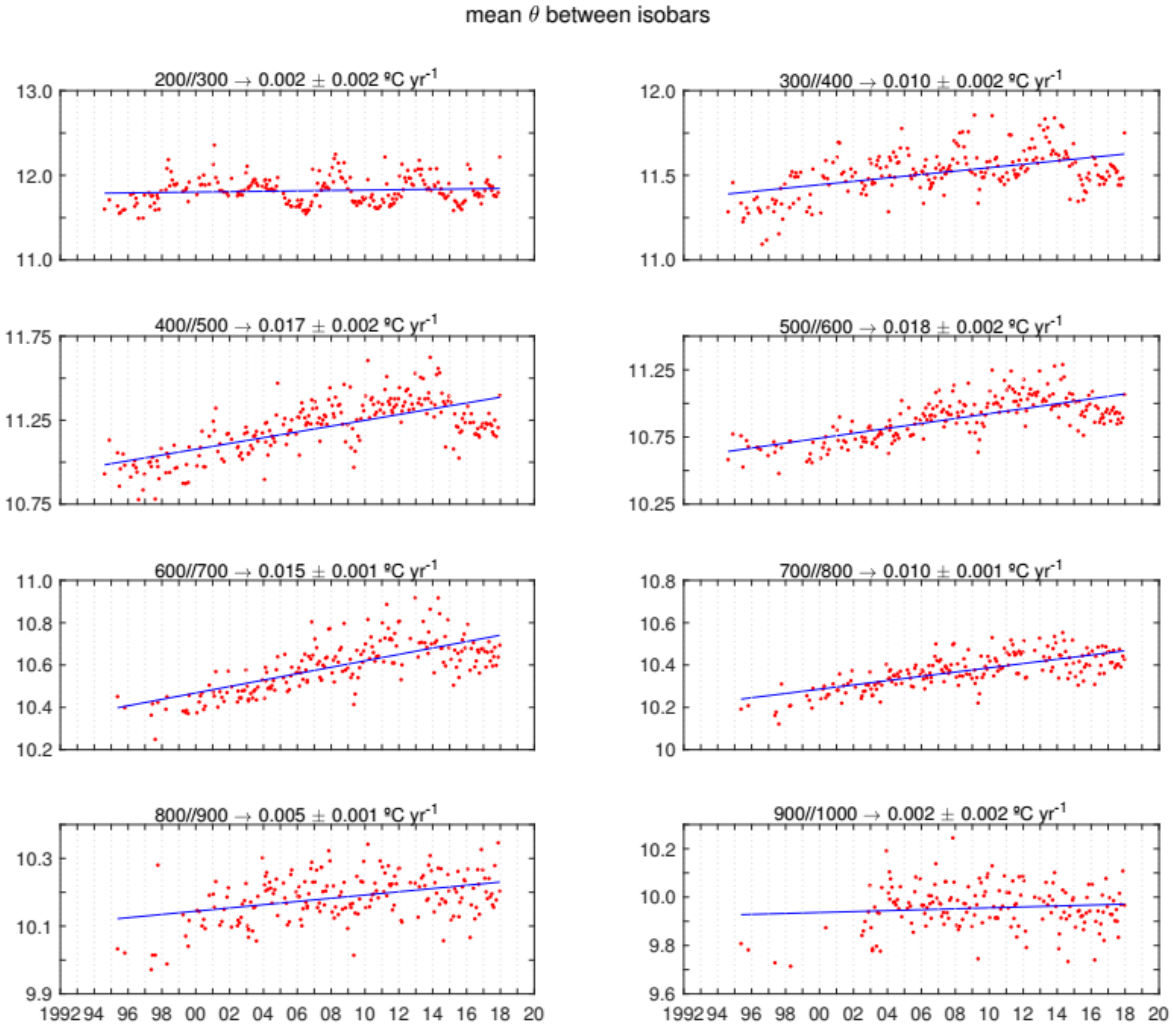

Figure 14. *ENACW and MW potential temperature at Santander station 7(43º 48'N, 3º 47'W) (outer slope).*

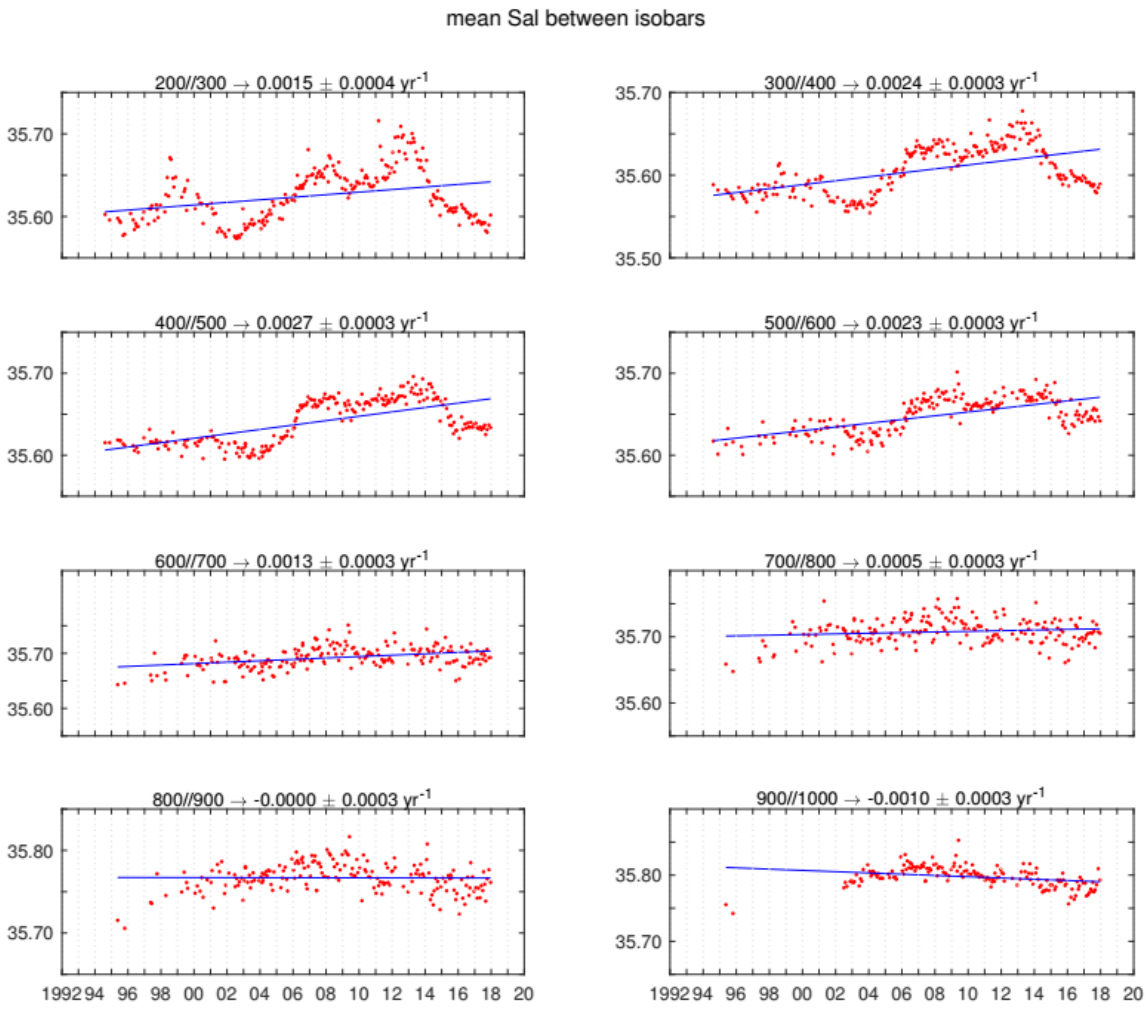

Figure 15. *ENACW and MW salinity at Santander station 7(43º 48'N, 3º 47'W) (outer slope).*

A Deep Sections program is being run by Spanish Institute of Oceanography since 2003, providing full-depth (>5500 m) hydrography and biogeochemistry at Western Iberia and Biscay. Cruises have been carried out semiannually for the period 2003-2010 and annually after that. The Finisterre section, about ~400 km, reaches the center of the Iberian Abyssal Plain. The section has been occupied 21 times so far.

Figure 16 shows the Finisterre section, Figure 17 the hydrographic anomaly averaged across the section and Figure 18 shows the overall trends observed. Roughly, Central Waters (200-800) have behaved as in Biscay. Lower thermocline waters (MW and LSW) subjected to strong variability linked to large-scale atmospheric patterns and the main highlight is the passage of a cold and fresh anomaly in late 00`s. No relevant changes have been observed in deep waters (2000-5500 m). 2017 continues the upwards swing of temperature and salinity observed in these intermediate waters in 2014 concurrent with the decrease at Eastern North Atlantic Central Waters level.

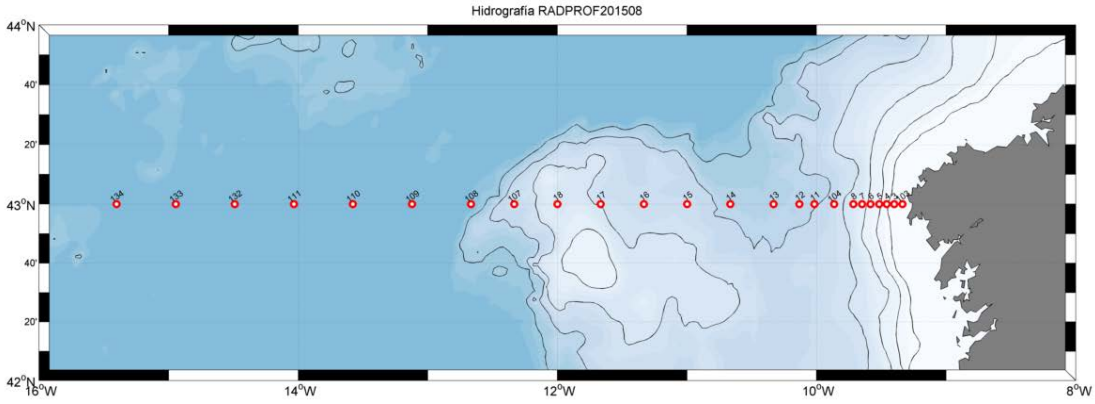

Figure 16. Finisterre Section from the 'Instituto Español de Oceanografía' in NW Iberia.

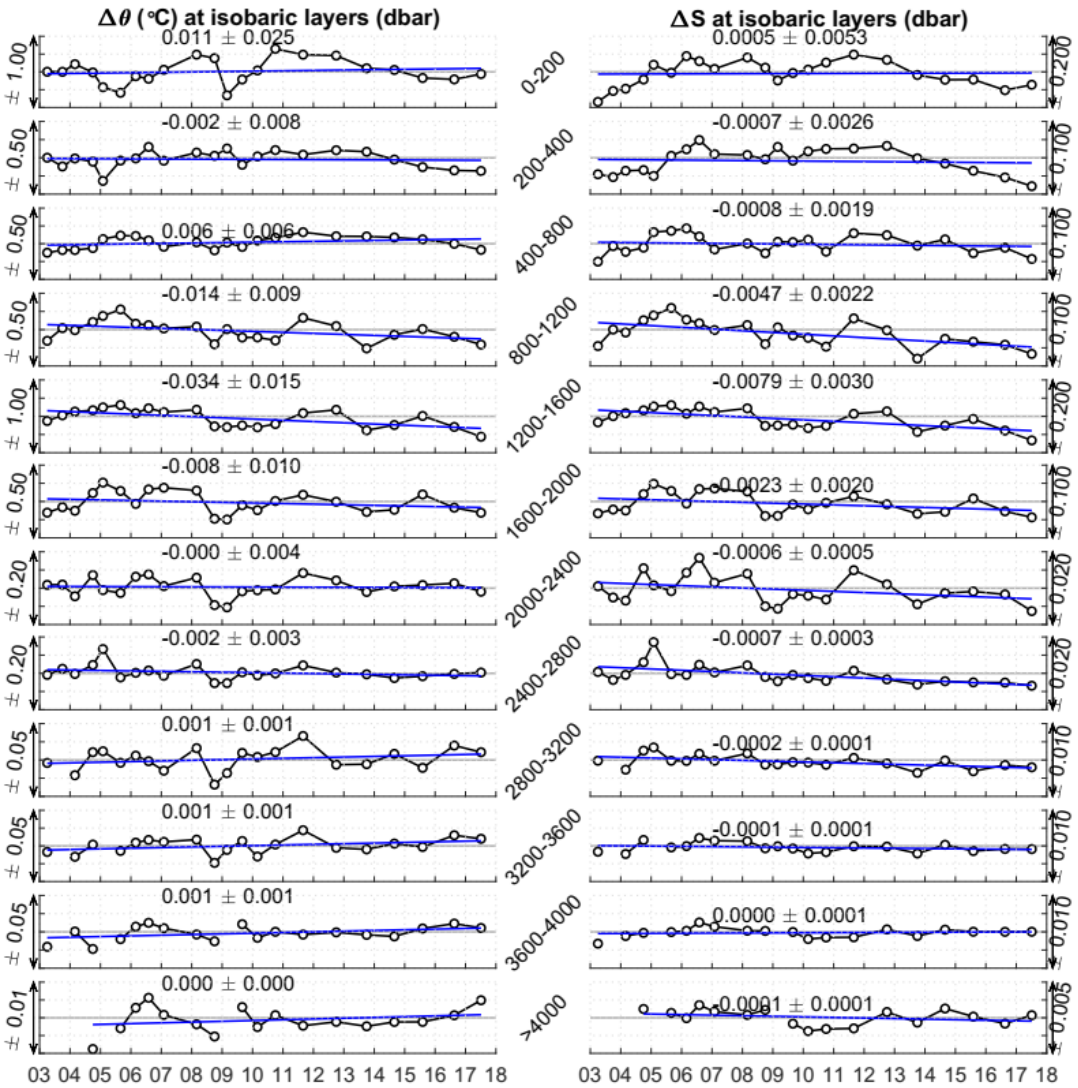

Figure 17. Timeseries of anomalies in hydrographic properties in the Finisterre section. Seasonal cycle at deep waters is removed.

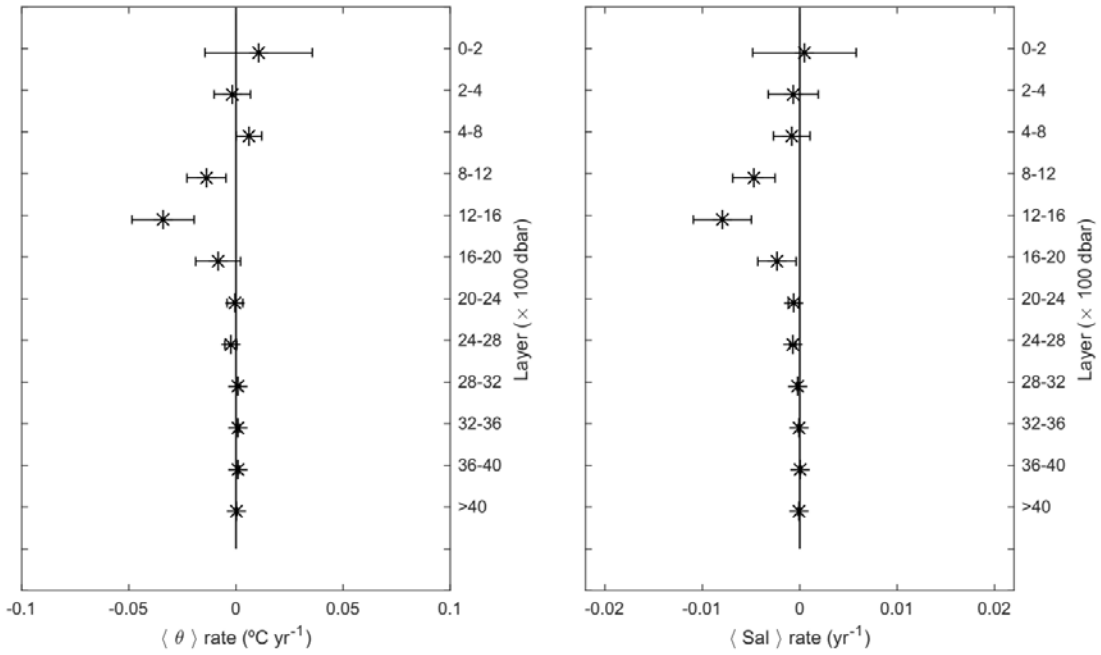

Figure 18. Overall linear trends derived from timeseries shown in Fig.17

4 REFERENCES

AEMET, 2018. Resumen anual climatológico 2017. Retrieved from http://www.aemet.es/documentos/es/serviciosclimaticos/vigilancia_clima/resumenes_climat/anuales/res_anual_clim_2017.pdf.

Prieto, E., C. Gonzalez-Pola, A. Lavin, R. F. Sanchez, and M. Ruiz-Villarreal (2013), Seasonality of intermediate waters hydrography west of the Iberian Peninsula from an 8 yr semiannual time series of an oceanographic section, Ocean Sci., 9(2), 411-429.

Valdés, L., A. Lavín, M. L. Fernández de Puelles, M. Varela, R. Anadon, A. Miranda, J. Camiñas, and J. Más (2002), Spanish Ocean Observation System. IEO Core Project: Studies on time series of oceanographic data, in Operational Oceanography: Implementation at the European and Regional Scales, edited by N. C. Flemming and N. Vallerga, pp. 99-105, Elsevier Science

Valencia, V., Franco, J., Borja, Á., and Fontán, A., 2004. Hydrography of the southeastern Bay of Biscay. In: Borja, A. and Collins, M. (Eds.), Oceanography and Marine Environment of the Basque Country. Elsevier Oceanography Series nº 70, Elsevier, Amsterdam, pp. 159-194.

Working Document **ICES 2018**
Working Group on Oceanographic Hydrography
15 May 2018

Gulf of Cádiz Waters

Ricardo F. Sánchez Leal
rleal@ieo.es,
IEO -Cádiz. Muelle de Levante s/n. Puerto Pesquero
E-11006 Cádiz, Spain

Main summary

The surface temperatures of the Gulf of Cadiz Atlantic water were in 2017 slightly above the 1996-2018 means. The ENACW was anomalously warm and saline, whereas the MOW was colder and less saline than the 2009-2017 average. The vertical distribution of long-term (2009-2018) temperature and salinity trends suggest strong warming of the surface layer, extended freshening and cooling of the underlying ENACW, warming and salinification of the upper Mediterranean waters and freshening of the deeper MOW.

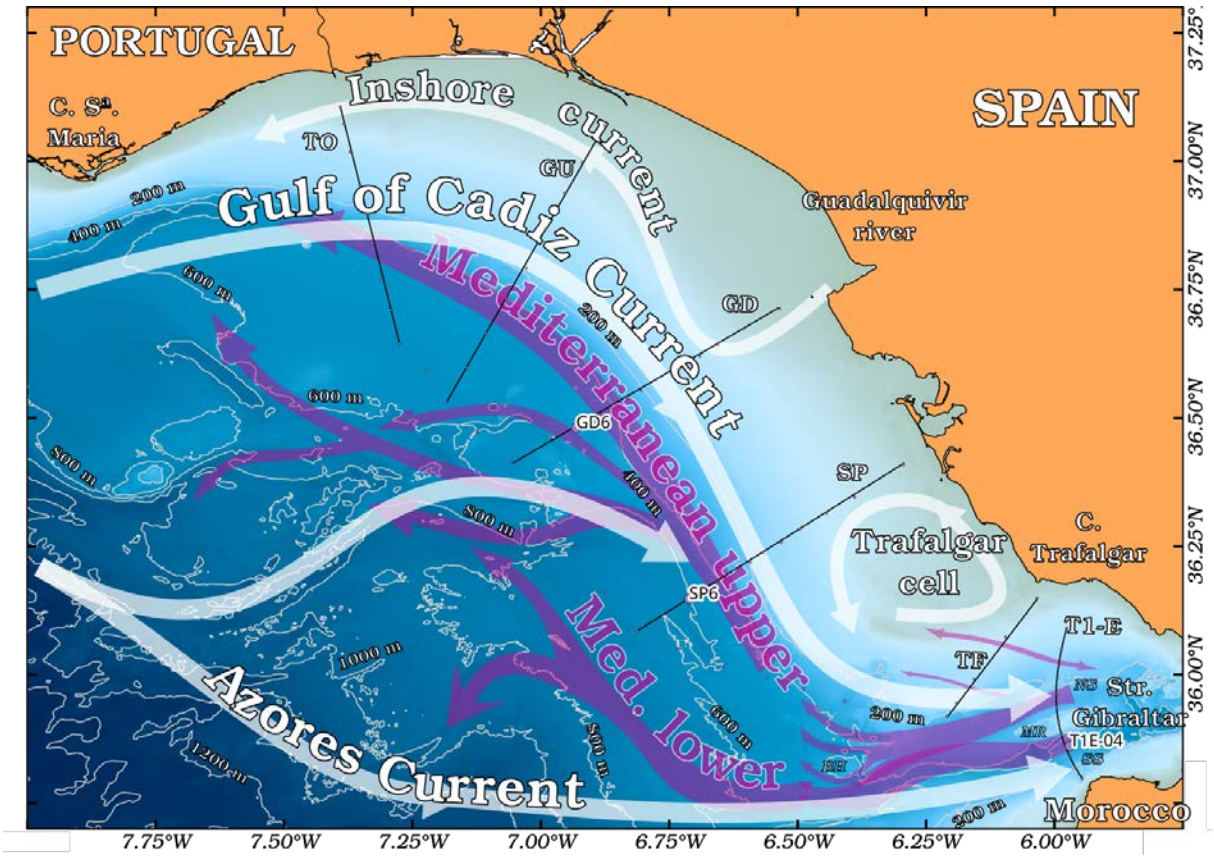

Figure 1. *Sketch of the main currents in the Gulf of Cádiz. White arrows depict the surface circulation. This is composed by (i) the baroclinic Gulf of Cádiz Current (Peliz et al., 2007), that advects relatively fresh and cool waters from the Portuguese Coastal Transition Zone to feed the Atlantic Inflow (AI) in the Med. basin; (ii) the meridional branch of the Azores Current, a rather barotropic frow that brings warmer more saline atlantic waters to supplement the AI into the Med; (iii) the inshore current system*

linked with the Guadalquivir River plume; and (iv) the Trafalgar cyclonic cell, an upwelling hotspot generated by tidal stirring over the Trafalgar Banks. Cyan arrows depict the subsurface circulation. This is governed by the Mediterranean Overflow, a branched, warm, saline and dense gravity current attached to the seafloor that follows the intricate bottom topography. We also include the STOCA project standard sections (black lines) and fixed oceanographic station under the responsibility of the Spanish Institute of Oceanography, Cádiz whose data are presented in this report (GD6 and SP6). Puertos del Estado provides data form a weather buoy located at GD6.

Introduction

The Gulf of Cadiz is located off the Southwestern Iberian Peninsula, where the Atlantic Ocean and the Mediterranean Sea are connected through the Strait of Gibraltar. There, the water exchange is governed by a two-layered inverse estuarine circulation with Mediterranean Water (MW) flowing into the Gulf of Cadiz under Atlantic Water flowing into the Mediterranean Sea (e.g. Price et al., 1993). The traditional view of the surface circulation in the Gulf of Cadiz poses a clockwise flow on the slope as part of a larger-scale anticyclonic gyre and a counter-current on the inner shelf (Folkard et al., 1997, Criado-Aldeanueva et al., 2006, Teles-Machado et al., 2007). The clockwise flow conveys both Eastern North Atlantic Central Waters (ENACW) from the Portuguese Coastal Transition Zone (the Gulf of Cadiz Current, GCC) and the Azores Current to form the Atlantic Inflow (AI) towards the Mediterranean Sea (Sánchez and Relvas, 2003; Sanchez-Leal et al., 2017). The inshore counter-current transports waters westward during most of the year (Relvas and Barton, 2002, Sánchez et al., 2006). A number of mechanisms have been proposed as responsible for this pattern. Seasonal displacements of the Azores High have been related to the local upwelling-favorable winds (Fiúza et al., 1982) and its convergence to the Azores Current (Sánchez and Relvas, 2003). Besides local wind forcing (Teles-Machado et al., 2007), alongshore pressure gradients (Relvas and Barton, 2002) generated by the spatially heterogeneous wind field (Sánchez et al., 2006) and the buoyancy flux associated with continental runoff (García-Lafuente et al., 2006) seem to be the trigger for the onset of the inshore coastal counter-current.

From the geomorphological point of view, the Gulf is characterized by a wide continental shelf. The continental slope presents a complex seafloor with channels, ridges, canyons and even mud volcanoes down to the abyssal plains (García et al., 2009). Whereas the lower slope and abyssal plain are dominated by down-slope processes that are partly detached from the upper slope region, the middle slope and its complex contourite depositional system are dominated by along-slope processes driven by the Mediterranean Outflow (MO)(Hernández- Molina et al., 2006).

After plunging past the Spartel Sill (360 m deep), the MO turns into an undercurrent that flows under the ENACW along the main channel axis of the Strait of Gibraltar with a salinity of 38.3 and temperature of 13.3 ºC (Sanchez-Leal et al., 2017). The salinity wedge, initially about 10 km wide and 150 m thick, flows at speeds in excess of 1.5 m s^{-1} as a dense overflow. The MO water (MOW) experiences a gradual decrease in temperature, salinity and velocity due to mixing and entrainment with the ENACW during the first 140 km of its pathway (Baringer and Price, 1997, Sanchez-Leal et al., 2017). After, it is seen to follow the seafloor morphology as a multi-branched bottom-trapped gravity current (Madelain, 1970; Sanchez-Leal et al., 2017) before reaching a neutral equilibrium depth past Cape St. Vincent.

Air and sea-surface temperatures.

Fig. 2 shows the 2000-2017 time-series of daily SST and air temperatures at the Cadiz Buoy of Puertos del Estado. This buoy is geographically located at STOCA GD6 station. Both air and sea-surface temperatures show a statistically significant warming trend of about 0.31 ºC/decade over the last two decades. The smoothed time-series suggest the existence of interannual variability, with major departures in 2009, when temperatures were anomalously colder than average, and 2011, when these were anomalously warm. Fig 2 (bottom panels) show the detrended time series. In 2016-2017 temperatures were higher than the average. However, a relative maximum was observed by the end of 2016. Temperatures exhibited a slight decrease over 2017. 2018 seems to be the first year of a cooler-than-average phase.

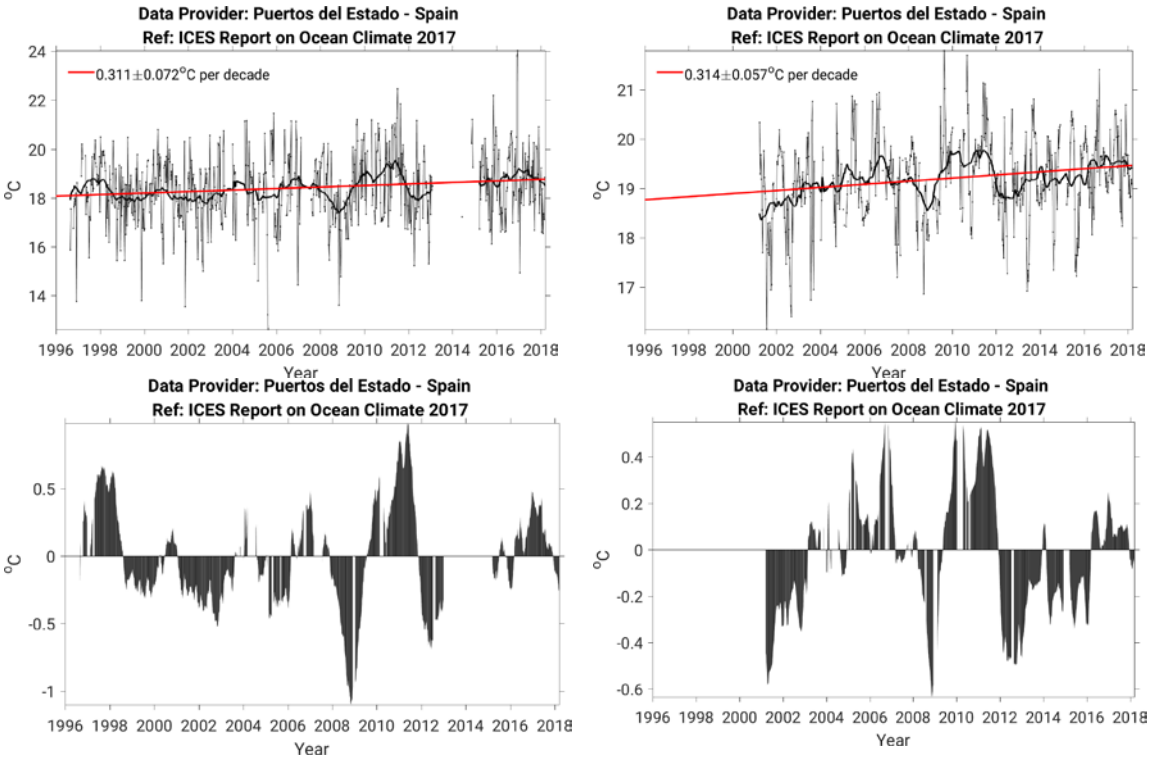

Figure 2. *Temperature time-series at the Cadiz weather buoy of Puertos del Estado, a SeaWatch ODAS platform that has been measuring the Gulf of Cadiz ocean waters since 1997 (www.puertos.es). (Top-Left): Daily means of air temperature (black thin line). The black bold line represents a 12-month running mean filter. The linear trend (0.31 ºC/decade, red line) is statistically significant,(p-value<0.01) (Top-Right): Idem but for the sea-surface temperatures. The linear trend (0.31 ºC/decade, red line) is statistically significant (p-value<0.01). (Bottom-Left): Time series of detrended air temperature anomalies. (Bottom-Right): Idem but for sea-surface temperatures.*

Fig. 3 shows the comparison of daily SST and air temperatures at the Cadiz Buoy and the seasonal daily means. The seasonal cycle is clear with highest temperatures around August (air) and September (sea-surface) and lowest in February (air) and March (sea-surface). The sea-surface temperatures illustrate how 2017 was a year with strong contrasting seasonal variability. Hence, relatively warm spring, cool summer and warm fall featured the air but particularly the sea-surface temperatures.

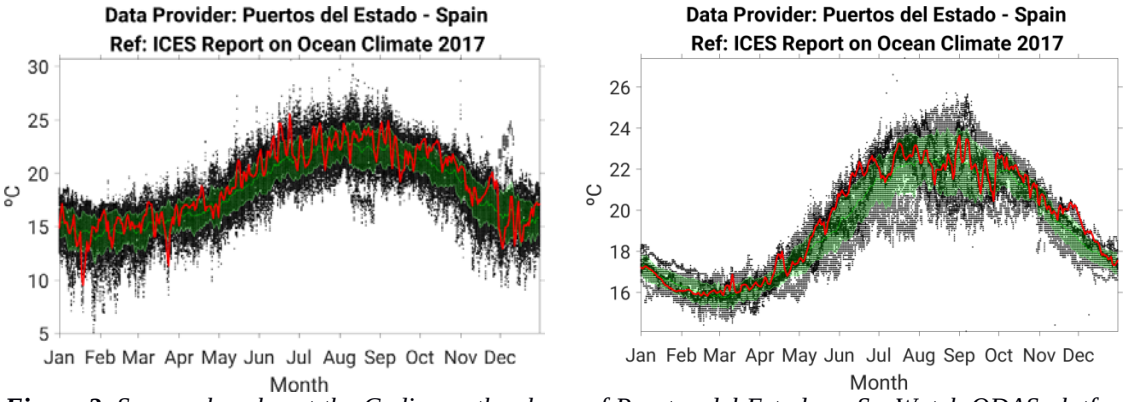

Figure 3. *Seasonal cycles at the Cadiz weather buoy of Puertos del Estado, a SeaWatch ODAS platform that has been measuring the Gulf of Cadiz ocean waters since 1997 (www.puertos.es). (Left): Daily means of air temperature (black dots). The green line and shades depict the climatological mean and standard deviation. The red line are the daily means for 2017. (Right):Idem but for the sea-surface temperatures.*

Water column: mean fields and temporal variability

The SP standard section provides an illustrative example of the stratification of the water column and the meridional alignment of water masses and currents in the eastern Gulf of Cádiz (Fig. 4). Besides the upper, mixed layer, two water masses prevail.

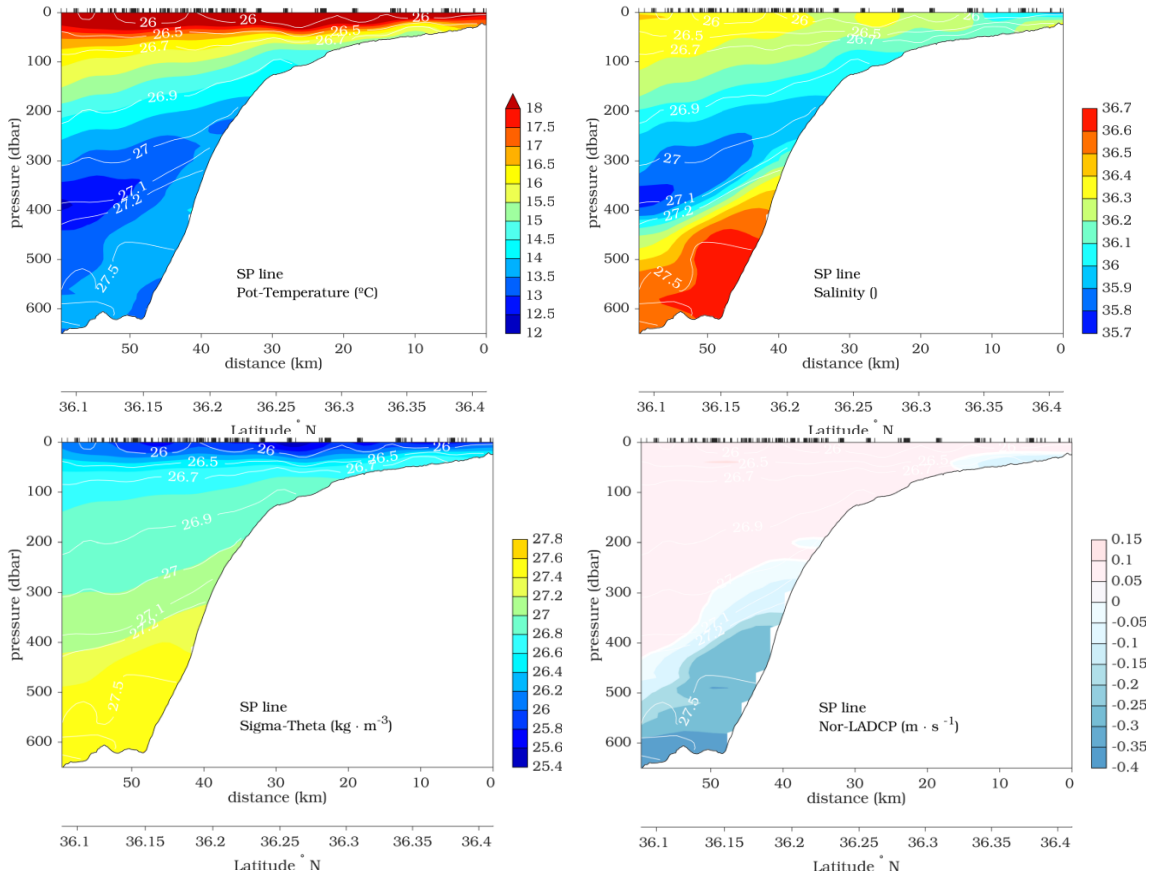

Figure 4. *SP standard section of the STOCA program. Mean (2009-2018) fields along the transect. (Top-left): Potential temperature (ºC); (Top-Right): Salinity; (Bottom-Left): Potential density anomaly (kg m^{-3}); (Bottom-Right): Lowered-ADCP velocity across the section (m s^{-1}). Selected potential density contours are plotted in every panel. Colorbars indicate magnitude (units are indicated in the insets). SP6 lays at*

about 50 km off the coast.

The water column is formed by the superposition of three well-defined water masses. The surface mixed layer (hereinafter, SML) occupies the top tens of meters. It is formed by waters above the seasonal thermocline. Below the SML, salinity (< 35.8) and temperature (< 13 ºC) minima define the base of the ENACW. It appears as a near-straight line in the T-S diagrams (fig. 6) that extend down to 375 m approximately where densities range between 27 and 27.1 kgm^{-3}. However, its vertical extent depends on the distance from the coast. The ENACW core lays lower (below 300 m) offshore than onshore (about 250 m).

Below the ENACW salinity minimum, salinity, temperature and density values rise sharply. Near the bottom, high salinities (> 36.2) flood practically all grounds laying deeper than 300 m. Temperatures are also higher than at the ENACW core (between 13.5-14 ºC) and densities in excess of 27.2 kgm^{-3} are common. Pushed by the density-driven Mediterranean Overflow, these saline water types are a result of mixing between through the eastern Gulf of Cadiz MW and ENACW (Sanchez-Leal et al., 2017). Although its core properties vary along the MOW pathway, these waters are commonly known as Mediterranean Overflow Waters (MOW) (Bellanco and Sanchez-Leal, 2016). Salinity contours illustrate the vertical extent. This mass spreads horizontally through the lower slope (Sanchez-Leal et al., 2017). Like the layers above, the boundary between ENACW-MOW deepens offshore and shoals as it approaches the shelf break.

Apart from the SML, strongly influenced by fluctuations of meteorological origin (Bellanco and Sanchez-Leal, 2016), observations suggest seasonal and longer-term variability patterns at both ENACW and MOW levels (Fig. 5). Using the 0.125 Kg/m^{-3} density criterion (density difference between the near-surface and the base of the SML) we estimate that the SML exhibits the expected seasonal cycle, with winter (March) maxima and summer (September) minima(about 200 m in SP6, fig. 5, Top-Left panel). Colder, less saline and denser waters occupy the deeper, winter SML. Conversely, warmer, saltier and lighter waters form the highly stratified and shallower, summer SML that features a sharp thermo- and pycnocline. The onset of the erosion of the seasonal thermocline occurs by the end of September.

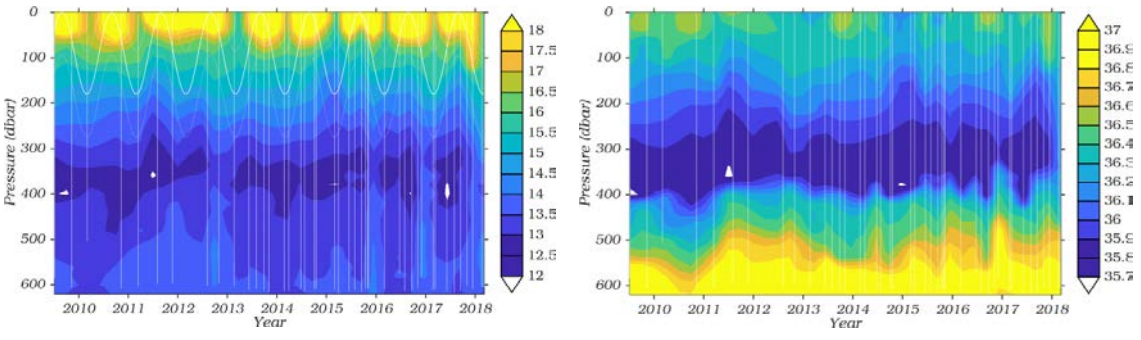

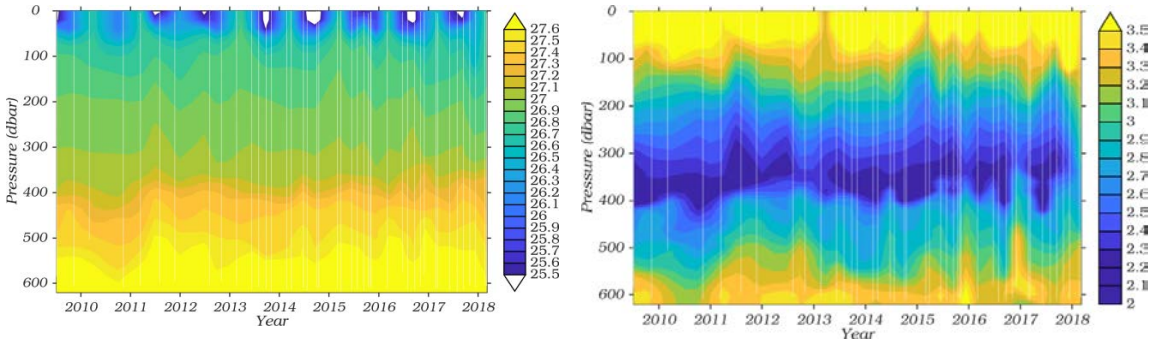

Figure 5. *2009-2018 evolution of water mass properties at SP6 (STOCA program). (Top-left): Potential temperature (ºC); (Top-Right): Salinity; (Bottom-Left): Potential density anomaly (kg m^{-3}); (Bottom-Right): Spiciness. Observation points are indicated for reference. The*

These seasonal oscillations also emerge deeper in the water column. One way to look at this variability is by comparing the mean T-S curves at SP6 (Fig. 6). Upper waters (down to 50 m depth) were colder (about 0.3 ºC colder) and fresher (0.04) than the 2009-2017 mean. On the contrary, waters below 50 m were warmer than the average (between 0.1-0.3 ºC). In fact, the ENACW was anomalously warm in 2017 (the warmest year of the time-series). The water column down to 350 m depth was less saline than the previous years (about 0.06 fresher than the mean). MOW was colder and less-saline than the average.

The latest data taken in 2018 (March) show an anomalously saline lower ENACW and cold upper MOW, suggesting strong mixing between the two.

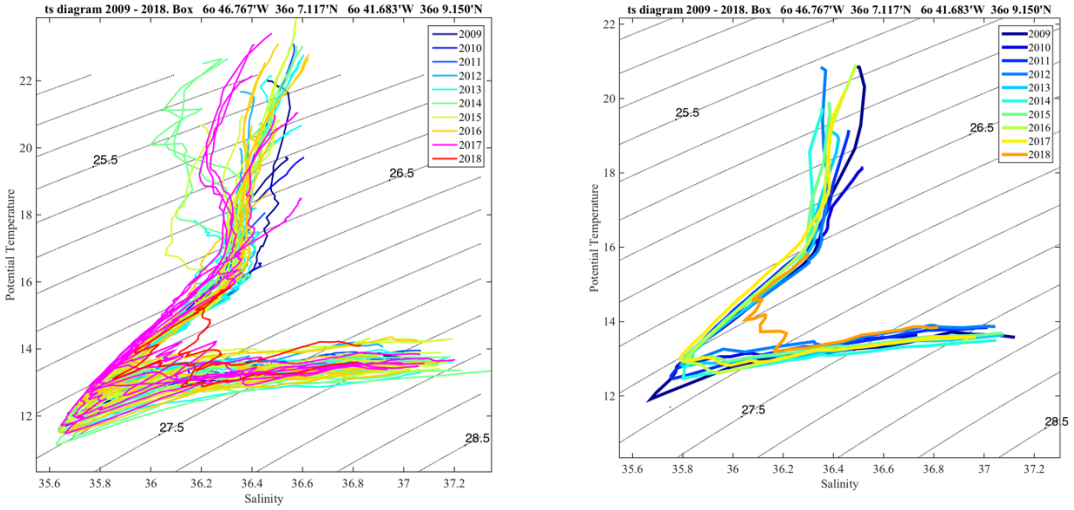

Figure 6. *2009-2018 T-S curves at SP6 (STOCA program). Curves are color coded by date. (Left): All observations. 2007 is coded in magenta. (Right): Mean T-S curves.*

Water column trends

Fig. 7 shows the vertical distribution of 2009-2018 potential temperature and salinity trends (along with the 95% CI) across the water column at station SP6. The graphs illustrate the contrasting variability at each water mass. Surface (top 50 m of the water column) waters experience significant warming. On the contrary, ENACW extending from 50-350 exhibit cooling (about 0.3 ºC per decade) and significant freshening (0.1 per decade). The MOW, present everywhere below 350 m depth, exhibit two significant salinification trend peaks between 350 and 420 m and between 450-540 m depth,

respectively. The former also shows a non-significant warming trend. Below 530 m, the deeper MOW exhibits a significant freshening with no associated significant warming trend.

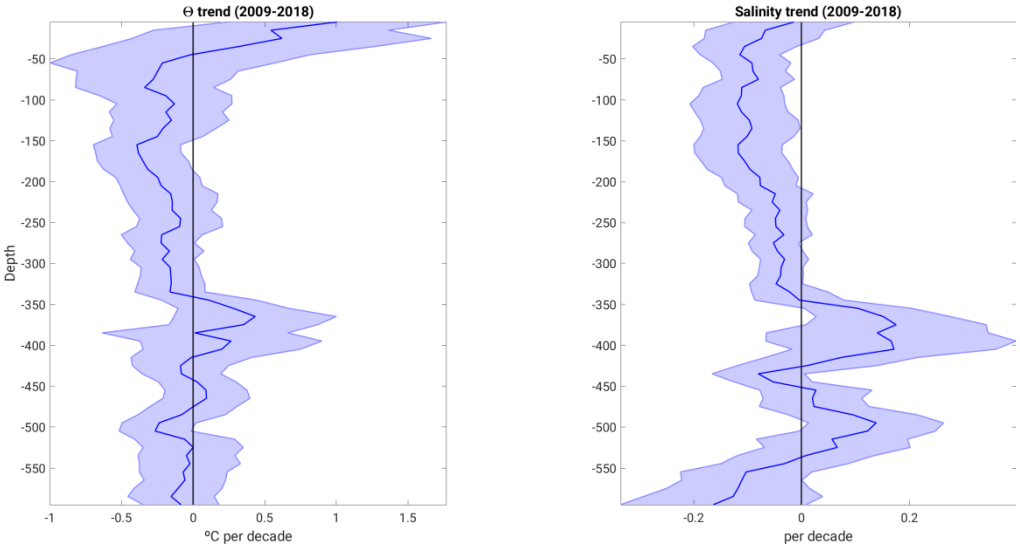

Figure 6. *2009-2018 potential temperature (ºC per decade; Left panel) and salinity (per decade; Right panel) at SP6 (STOCA program). The 95% C.I. is shaded.*

References

M. J. Bellanco, R. F. Sánchez-Leal, Spatial distribution and intra-annual variability of water masses on the Eastern Gulf of Cadiz seabed. Cont. Shelf Res. 128, 26–35 (2016).

M. O. Baringer, J. F. Price, Mixing and spreading of the Mediterranean outflow. J. Phys. Oceanogr. 27, 1654–1677 (1997).

Criado-Aldeanueva, F., J. García-Lafuente, J. M. Vargas, J. Del Río, A. Vázquez, A. Reul, and A. Sánchez, Distribution and circulation of water masses in the Gulf of Cadiz from in situ observations, Deep Sea Res., Part II, 53, 1144–1160 (2006)

Fiúza, A.F.G., Macedo, M.E., Guerreiro, M.R., Climatological space and time variation of the Portuguese coastal upwelling. Oceanol. Acta 5, 31–40 (1982)

Folkard, A. M., P. A. Davies, A. F. G. Fiúza, and I. Ambar, Remotely sensed sea surface thermal patterns in the Gulf of Cadiz and Strait of Gibraltar: Variability, correlations, and relationships with the surface wind field, J. Geophys. Res., 102, 5669–5683 (1997),

García-Lafuente, J., J. Delgado, F. Criado-Aldeanueva, M. Bruno, J. Del Río, and J. M. Vargas, Water mass circulation on the continental shelf of the Gulf of Cadiz, Deep Sea Res., Part II, 53, 1182–1197 (2006)

M. García, F. J. Hernández-Molina, E. Llave, D. A. V. Stow, R. León, M. C. Fernández-Puga, V. Diaz del Río, L. Somoza, Contourite erosive features caused by the

Mediterranean Outflow Water in the Gulf of Cadiz: Quaternary tectonic and oceanographic implications. Mar. Geol. 257, 24–40 (2009)

F. Madelain, Influence de la topographie du fond sur l'écoulement méditerranéen entre ledétroit de Gibraltar et le cap Saint-Vincent. Cah. Océanogr. 22, 43–61 (1970)

A. Peliz, J. Dubert, P. Marchesiello, A. Teles-Machado, Surface circulation in the Gulf of Cadiz: Model and mean flow structure. J. Geophys. Res. 112, C11015 (2007)

J. F. Price, M. O. Baringer, R. G. Lueck, G. C. Johnson, I. Ambar, G. Parrilla, A. Cantos, M. A. Kennelly, T. B. Sanford, Mediterranean outflow mixing and dynamics. Science 259, 1277–1282 (1993).

Relvas, P., and E. D. Barton, Mesoscale patterns in the Cape São Vicente (Iberian Peninsula) upwelling region, J. Geophys. Res., 107(C10), 3164 (2002)

Sánchez, R., and P. Relvas, Spring-summer climatological circulation in the upper layer in the region of Cape St. Vincent, southwest Portugal, ICES J. Mar. Sci., 60, 1232–1250 (2003)

Sánchez, R.F., Mason, E., Relvas, P., da Silva, A.J., Peliz, Á., On the inner-shelf circulation in the northern Gulf of Cádiz, southern Portuguese shelf. Deep-Sea Res. II Top. Stud. Oceanogr. 53, 1198–1218 (2006)

Ricardo F. Sánchez-Leal, María Jesús Bellanco, Luis Miguel Fernández-Salas, Jesús García-Lafuente, Marc Gasser-Rubinat, César González-Pola, Francisco J. Hernández-Molina, Josep L. Pelegrí, Alvaro Peliz, Paulo Relvas, David Roque, Manuel Ruiz-Villarreal, Simone Sammartino, José Carlos Sánchez-Garrido. The Mediterranean Overflow in the Gulf of Cadiz: A rugged journey. Science Advances (2017)

Teles-Machado, A., Á. Peliz, J. Dubert, and R. F. Sánchez, On the onset of the Gulf of Cadiz Coastal Countercurrent, Geophys. Res. Lett., 34, L12601 (2007)

Contribution to the ICES Report on Ocean Climate 2017 - Canary Basin.

Pedro Vélez-Belchí, Spanish Oceanographic Institute

North-atlantic-upper-ocean - Canary Basin.

Highlight

During 2017, there was a slightly decrease in the warming and increase in salinity, if compared to the previous years, following the trend initiated in 2015; 2014 was the saltier and warmest year in the record for the NACW waters.

The upwelling of the CCLME continues to strengthen. 2015 was the coolest and fresher year in the record for the upwelling influenced surface waters.

Description

The Canary Basin sits at the boundary between the oceanic waters of the subtropical Atlantic gyre and the upwelling waters from the Canary Current Large Marine Ecosystem (CCLME) off the coast of Northwest Africa. Since the early 2000's the Canary Islands archipelago region has been monitored by the Spanish Institute of Oceanography [Tel et al, 2016]; the oceanic waters west of Lanzarote (stations 11-23, Figure 1) and the Coastal Transition Zone (CTZ) of the upwelling region of the Canary Current Large Marine Ecosystem (stations 1-10, Figure 1)

At the upper levels, the area is under the influence of the southward flowing Canary current and the Canary Upwelling current, associated to the upwelling front (Figure 1). At intermediate levels, it is under the influence of the tongue of slow propagating Mediterranean waters and the slope current known as the Canary Intermediate Poleward Current [Hérnandez-Guerra et al, 2017; Vélez-Belchí et al, 2018].

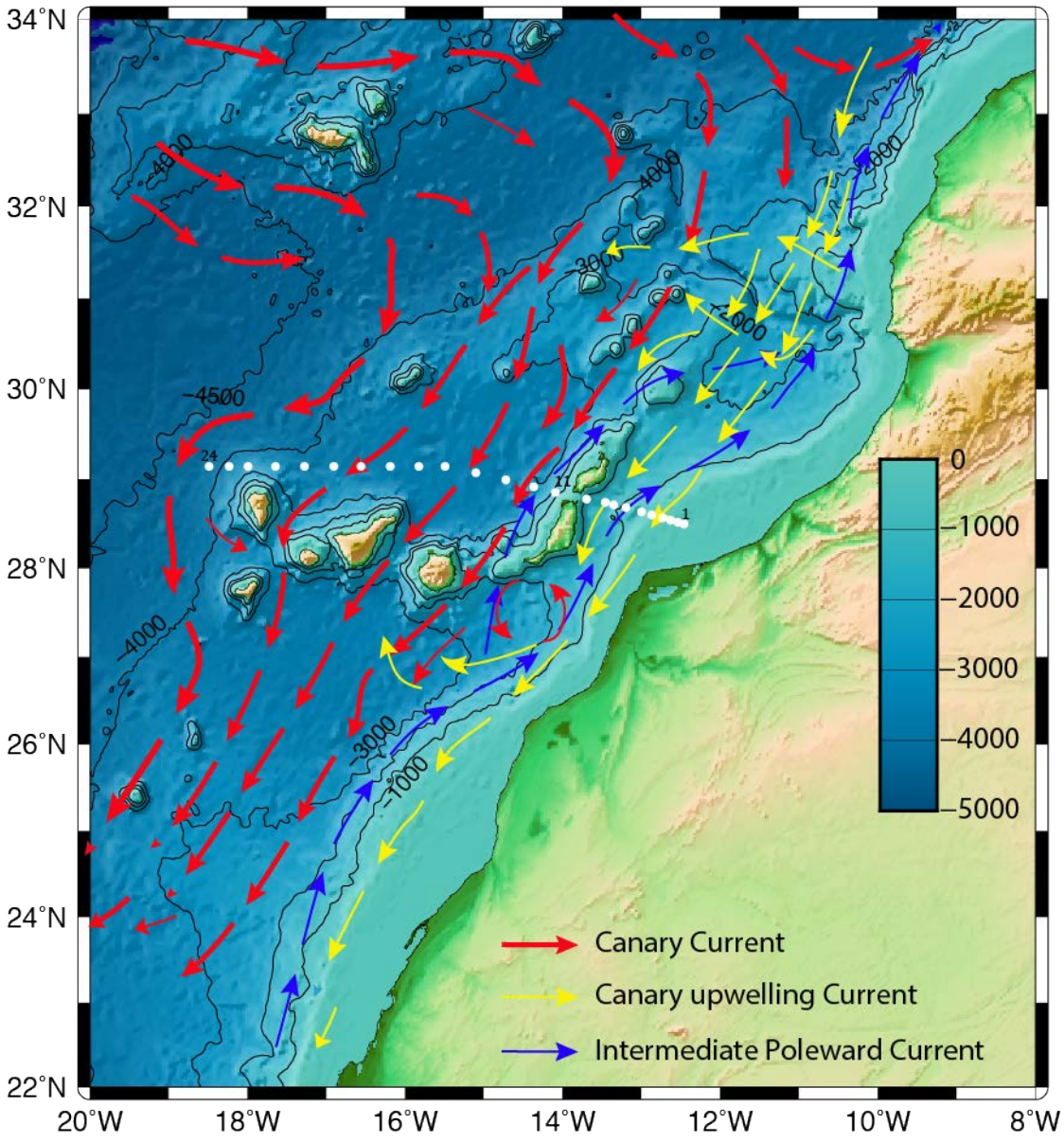

Figure 1. Circulation schematic for the Canary Basin. Red arrows show the southward Canary Current of, mainly, NACW and intermediate waters. Yellow arrows show the Canary Upwelling current that flows in the thermocline waters. The white dots represent the distribution of the 24 hydrographic stations sampled in the Canary Islands archipelago region since 1997. Stations 1-10 are used to estimate changes in the CTZ and stations west of Lanzarote (11-24) **the oceanic waters**

The waters above the seasonal thermocline, γ_n < 26.850 kg m-3, are characterized on the θ/S diagram by scattered temperature and salinity values due to seasonal heating and evaporation. These waters occupy the upper 300 m in the oceanic region, and the upper 100 m in the stations under the effect of the coastal upwelling which are considered the surface waters. Below the seasonal thermocline and through the permanent thermocline is the North Atlantic Central Water (NACW), roughly delimited by 26.850 <γ^n< 27.380 kg m-3, between 300 m and 700 m

depth. These waters are characterized on the θ/S diagram by an approximately straight-line relationship between potential temperature (11.4ºC<θ<14.9ºC) and salinity (35.6<S<36.1). At intermediate levels, between 27.380 < γ^n < 27.820 kg m-3, two distinct water masses are found in the Canary Islands region, the fresher (S<35.3) and slightly lighter Antarctic Intermediate Waters (AAIW), and the saltier (S>35.4) and heavier Mediterranean Waters (MW).

Report

In the oceanic region, between the 1990s and the early 2000s there was a decrease in the temperature and salinity in the all upper–layer waters, than ended in the mid-2000s when began a markedly increase in both, temperature and salinity until 2014, that is the hottest and saltier year in the record. Since 2015, both temperature and salinity has decreased, and at the end of 2017, the mean temperature and salinity was similar to that found in the late 1990s [Vélez-Belchí et al, 2015].

In the depth stratum that characterize the NACW waters (200-800 dbar), there is an overall statistically significant warming of 0.12±0.07°C decade^{-1} and increase of salinity of 0.016±0.012°C per decade^{-1} (Figure 2). The overall increase in temperature and salinity almost compensate in density, corroborating that the observed trends are due to deepening of the isoneutral surfaces rather than changes along the isoneutral surfaces. This overall increase in salinity and temperature for the NACW waters was also observed in the CTZ, although with slightly smaller values for the trend due to the influence of the upwelling. The variability in the CTZ is higher due to the proximity of the upwelling region, and the frequent intrusions of upwelling filaments. For the same reason, the uncertain is higher in the trend estimations.

The surface waters in the CTZ shows a non-statistical significant cooling of -0.33±0.49°C decade^{-1}, and a non-statistical significant decrease in salinity of -0.059±0.069 decade^{-1}, both coherent with an increase in the upwelling in the Canary Current Large Marine Ecosystem (CCLME). The upwelling of the CCLME continues to strengthen, and 2015 was the coolest and fresher year in the record for the upwelling influenced surface waters. Sea surface temperature observations from satellite observations (Figure 4) corroborate the in-situ observations for the changes in the upwelling regime, with different areas showing increase in the upwelling. However, the magnitude of the observed trend in the satellite SST are different, probably due to the thin layer of ocean that the satellite observes.

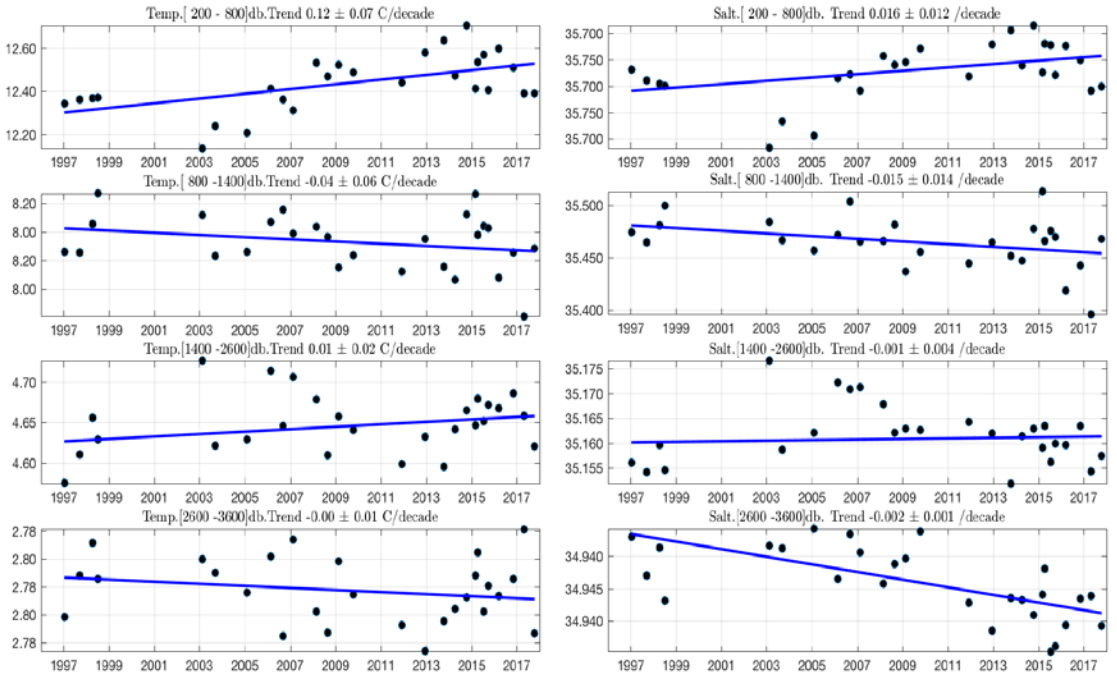

Figure 2. Time series of hydrographical properties at different depth stratums in the oceanic waters of the Canary basin.

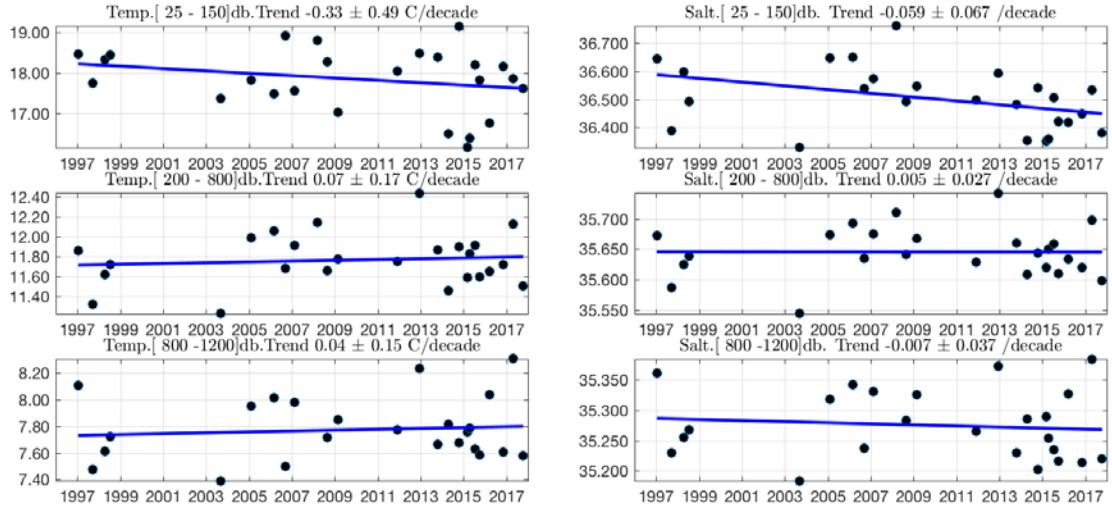

Figure 3. Time series of hydrographical properties at different depth stratums in the Coastal Transition zone of the Canary Current Large Marine Ecosystem (stations 1-5).

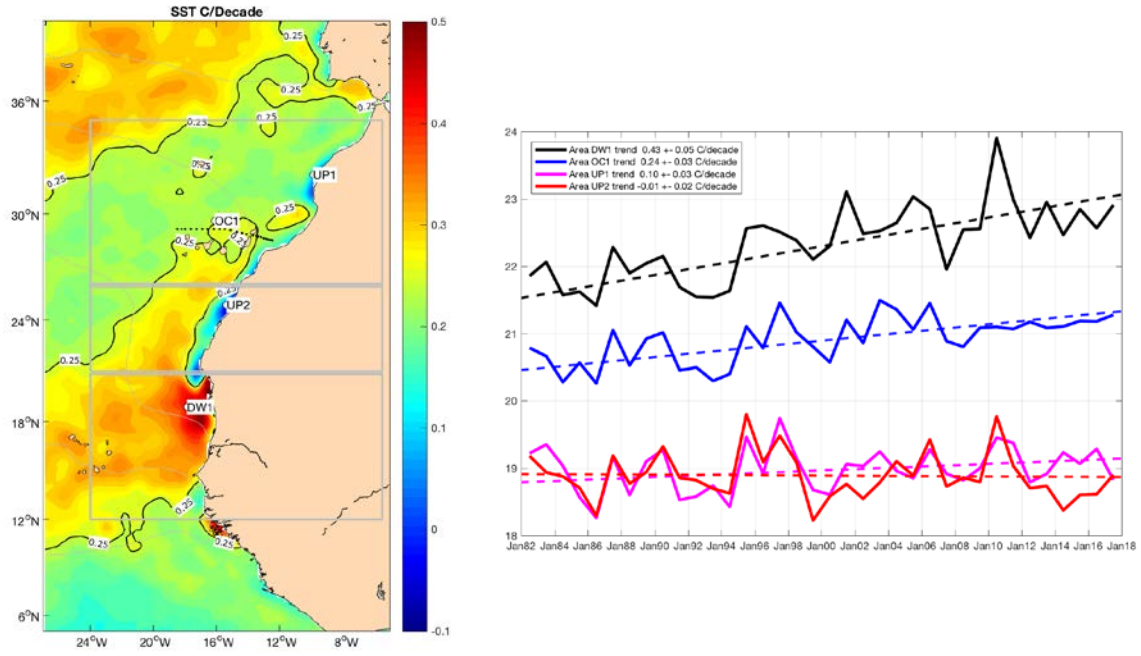

Figure 4. (a) Sea surface trends (°C decade-1) computed from NOAA high-resolution (1/4°) blended analysis of Daily SST for the 1982–2017 period. The dashed grey line denote the three upwelling areas as defined by Cropper et al. (2014): the weak annual upwelling zone (26°N-35°N), the permanent annual upwelling zone (21°N-26°N) and the Mauritania-Senegalese upwelling zone (12°N -20°N). The thin solid grey lines correspond to the isotherms (18°C, 20°C, 22°C, 24°C and 26°C) of the mean field for each season.

(b) Yearly values of the SST for the four locations represented in (a): UP1, west of Cape Beddouza in the weak permanent annual upwelling zone, UP2, south of Cape Bojador in the permanent annual upwelling zone, OC1, in the oceanic waters north of the Canary Islands, and DW1, west of Cape Timiris, in the Mauritania-Senegalese upwelling zone. Trend values (dashed line in °C decade-1), and statistical significant range at the 95% confidence level are indicated in the legend for each one of the locations.

North-atlantic-intermediate - Canary Basin.

In the stratum corresponding to the intermediate waters (800-1400 dbar), continue the weak cooling and decrease in salinity since the 1990s, however it is not statistically significantly different from zero, neither in the oceanic region nor in the CTZ. Both time series show high variability due to the two very different intermediate water masses present in the region, i.e the Mediterranean waters (MW) and the Antarctic Intermediate Waters (AAIW)

North-Atlantic-deep-waters - Canary Basin.

In the layer corresponding to the upper NADW (1700-2600 dbar), there was a weak warming and increase in salinity that is not statistically significantly different from zero. However, in stratums corresponding to the NADW (2600-3600 dbar), a marginally statistical significant cooling (-0.01±0.01°C decade-1) and freshening (-0.002±0.002°C decade^{-1}) is observed.

Bibliography

Hernández-Guerra, A., Espino-Falcón, E., Vélez-Belchí, P., Pérez-Hernández, M.D., Martínez-Marrero, A., Cana, L. (2017). Recirculation of the Canary Current in fall 2014. Journal of Marine Systems, 174, pp. 25-39, doi:10.1016/j.jmarsys.2017.04.002

Tel, E., Balbin, R., Cabanas, J.-M., Garcia, M.-J., Garcia-Martinez, M. C., Gonzalez-Pola, C., Lavin, A., Lopez-Jurado, J.-L., Rodriguez, C., Ruiz-Villarreal, M., Sánchez-Leal, R. F., Vargas-Yáñez, M., and Vélez-Belchí, P. (2016) IEOOS: the Spanish Institute of Oceanography Observing System, Ocean Sci., 12, 345-353, https://doi.org/10.5194/os-12-345-2016, 2016.

Vélez-Belchí, P., González-Carballo, M., Pérez-Hernández, M. D. and Hernández-Guerra, A. (2015). Open ocean temperature and salinity trends in the Canary Current Large Marine Ecosystem. In: Valdés, L. and Déniz-González, I. (eds). Oceanographic and biological features in the Canary Current Large Marine Ecosystem. IOC-UNESCO, Paris. IOC Technical Series, No. 115, pp. 299-308.

Vélez-Belchí, P., M. D. Pérez-Hernández, M. Casanova-Masjoan, L. Cana, and A. Hernández-Guerra (2017), On the seasonal variability of the Canary Current and the Atlantic Meridional Overturning Circulation, J. Geophys. Res. Oceans, 122, 4518–4538, doi:10.1002/2017JC012774.

Faroese Waters 2017

By Karin Margretha H. Larsen

Hydrographic conditions in Faroe waters are monitored by regular CTD cruises along four standard sections three times a year. In addition, ADCPs are moored on two of these sections (Figure 1). These activities are designed to monitor the properties (T and S) and volume transport of the Faroe Bank Channel (FBC) overflow and the Atlantic inflow in the Faroe Current north of the Faroes. Additionally, we collaborate with Marine Science Scotland in Aberdeen on monitoring the Atlantic water flow through the Faroe-Shetland Channel.

Time series plots of the temperature (Figure 2) and the salinity (Figure 3) of the Atlantic water on the section across the FBC and northwards from the Faroes show the increased temperatures and salinities from the mid-1990s that were high through the 2003-2011period. In 2012 both temperatures and salinities declined, but whereas annual average temperatures have stayed close to the long-term mean, salinities first stagnated, but then dropped suddenly in autumn 2016 and stayed at this lower level throughout 2017. In 2017 temperatures were just above the long term mean (1988-2010), while salinities were record low.

On the Faroe Shelf the annual average temperature has been relatively high since the early 2000s, and in 2017 the annual averaged temperature was the fourth highest in the recent decade (Figure 4). All months except December were above average. The conditions thus still remain warm in a century-long perspective as indicated by the Faroe coastal temperature time-series from Mykines (Figure 4, left panel). The long term trend in salinity on the Faroe Shelf (Figure 5) follows the trend observed in off-shelf waters, but with some lag. Salinities increased from the start of the observations in 1995 to record high values in 2010. Since 2010 salinities have been decreasing and this trend accelerated in the latter half of 2016. In 2017 the trend ceased, but the salinities stayed at this low level, such that all for months in 2017 the values are lowest on record (since 1995).

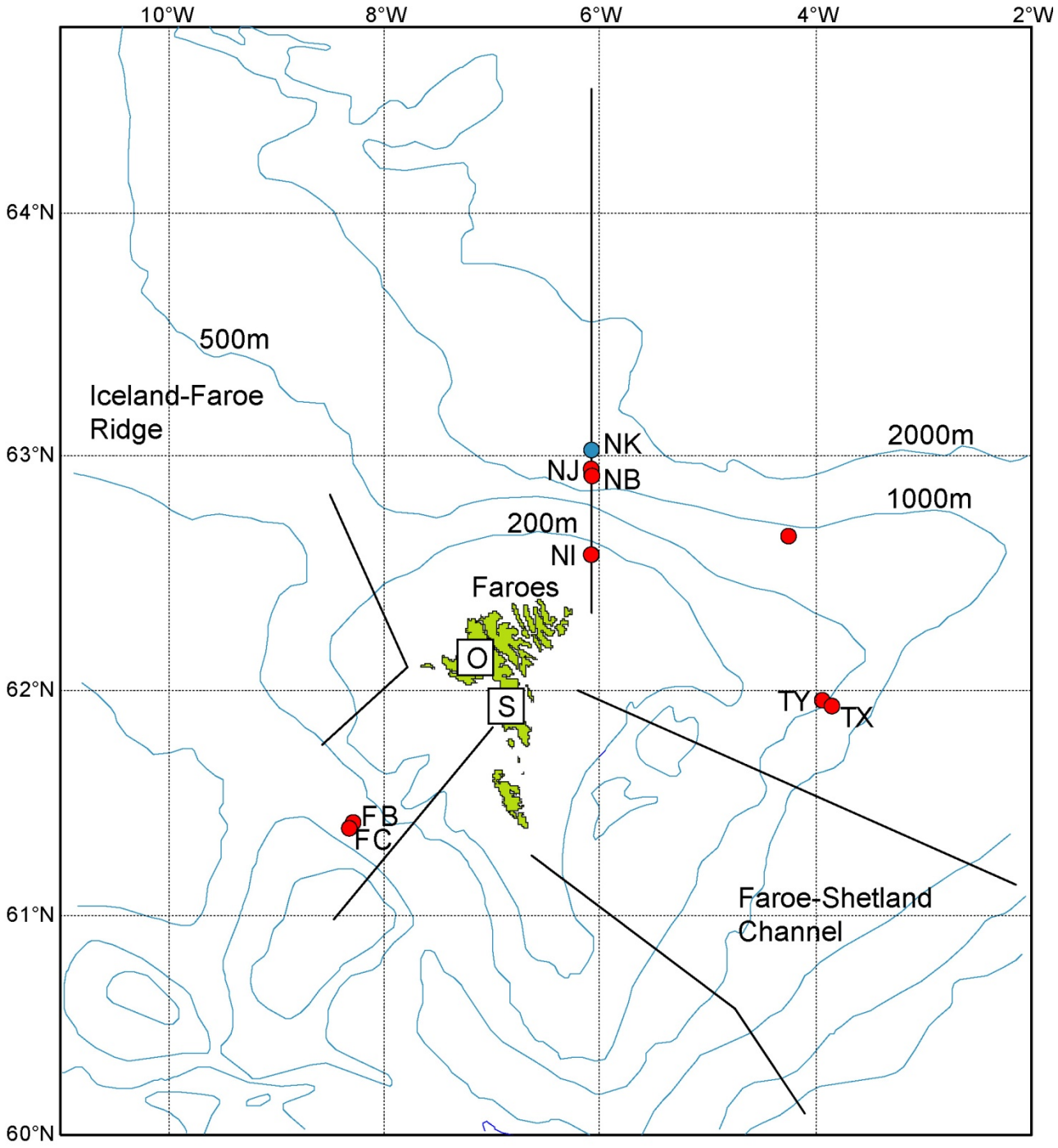

Figure 1. Standard sections 2017 (black lines) and moored ADCPs (red circles) at the top of traditional moorings (NB, NJ, FB, FC, TX and TY) or in trawl-protected frames (NI) deployed in 2017. Blue circle is an Aanderaa mooring. Squares with the letters O and S indicate the coastal stations Oyrargjógv and Skopun, respectively.

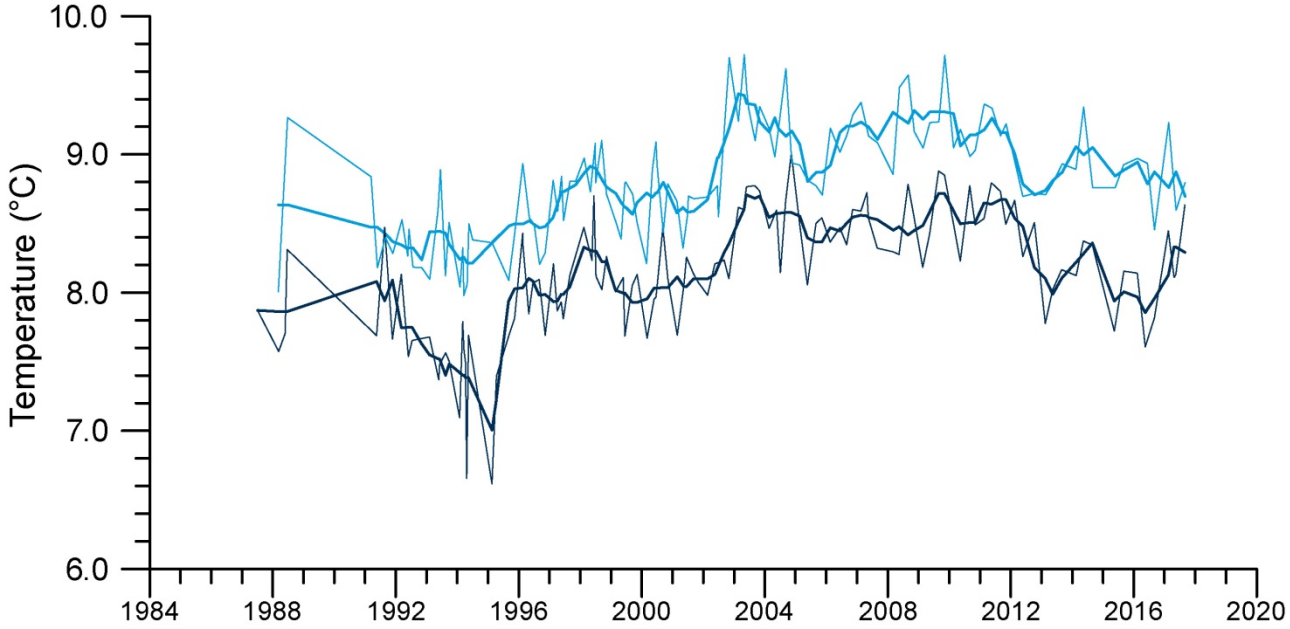

Figure 2. De-seasoned temperature from individual cruises (thin lines) in the FBC (light blue) and the core of the Faroe Current (dark blue). Thick lines are annual means. The figure represents the average temperature in that 50 m layer on the section that has the highest salinity (the core).

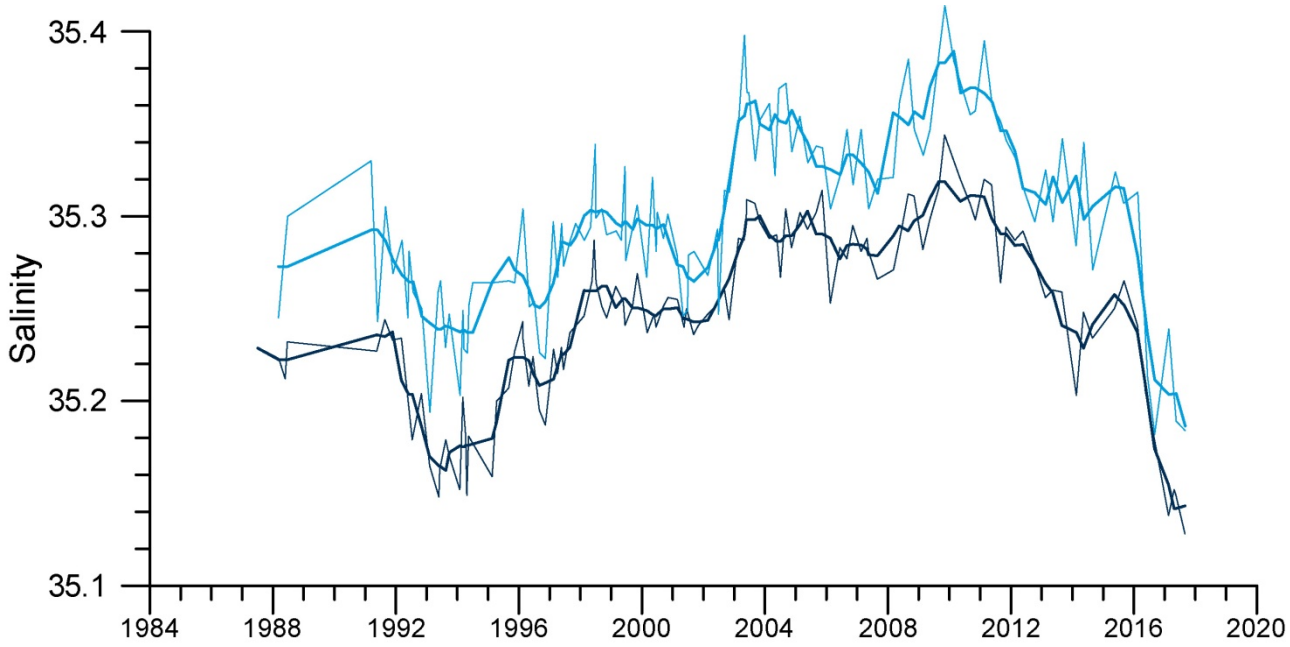

Figure 3. De-seasoned salinity from individual cruises (thin lines) in the FBC (light blue) and the core of the Faroe Current (dark blue). Thick lines are annual means. The figure represents the average salinity in that 50 m layer on the section that has the highest salinity (the core).

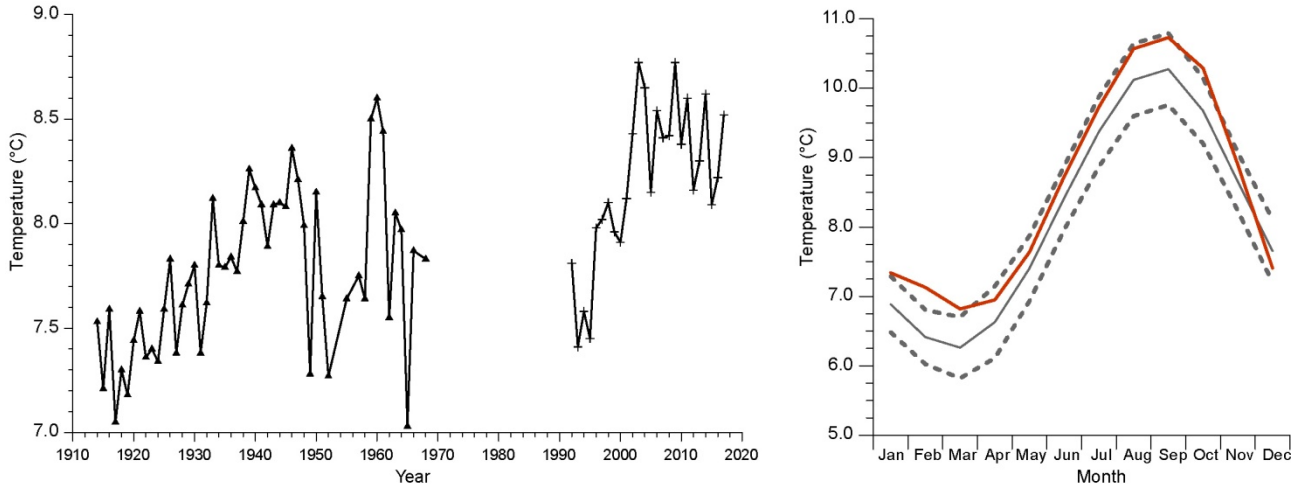

Figure 4. Annually averaged Faroe coastal temperature (left panel) monitored daily in Mykines 1914-1969 and several times daily at the neighbouring site Oyrargjógv from 1992. In the Mykines timeserie, years with less than 8 months of observations are omitted. The right panel shows the monthly averaged Faroe coastal temperature monitored at Oyrargjógv in 2017 (red line) and the monthly mean climatology from Oyrargjogv (1991-2010) (grey line) ± one standard deviation (dotted lines). Inter-comparison experiments support that the two coastal sites Oyrargjogv and Mykines represent the same water mass (Larsen et al, 2008).

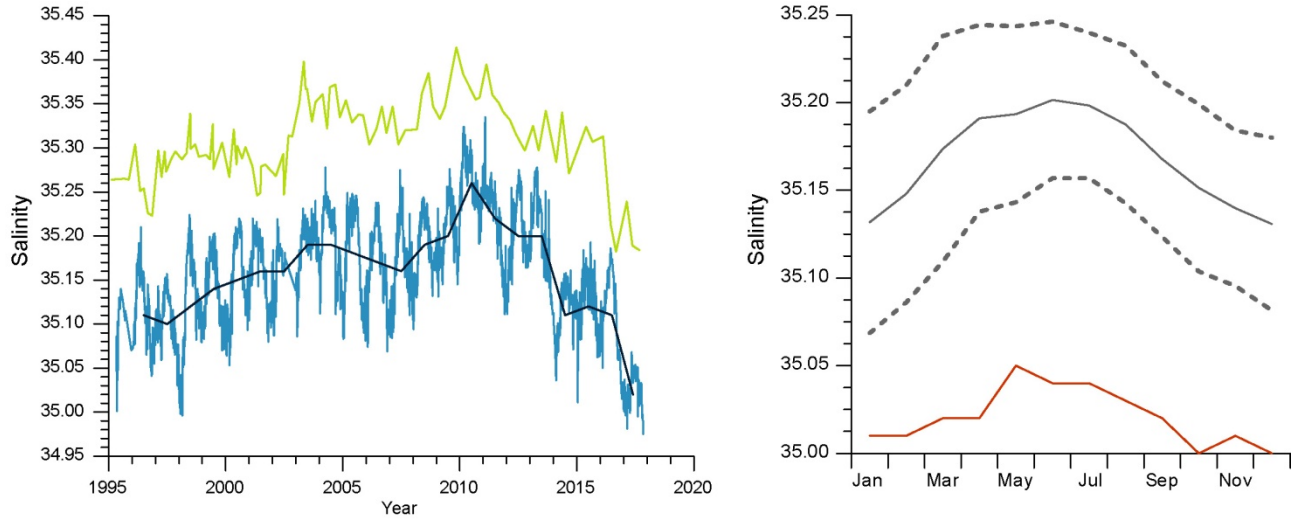

Figure 5. Individual observations (blue) and annually averaged (dark blue) Faroe coastal salinity (left panel) monitored weekly at coastal station Skopun since May 1995. Also shown (light green) is the salinity from the FBC (Figure 3, thin light blue) . The right panel shows the monthly averaged Faroe coastal salinity in 2017 (red line) and the monthly mean climatology (1995-2010) (grey line) ± one standard deviation (dotted lines).

BUNDESAMT FÜR SEESCHIFFFAHRT UND HYDROGRAPHIE

Area Report

Eco-Region Greater North Sea 2017

Holger Klein, Alexander Frohse, Peter Loewe, Achim Schulz

Federal Maritime and Hydrographic Agency

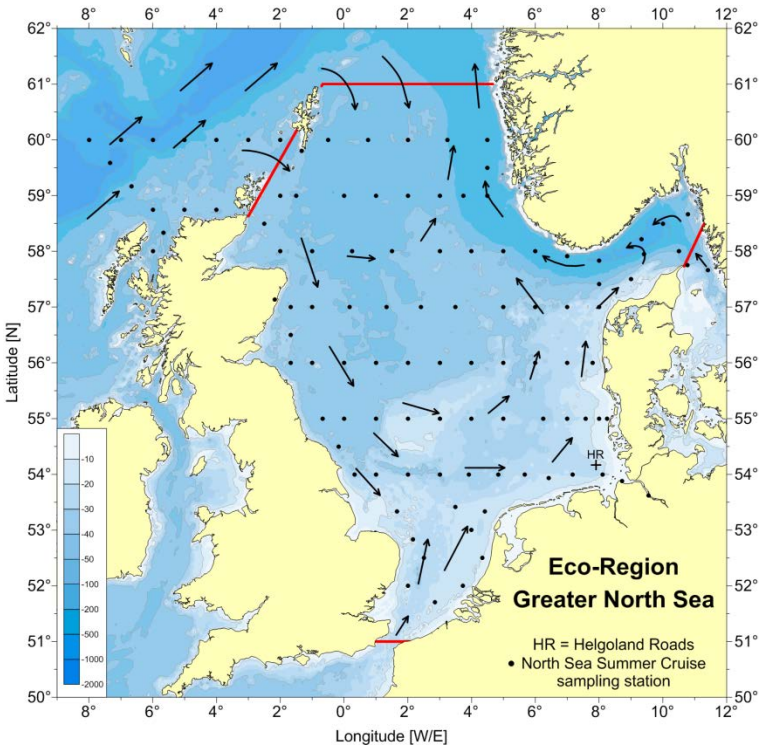

1 North Sea 2017: Annual Survey

1.1 Global Radiation

During spring 2017 the monthly means of global radiation at the East Frisian island of Norderney exceeded the means of the reference period 1981-2010 (Fig. 1.1), but the June value was about one standard deviation below the reference period. During fall the values were again below the long-term mean and also the annual average of daily global radiation totals at Norderney was slightly below the reference period.

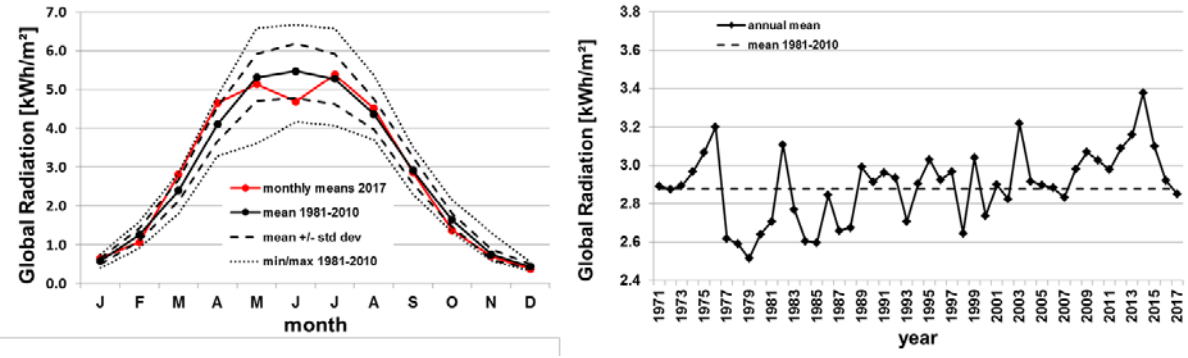

***Fig. 1.1**: Left: Red: Seasonal cycle of monthly averaged daily global radiation totals 2017 in kWh/m² at Norderney. Black: Monthly means of the 1981-2010 base period ± standard deviations (broken lines) and extreme values (dotted lines). Right: Annually averages of daily global radiation totals at Norderney 1971-2017 in kWh/m². Broken line: mean of the base period 1981-2010. Data provider: German Meteorological Service (DWD).*

1.2 Elbe River Run-Off

During the first month of 2017 all monthly run-off volumes were below the reference period 1981–2010 (Fig. 1.2) and slightly above the reference period during November in December. The annual run-off volume of 18.2 km³/a was still relatively low, but higher compared to the three previous years.

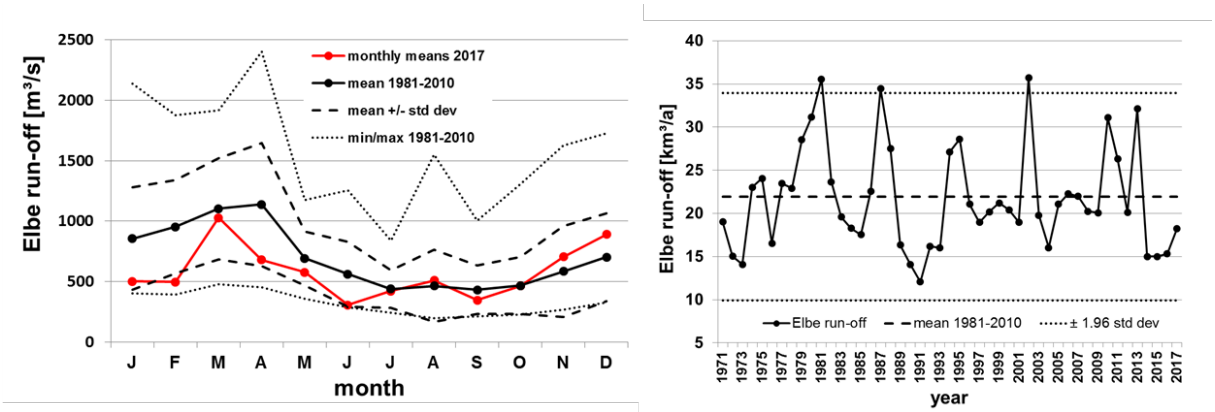

***Fig. 1.2:** Left: Monthly means of Elbe discharge at the water gauge Neu Darchau in m³/s in 2017and 1981-2010 mean ± standard deviations. Right: Total annual run-off in in km³/year 1971-2017 and 1981-2010 mean ±1.96 standard deviations. Data provider: BfG / WSA Lauenburg.*

1.3 North Sea SST

In 2017 all monthly means of area averaged North Sea SSTs were at between 0.1 and 0.9 K above the reference period 1981-2010. The monthly SST maximum of 16.0 °C occurred in August (Fig. 1.3, left). The 2017 annual mean of area averaged North Sea SST of 10.8 °C was slightly lower than in 2016 but with an anomaly of +0.6 K still above the long-term mean (Fig. 1.3, right).

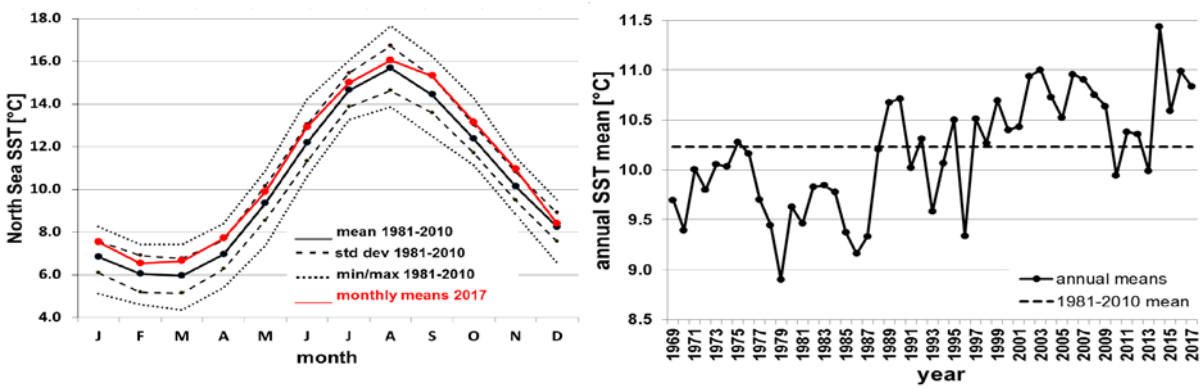

***Fig. 1.3**: Left. Monthly means of area averaged North Sea SST in °C for 2017 (red line). Black solid line: mean of reference period 1981-2010 ± standard deviation (broken lines), dotted lines: min/max of reference period. Right: Annual North Sea SST means 1969-2017 in °C. Broken line: 1981-2010 mean.*

The spatial pattern of monthly North Sea SST anomalies relative to the reference period 1971–1993 are shown at:
http://www.bsh.de/de/Meeresdaten/Beobachtungen/Meeresoberflaechentemperatur/anom.jsp#SSTJ

1.4 Temperatures at Light Vessel *German Bight*

The vertical temperature distribution in the German Bight is exemplarily documented by the temperature records of the MARNET[1] station on the unmanned light vessel *German Bight* (54° 10' N; 007° 27' E, water depth 38 m) at depths between 3 and 30 m for the period 2015 to 2017 (Fig. 1.4). Gaps in the time series are caused by technical problems, bio-fouling or dockyard lay time for maintenance. The thin horizontal grey lines gives the climatological seasonal extreme values in the surface layer according to Janssen et al. (1999)[2] with a seasonal range of about 13.5 K. The winter minimum 2016/2017 was more than 1.5 K above the climatological cycle. In 2017 stratification started during the first week of May and reached a maximum range of 4.2 K early in the beginning of June. In the German Bight the stratification broke down at the end of July due to strong winds. There are no values for August, but near-by in-situ measurements showed a seasonal maximum of about 19 °C in the surface layer in the midst of August.

[1] http://www.bsh.de/en/Marine_data/Observations/MARNET_monitoring_network/index.jsp
[2] Janssen F., C. Schrum and J.O. Backhaus, 1999: A Climatological Data Set of Temperature and Salinity for the Baltic Sea and the North Sea, German Journal of Hydrography, Supplement 9, 245pp.

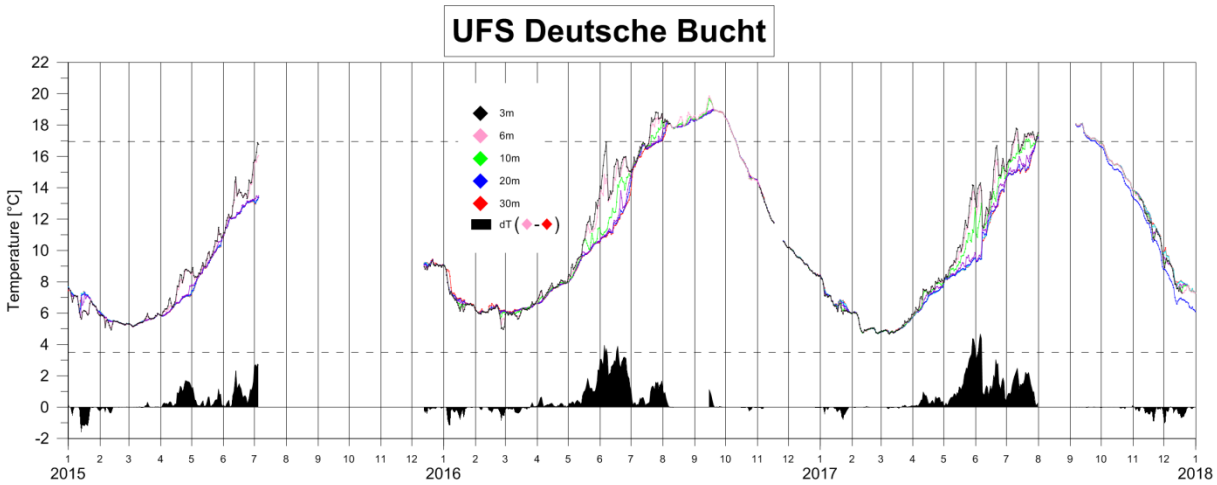

Fig. 1.4: *Temperatures [°C] at light vessel "German Bight" 2015–2017. Broken lines: climatological seasonal maximum and minimum of the surface layer according to Janssen et al., 1999.*

2 North Sea Summer Status 2017

2.1 The BSH North Sea Summer Surveys

The North Sea summer state is primarily assessed by the data of the annual *BSH North Sea Summer Surveys* (NSSS) which started in 1998. They cover the entire North Sea with seven zonal coast to coast sections between 54° and 60°N and additional stations between 54°N and the eastern entrance of the English Channel. The surveys were realised at a time when thermal stratification is expected to be at its maximum and phytoplankton production has passed its maximum. With the exception of the first survey in 1998 all surveys served a fixed grid of vertical CTD casts (temperature, salinity, fluorescence for chlorophyll-a, and turbidity, and oxygen saturation. Additionally, ship-mounted temperature-, salinity-, and optical sensors provided data at about 4 m depth.

For the assessment of the North Sea status a 10 years reference period (RP) from 2000 to 2010 was defined which skips the year 2002 because the 2002 survey was much too early with regard to the seasonal cycle.

2.2 North Sea Summer Temperature and Salinity Distribution

Temperature

During summer the surface temperatures in the southern North Sea exceeded the long-term mean (2000-2010) by 0.5 to 1.0 K. In the outer Firth of Forth estuary and over the Norwegian trench the surface temperatures lay up to 1 K below the long-term mean. The bottom temperatures exceeded the long-term mean over large areas with anomalies greater +4 K over Dogger Bank and up to +3 K above Jyske Rev and west off Jutland (Fig. 2.2a).

The maximum vertical temperature gradient in the thermocline was 2.9 K/m on the 57°N section. The 54°N section was vertically mixed with vertical gradients <0.5 K/m. Generally, the thermocline depth in the North Sea varied between 15 m on the 55°N section and 99 m over the Norwegian Trench (Table 1). There was a strong thermocline in the central North Sea and a weakening of thermocline strength from south to north (in Fig. 2.2c, d). The differences between surface and bottom temperature exceeded 8 K over the Norwegian Trench and in a small ribbon north of Dogger Bank (Fig. 2.2b).

Compared to 2016 the total heat content increased slightly to 1.677×10^{21} J and exceeded the reference mean of 1.631×10^{21} J by 0.5 standard deviations (see Table 2 and Fig. 2.2g).

Salinity

The southern boundary of Atlantic Water (AW) >35 psu intruding from the north was located at about 58°N in the surface and at 57°N in bottom layer. At the surface as well as in the bottom layer AW intruded in a broad front. The general spatial pattern showed in both layers only minor deviations from the pattern of the reference period. Only over Viking and Bergen Bank, Utsiragrund and at the southern tip of Norway occurred positive anomalies up to 1 psu in the surface layer. Positive anomalies of the same order of magnitude are also observed in both layers in the inner German Bight (Fig. 2.2e, f).

Compared to 2016 the total salt content increased slightly to 1.105×10^{12} t which is still 1.5 standard deviations below the 2000-2010 mean (Fig. 2.2g and Table 2).

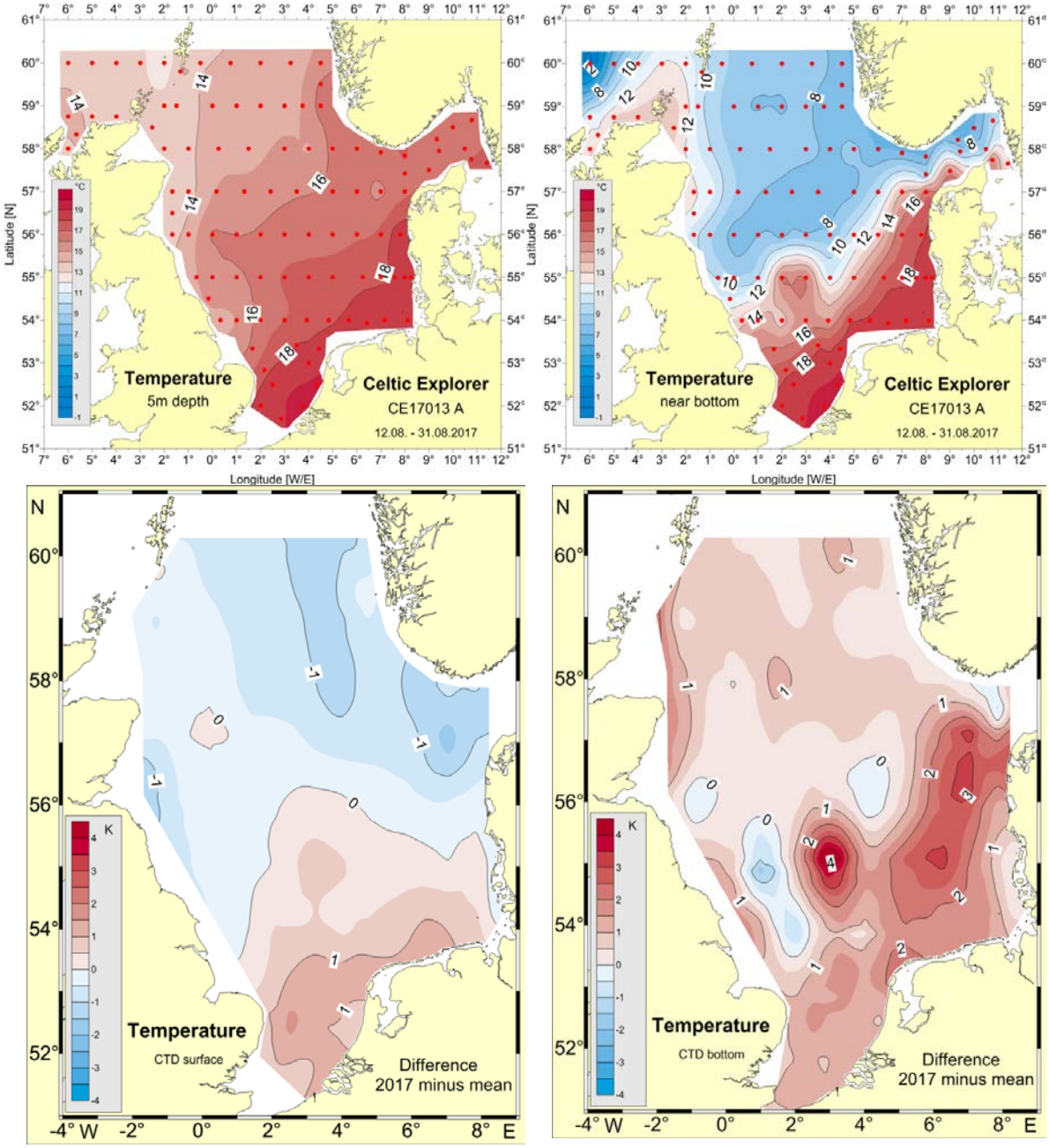

***Fig. 2.2a**: Top: Horizontal surface (left) and bottom (right) temperature distribution in °C. Bottom: Horizontal surface (left) and bottom (right) temperature anomalies (2017 – reference period 2000-2010) in K.*

section	vertical gradient (≥0.5 K/m)		depth of thermocline [m]	
	min	max	min	max
60° N	**0.5**	0.7	19	65
59° N	**0.5**	1.2	30	34
58° N	**0.5**	2.8	22	**99**
57° N	**0.5**	**2.9**	15	38
56° N	1.1	2.1	24	33
55° N	**0.5**	2.7	**17**	28
54° N	-	-	-	-
mean±std	0.6±0.2	2.1±0.9	21.2±5.4	49.5±27.6

Table 1: *Extreme values of vertical temperature gradients and thermocline depths (depth of maximum gradient) along zonal sections. Last line: Mean and standard deviation over all sections.*

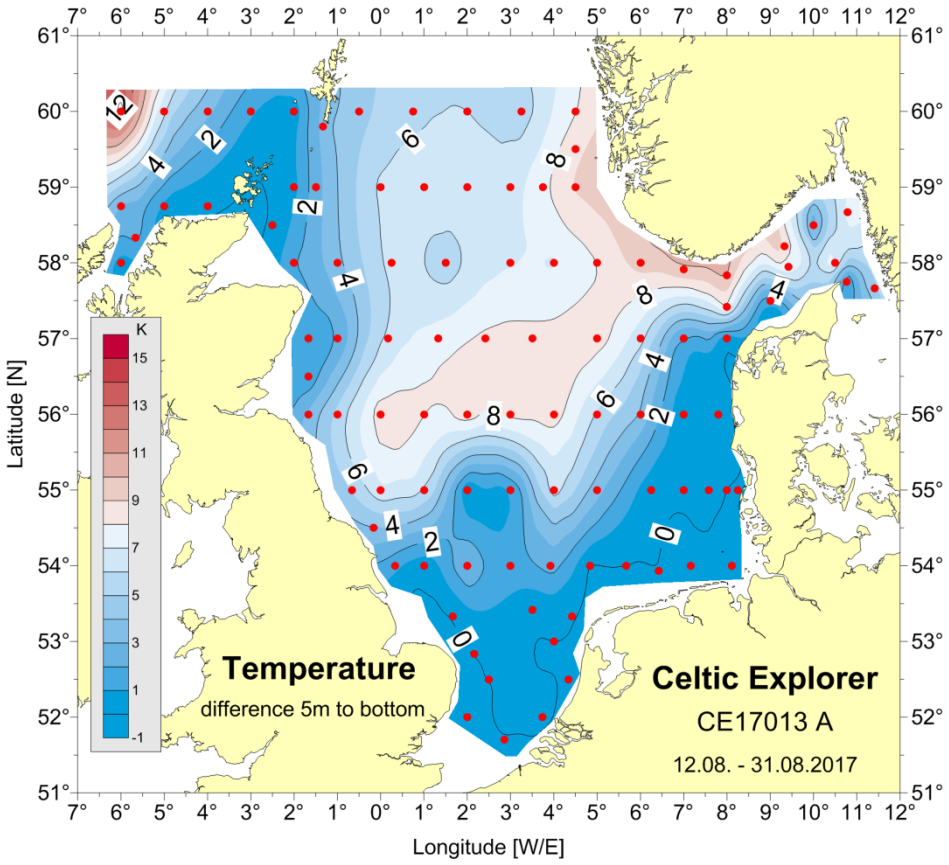

Fig. 2.2b*: Difference surface temperature minus bottom temperature in K.*

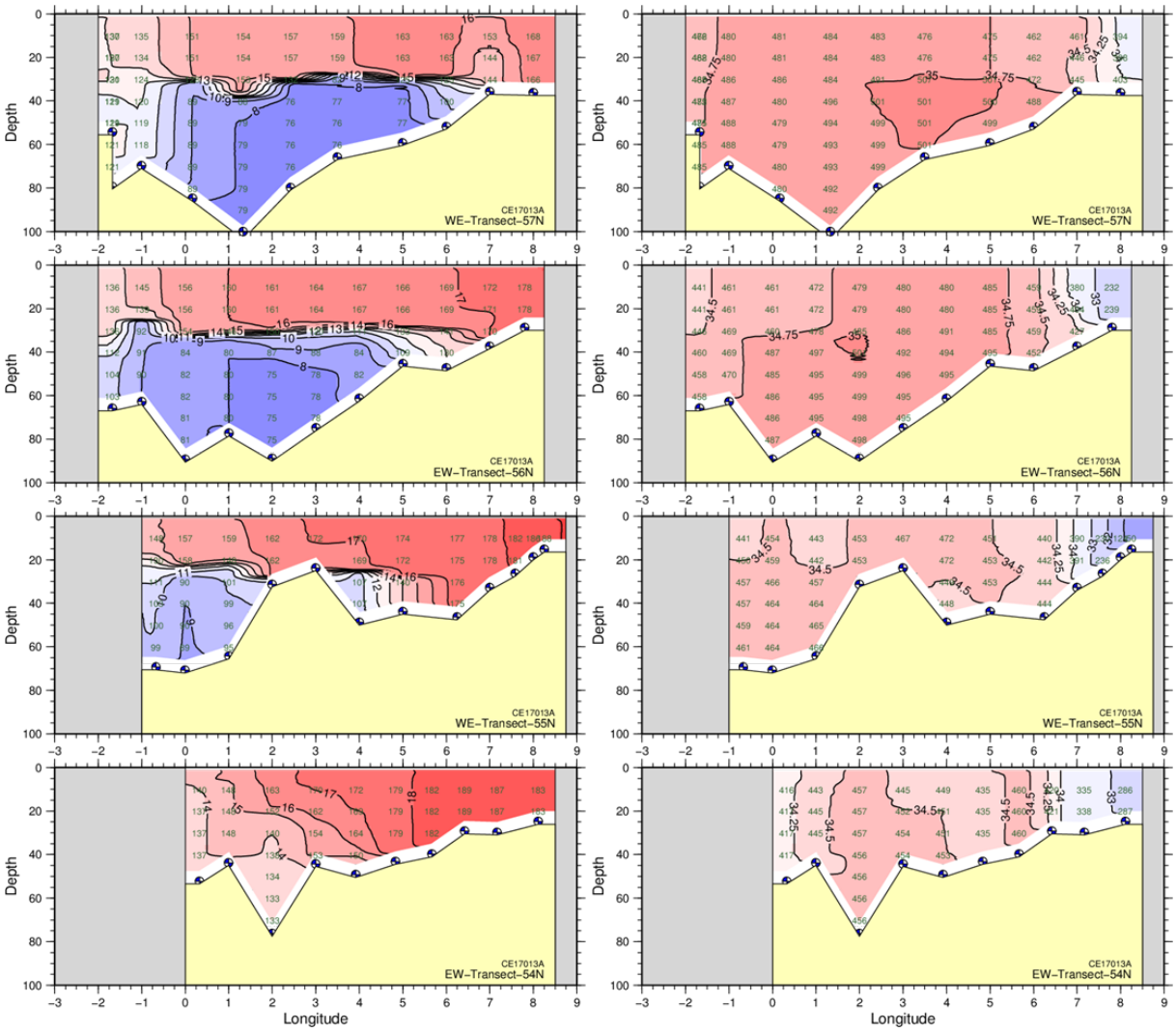

Fig. 2.2c: *Vertical temperature (left) and salinity (right) sections along 54°, 55°, 56°, and 57° N basing on CTD data. The numbers in the temperature sections give the temperatures×10 in °C for selected data points. The numbers in the sanity section give the (salinities×100) - 3000 for selected data points in psu.*

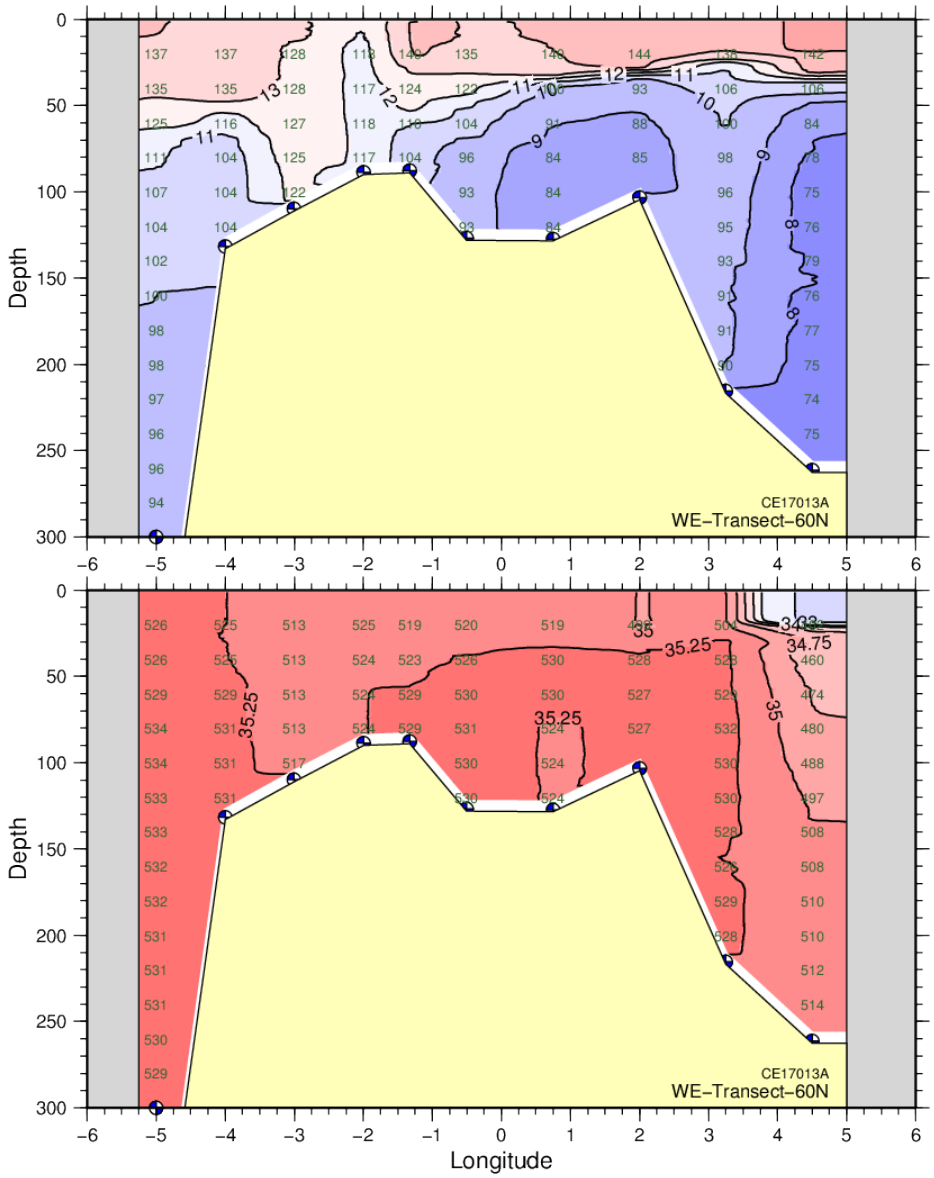

Fig. 2.2d: *Vertical temperature (top) and salinity (bottom) sections in °C along the 60° N basing on CTD data. The numbers in the temperature sections give temperatures×10 in °C for selected data points. The numbers in the sanity section give the (salinities×100) - 3000 for selected data points in psu.*

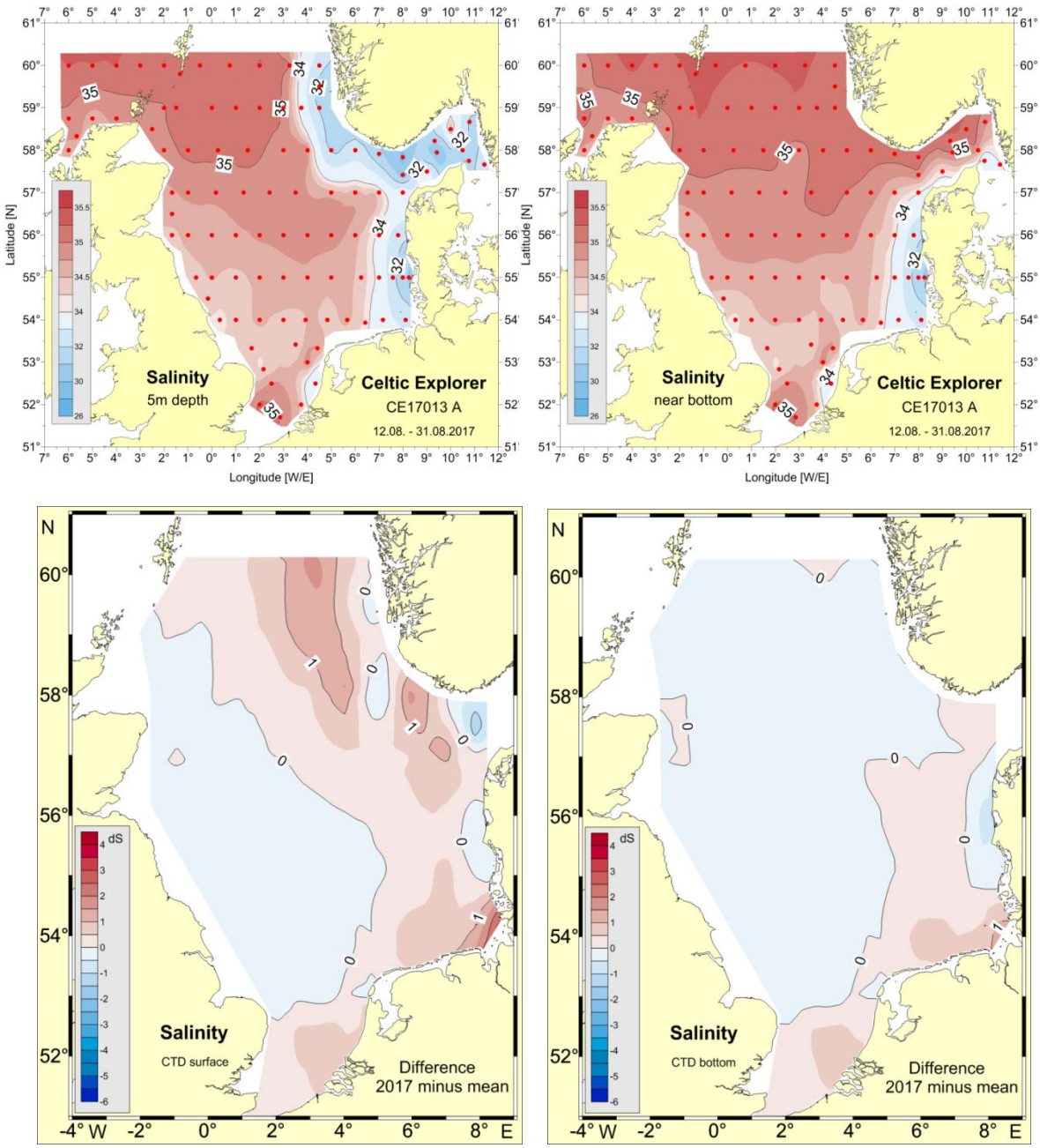

Fig. 2.2e: *Top: Horizontal surface (left) and bottom salinity distribution (right). Bottom: Salinity anomalies (2017 – reference period 2000-2010), in the surface (left) and bottom layer (right).*

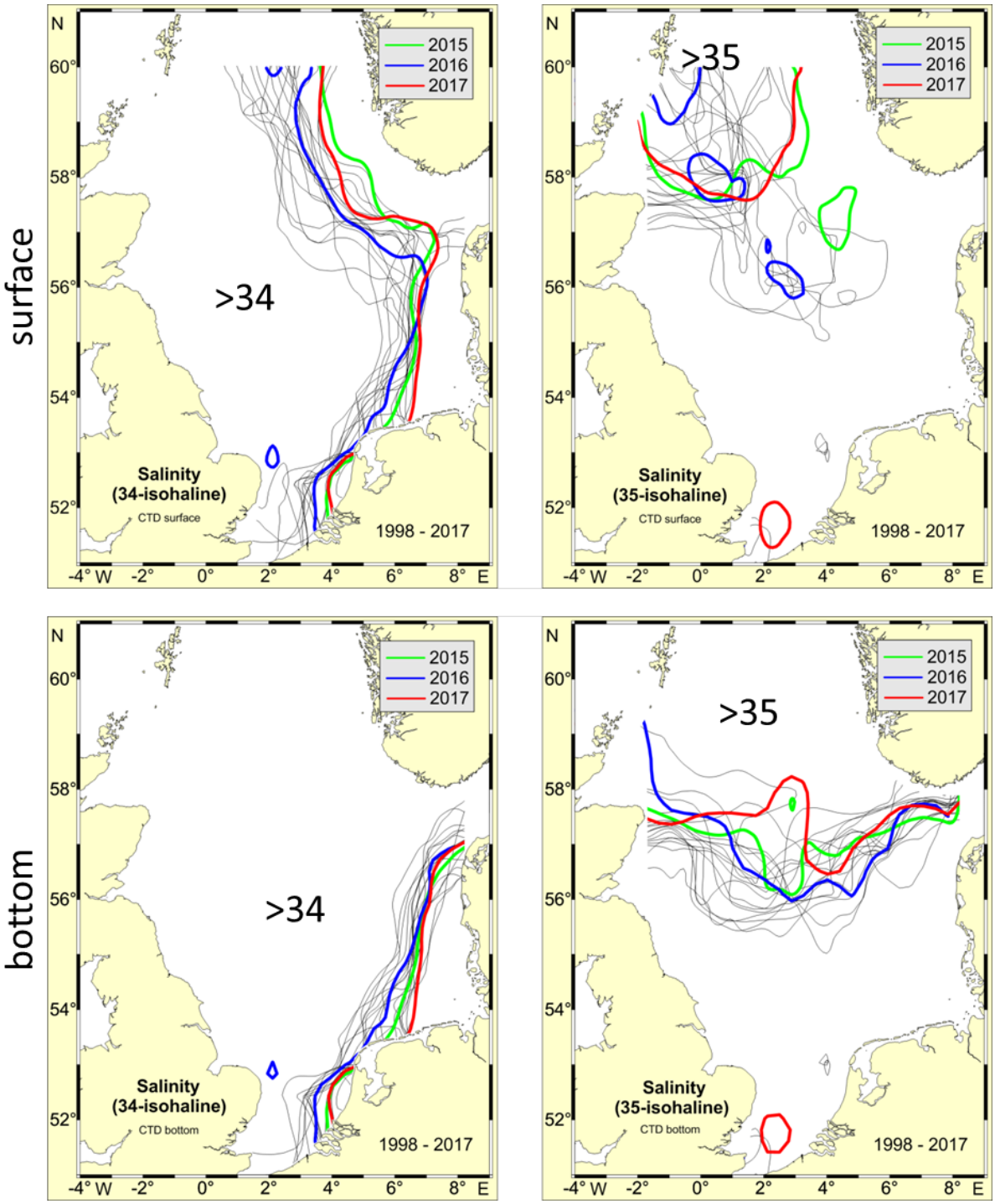

Fig. 2.2f: *Position of the 34 (left) and 35 (right) isohalines 1998 – 2017. Top panel: surface layer, bottom panel: bottom layer. Red: 2017, blue: 2016, green: 2015, and grey: 1998-2014.*

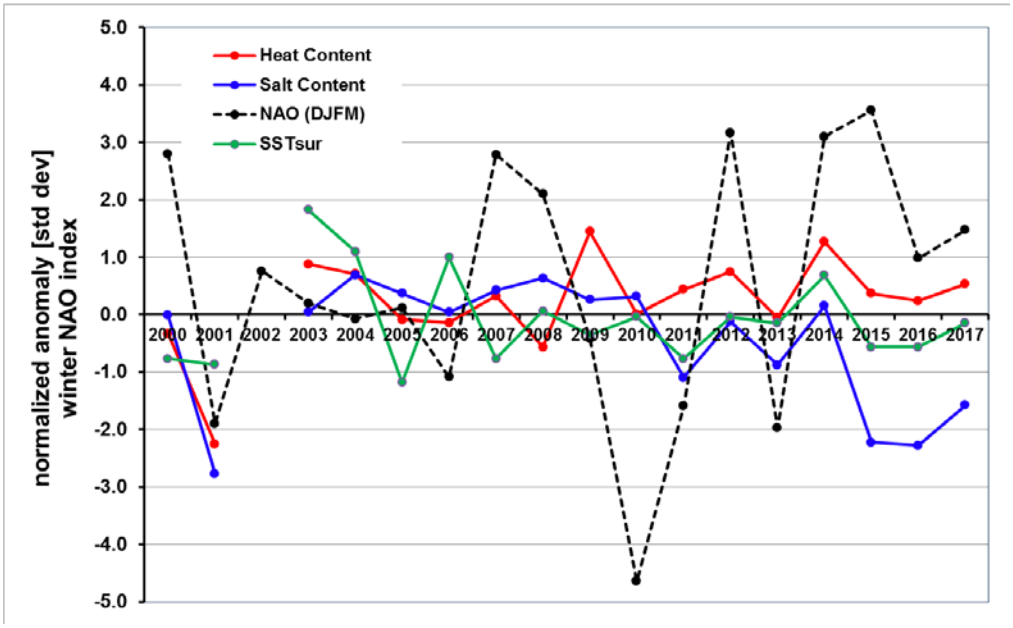

Fig. 2.2g: *Normalised anomaly of total heat and salt content and mean SST of survey period in standard deviations. Broken line: Hurrell winter NAO index (station based, DJFM)[3], reference period 2000-2010 but without 2002.*

3 Summary Table

		Annual Means				North Sea Summer Survey Data					
		annual SST		Elbe run-off		SST survey period		total Heat Content		total salt cntent	
year	NAO winter index[1)]	$mean_l$ [°C]	Δ [std dev]	mean [km³/a]	Δ [std dev]	$mean_r$ [°C]	Δ [std dev]	mean [x 10^{21} J]	Δ [std dev]	mean [x 10^{12} t]	Δ [std dev]
1999	1.70	10.7	0.84	21.22	-0.12	15.2	-0.87	1.427	-2.38	1.122	-0.66
2000	2.80	10.4	0.31	20.41	-0.25	15.3	-0.77	1.603	-0.33	1.134	-0.01
2001	-1.90	10.4	0.37	18.99	-0.48	15.2	-0.87	1.438	-2.25	1.083	-2.77
2002	0.76	10.9	1.29	35.69	2.24	15.4	-0.66	1.587	-0.52	1.131	-0.17
2003	0.20	11.0	1.40	19.79	-0.35	17.8	1.83	1.707	0.88	1.135	0.04
2004	-0.07	10.7	0.91	16.03	-0.97	17.1	1.10	1.692	0.71	1.147	0.69
2005	0.12	10.5	0.53	21.08	-0.14	14.9	-1.18	1.624	-0.08	1.141	0.37
2006	-1.09	11.0	1.32	22.29	0.05	17.0	1.00	1.619	-0.14	1.135	0.04
2007	2.79	10.9	1.23	21.98	0.00	15.3	-0.77	1.659	0.32	1.142	0.42
2008	2.10	10.7	0.95	20.25	-0.28	16.1	0.06	1.583	-0.56	1.146	0.64
2009	-0.41	10.6	0.74	20.06	-0.31	15.7	-0.35	1.755	1.44	1.139	0.26
2010	-4.64	9.9	-0.52	31.08	1.49	16.0	-0.04	1.632	0.01	1.140	0.31
2011	-1.59	10.4	0.28	26.30	0.71	15.3	-0.77	1.669	0.44	1.114	-1.09
2012	3.17	10.4	0.23	20.12	-0.30	16.0	-0.04	1.695	0.74	1.132	-0.12
2013	-1.97	10.0	-0.44	32.11	1.66	15.9	-0.15	1.627	-0.05	1.118	-0.88
2014	3.10	11.4	2.55	15.00	-1.13	16.7	0.68	1.740	1.32	1.137	0.15
2015	3.56	10.6	0.65	15.00	-1.13	15.5	-0.56	1.663	0.37	1.093	-2.23
2016	0.98	11.0	1.38	15.31	-1.08	15.5	-0.56	1.652	0.24	1.092	-2.28
2017	1.47	10.8	0.66	18.25	-0.60	15.9	-0.15	1.677	0.53	1.105	-1.53
reference period	-	**1981-2010**				**2000-2010**					

[1)] J. Hurrell NOA winter station based index (DJFM)

Δ is the normalized anomaly in standard deviation relative to the reference period

anomaly [std dev]	≤ -2	≤ -1	≤ 0	> 0	≥ 1	≥ 2

Table 2: *Winter NAO (DJFM), annual and area averaged North Sea SST, annual Elbe run-off, area averaged SST of the survey periods, total summer heat and total salt content, and normalised anomalies in standard deviations (Δ) 1999-2017.*

[3] https://climatedataguide.ucar.edu/sites/default/files/climate_index_files/nao_station_djfm.txt

Working Document **ICES 2018**
Working Group on Oceanographic Hydrography
23 April 2018

Norwegian Waters (Areas 8-11)

Kjell Arne Mork, Jon Albretsen, and Randi Ingvaldsen (editors)
Institute of Marine Research,
P.O. Box 1870 Nordnes, 5817 Bergen, Norway

Main summary

The temperatures of the inflowing Atlantic water were in 2017 above the long-term means (1981-2010) for the whole region. The salinity in the AW was below the long-term means in the south and close to or higher than the normal in the north. The heat content increased in the North and Norwegian Seas and it was record-high in the Norwegian Sea. In the Barents Sea the ice cover during 2017 was below the long-term mean during the whole year.

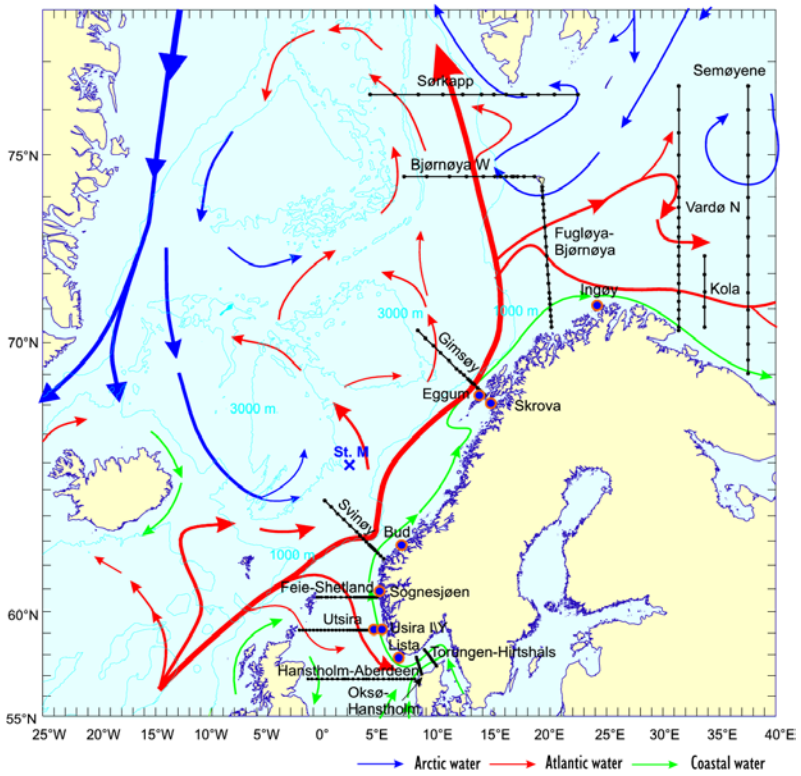

Figure 1. *Standard sections and fixed oceanographic station worked by Institute of Marine Research, Bergen. The main surface currents are also shown.*

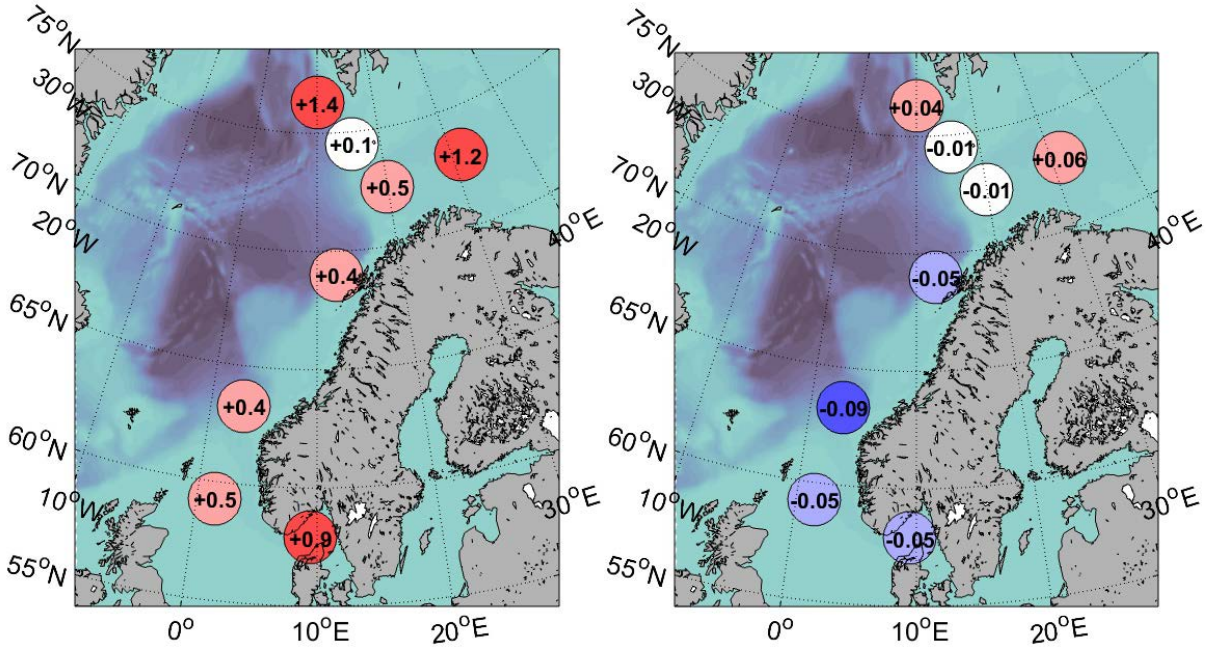

***Figure 2**. Annual temperature anomalies (a: left figure) and annual salinities (b: right figure) at the standard sections for 2017. The anomalies are relative to 1981-2010 and averages over 50-200 m depth.*

The Norwegian Sea

Kjell Arne Mork and Øystein Skagseth

Summary

- Record high heat content in the Norwegian Sea (spring 2017)
- The fresh water content in the Norwegian Sea is slightly above the long-term mean and there is a freshening trend
- The inflowing AW is warmer than normal and notable fresher in the south, but it is still saltier in the north compared to the long-term mean (Fig. 2).
- The salinity minimum in the Norwegian Sea Arctic Intermediate layer has ceased.

The hydrographic condition in the Norwegian Sea is characterized by relatively warm and salt water in the east due to the inflow of the Atlantic water from the south. In the west, however, the hydrographic condition is also influenced by the fresher and colder Arctic water that arrive from the Iceland and Greenland Seas (Fig. 1.)

Fig. 3 shows the development of temperature and salinity in the core of Atlantic Water for the sections in the eastern Norwegian Sea during 2017. For the three sections Svinøy, Gimsøy and Bear Island-West sections, the temperatures during 2017 were near or above normal. On average the temperature for 2017 at the Svinøy and Gimsøy sections were both 0.4°C above the normal, while at Bear Island-West section it was 0.1°C above the normal.

At the Svinøy section a declining trend for salinity started in 2016, and in 2017 the salinity was considerable lower than normal during the whole year. The salinity was also below normal during 2017 at the Gimsøy, while it was close to normal further north at the Bear Island-West section. At the Sørkapp-W section the salinity was still above normal in 2017. On average, the salinity for 2017 is 0.09, 0.05, and 0.01 below the normal for the Svinøy, Gimsøy, and Bear Island-West sections, respectively, while it was 0.04 above the normal at the Sørkapp-W section.

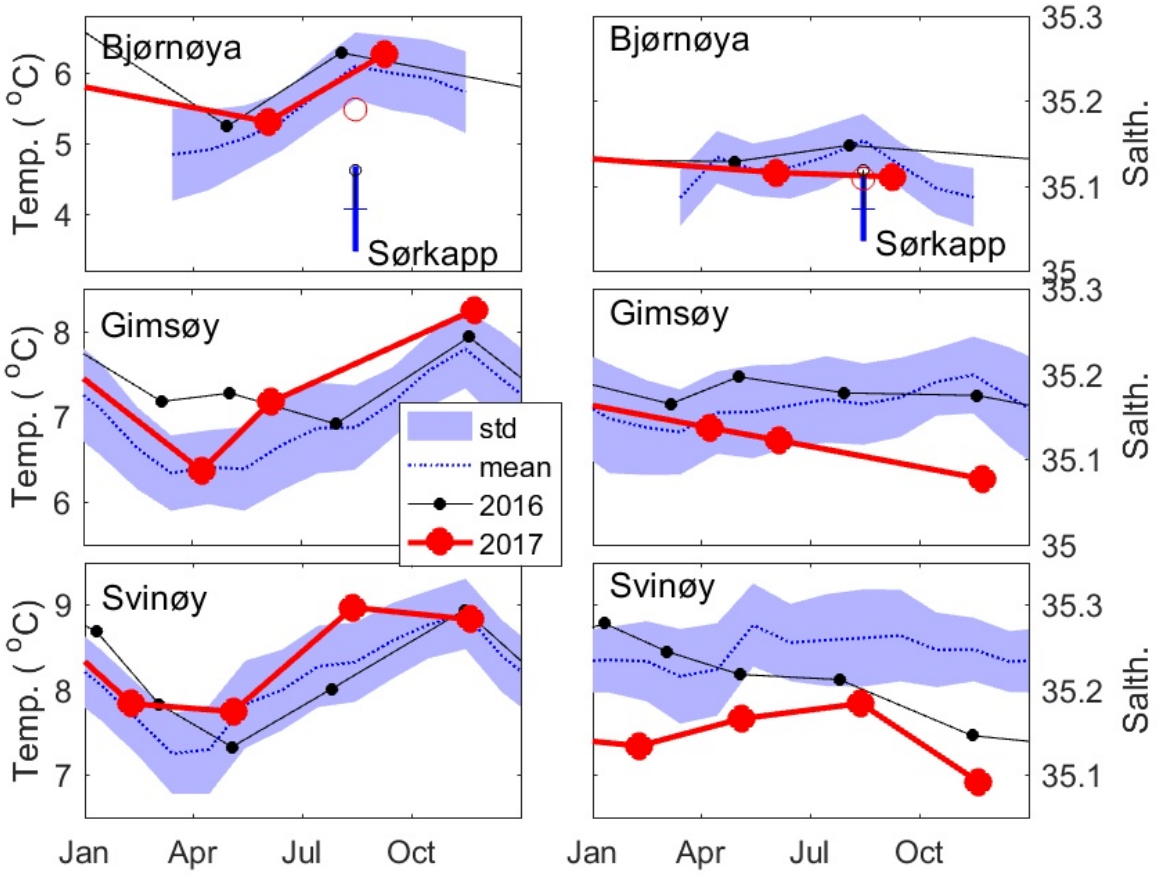

Figure 3. *Temperature (left) and salinity (right) in the core of Atlantic water), averaged between 50 and 200 m depth, for the sections Bjørnøya-W (upper figures), Gimsøy-NW (middle figures), Svinøy section (lower figures) and Sørkapp-W section (in the upper figure, only for August) for the years 2017 and 2016.*

There has been a linear increase of temperature and salinity in all sections from the 1970s to present where 2007 was the warmest year ever, with the exception of the Sørkapp-W section, since the time-series started in 1977 (Figure 4). Then the annual mean temperatures in the sections were 0.6-0.8ºC above the long-term means. After around 2000, the annual means have usually been over the long-term means but have had several oscillations of 2-5 years duration. The temperature seem to have a slight downward trend the recent years at the Svinøy section while further north, particular in the Sørkapp-W section, the temperature has increased. The Atlantic water along the continental slope has since the mid-1990s been significant saltier in all sections until the recent years. In the recent years there was a

remarkable downward trend in salinity especially for the two southernmost sections. At the Sørkapp-W section the salinity has the last 10-15 years been stable and higher than normal.

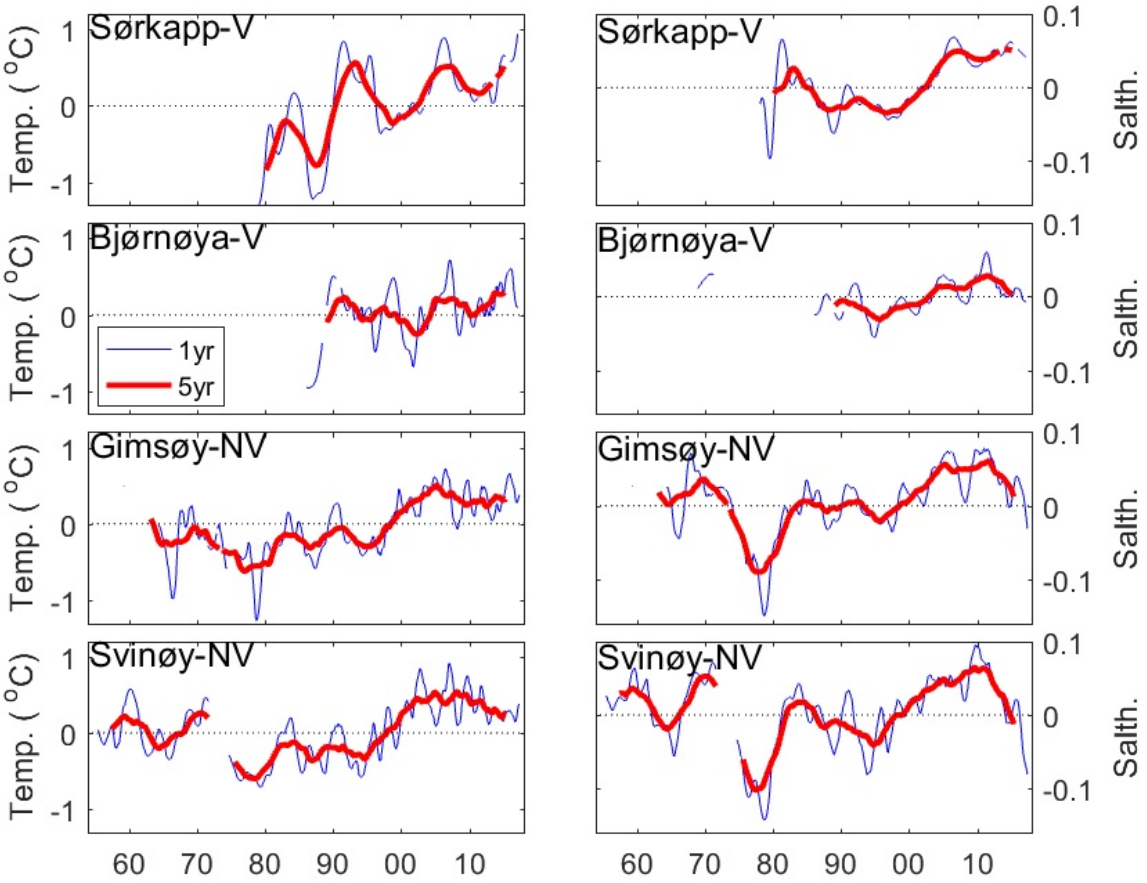

Figure 4. *Temperature (left) and salinity (right) anomalies in the core of Atlantic water, averaged between 50 and 200 m depth, for the sections Svinøy-NW, Gimsøy-NW, Bjørnøya-W and Sørkapp-W. Both yearly and five years averages are shown. The anomalies are calculated relative to the 1981-2010 averages.*

In the period from the end of April to beginning of June an international coordinated pelagic cruise has been performed every year since 1995. Figure 5 shows the temperature distribution, averaged between 0-50 m, 50-200 m and 200-500 m depth in 2017, and the anomalies relative to the long-term mean. The increased influence of the colder and fresher East Icelandic Current in the southern Norwegian Sea is clearly visible. The temperature was lower than normal in the southern and eastern Norwegian Sea. In the basins, at all depths, the temperatures were considerable higher than normal, and in some areas it was more than 1°C higher than normal. The salinity was lower than normal at all depths with the exceptions of coastal areas, and in some extent the western areas (Figure 6). Especially, the southern part was fresher than normal.

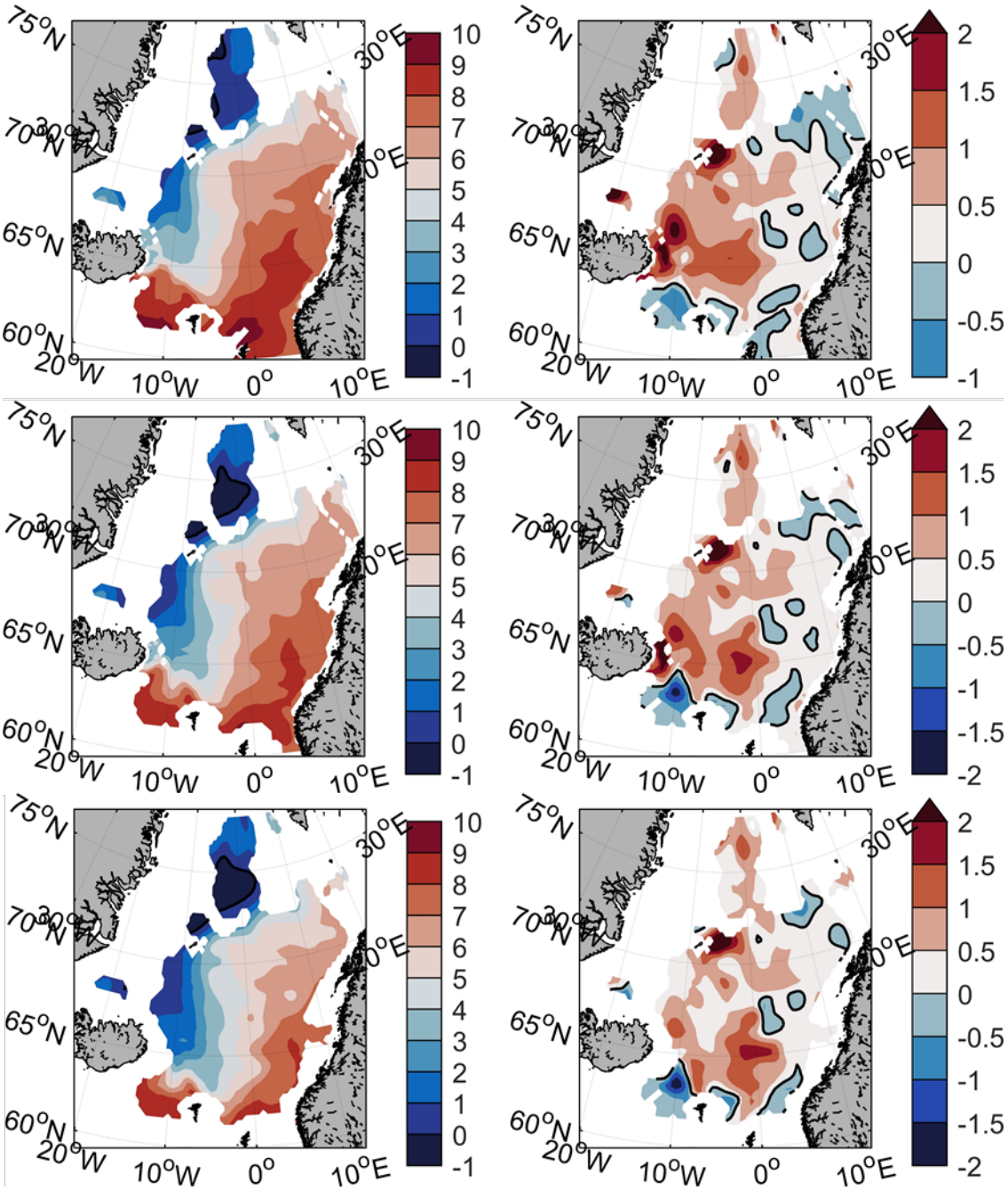

Figure 5. *Left: Temperature, averaged over 50-200 m depth, in May 2017. Right: temperature anomalies, averaged over 0-50m (upper), 50-200 m depth (middle), and 200-500 m (lower) relative to a 1995-2017 mean.*

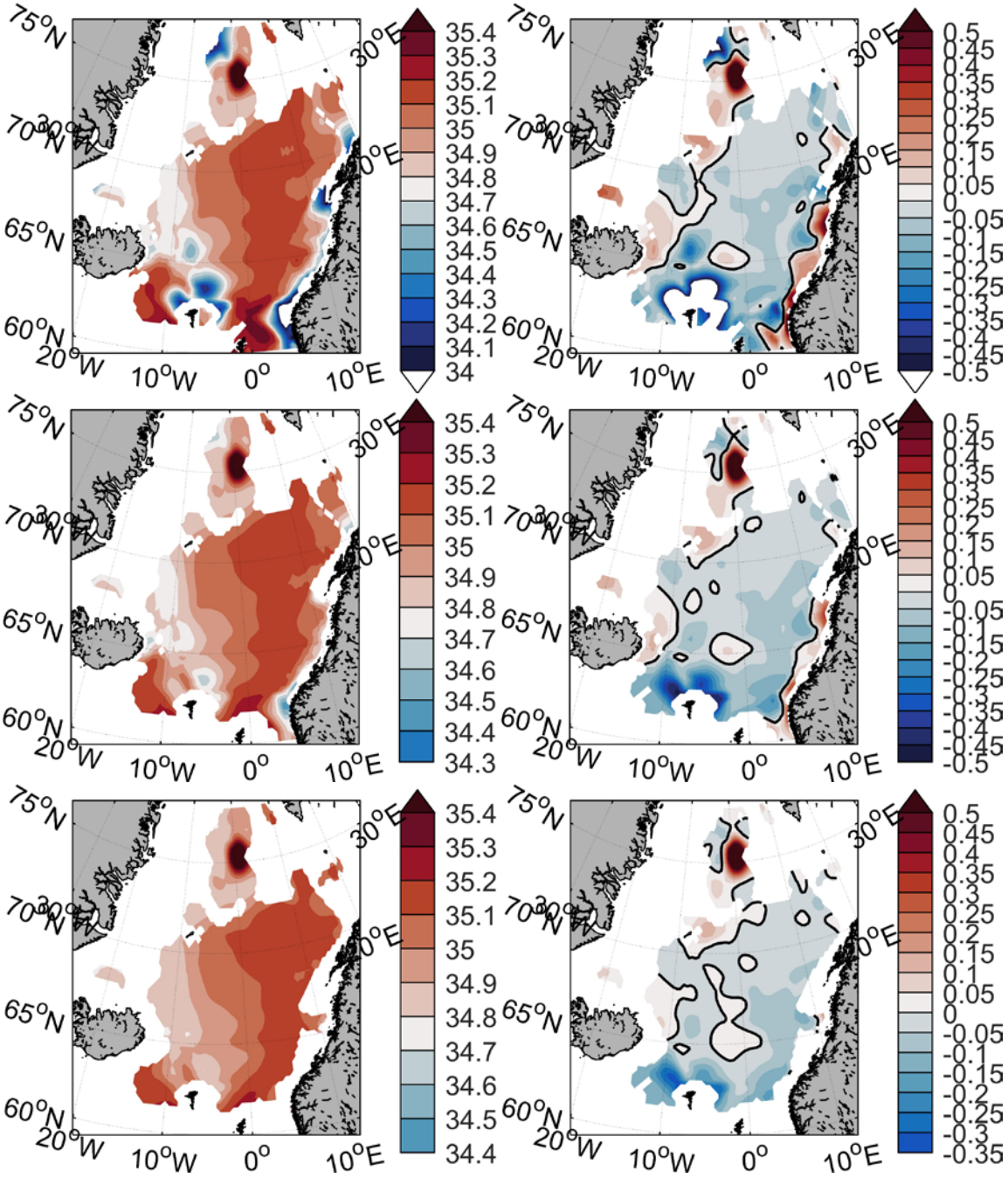

***Figure 6**. Left: Salinity, averaged over 50-200 m depth, in May 2017. Right: salinity anomalies, averaged over 0-50m (upper), 50-200 m depth (middle), and 200-500 m (lower) relative to a 1995-2017 mean.*

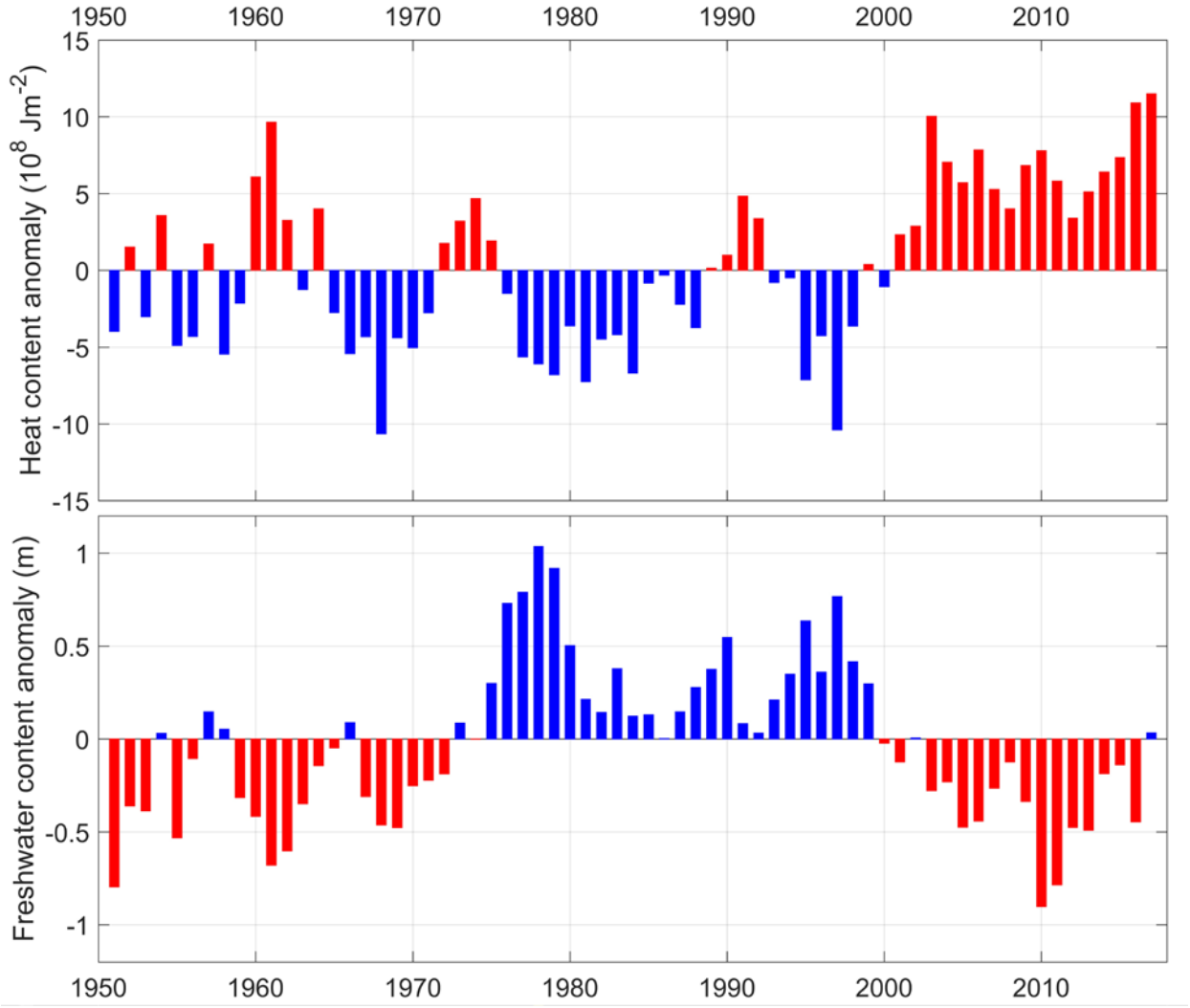

Figure 7. *Heat (upper) and freshwater (lower) content anomaly during spring (1951-2017) in Atlantic Water, averaged over the Norwegian Sea. Note that the y-axis is reversed for the freshwater content.*

The heat content of AW in the Norwegian Sea has since 2000 been above the long-term-mean (Figure 7). Following a five-year period of increasing heat content, the upper layer of the Norwegian Sea reached a new record-high value in 2017. The freshwater content anomaly was at minimum in 2010 (i.e., the water mass was saltier than normal) and increased afterwards to slightly positive in 2017.

The area of total occupied Atlantic Water in the Svinøy section is shown in Figure 8. After a relatively low extension of AW in the first half of the 1990s the area of AW has increased. In 2017 the area was higher than the long-term mean for both the spring and summer. The averaged temperature in the occupied AW has increased linearly since 1978 and has, during the whole period, become 0.8ºC warmer for both spring and summer. In 2017 the temperatures increased from 2016, and were 0.6ºC and 0.5ºC higher than the long term means for spring and summer, respectively.

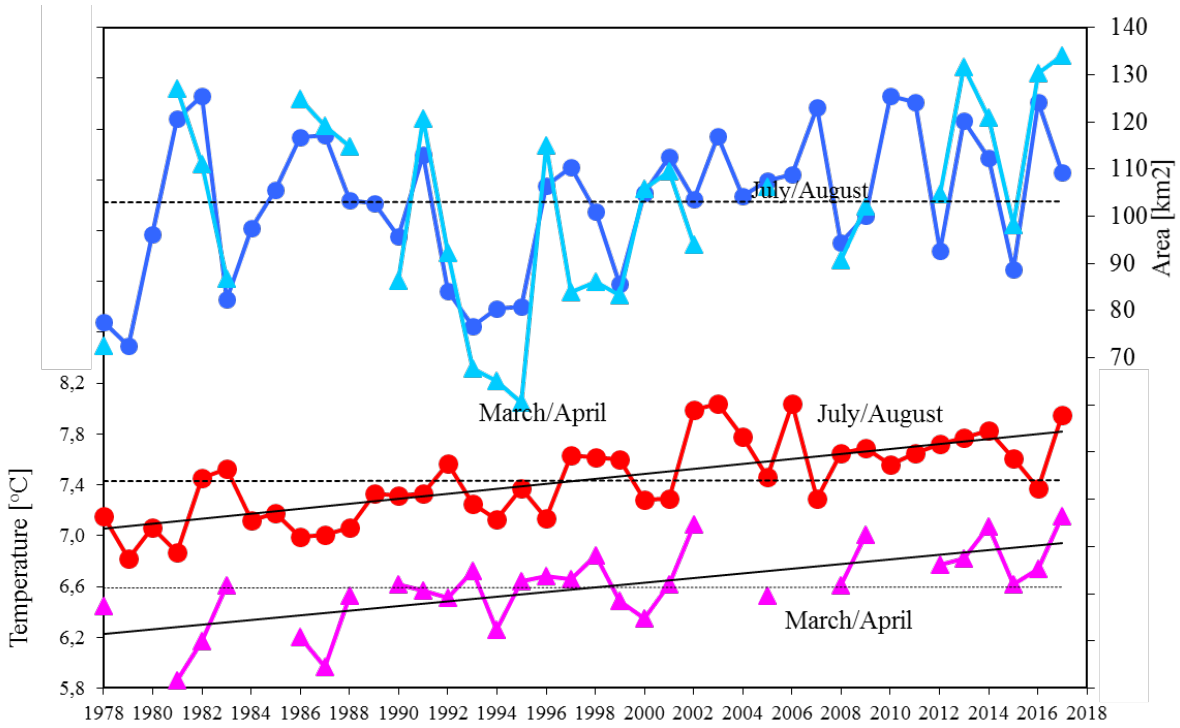

Figure 8. *Area of Atlantic water and averaged temperature of AW in the Svinøy section for spring (March/April) and summer (July/August).*

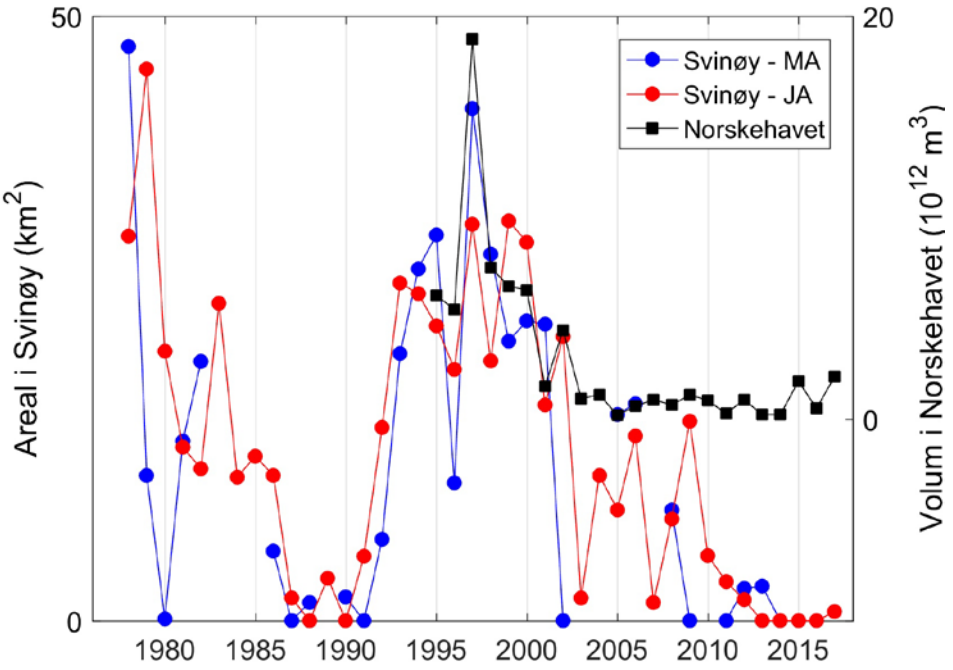

Figure 9. *Amount of Arctic water (salinity<34.9) at the four westernmost stations in the Svinøy-NW section at 50-500 m depth in spring (March-April, MA) and summer (July-August, JA), and in the southern Norwegian Sea (62-68 N, 150-300 m depth).*

The variability of the inflow of Arctic water from the Iceland and Greenland Sea to the Norwegian Sea has potentially large climate and ecosystem effects because the temperature and salinity properties are very different from the Atlantic water. The amount of Arctic water is measured several times per year in the Svinøy section and once per year in the Norwegian Sea. Figure 9 shows that the amount of Arctic water has varied largely since the 1970s. It was high in the late 1970s and from the early 1990s to the early 2000s. In the late 1980s and after the 2000s the amount was small. In 2017, the amount of Arctic water in the Svinøy section and the Norwegian Sea was slightly above the bottom level.

Intermediate layer

The development of temperature and salinity in the upper 2000 m of the Norwegian Sea can be followed with monthly resolution using Argo data from 2002. Figure 10 shows all the locations of the Argo profiles in the Norwegian and Lofoten Basins.

The temperature and salinity from 2002 to 2018 in the Norwegian Basin are shown in Figure 11. Below 500 m there has been a decrease in temperature during this period. The salinity minimum (S<34.9) at 500-1000 m depth existed until around 2013-2014 and afterwards it disappeared. In the Lofoten Basin the temperature declined at 1500 m depth and deeper (Figure 12). The salinity in the intermediate layer shows here similar trend as in the Norwegian Basin. After 2010 the salinity minimum has more or less disappeared.

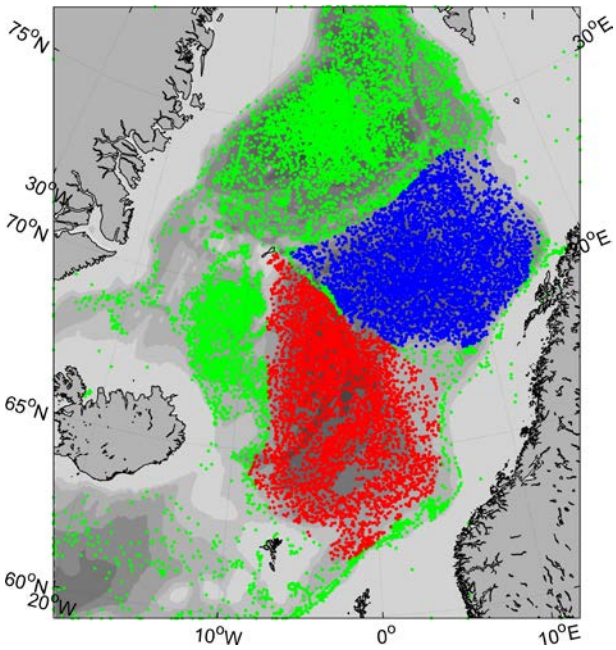

Figure 10. *Locations of all Argo profiles used (red dots: Norwegian Basin, blue dots: Lofoten Basin).*

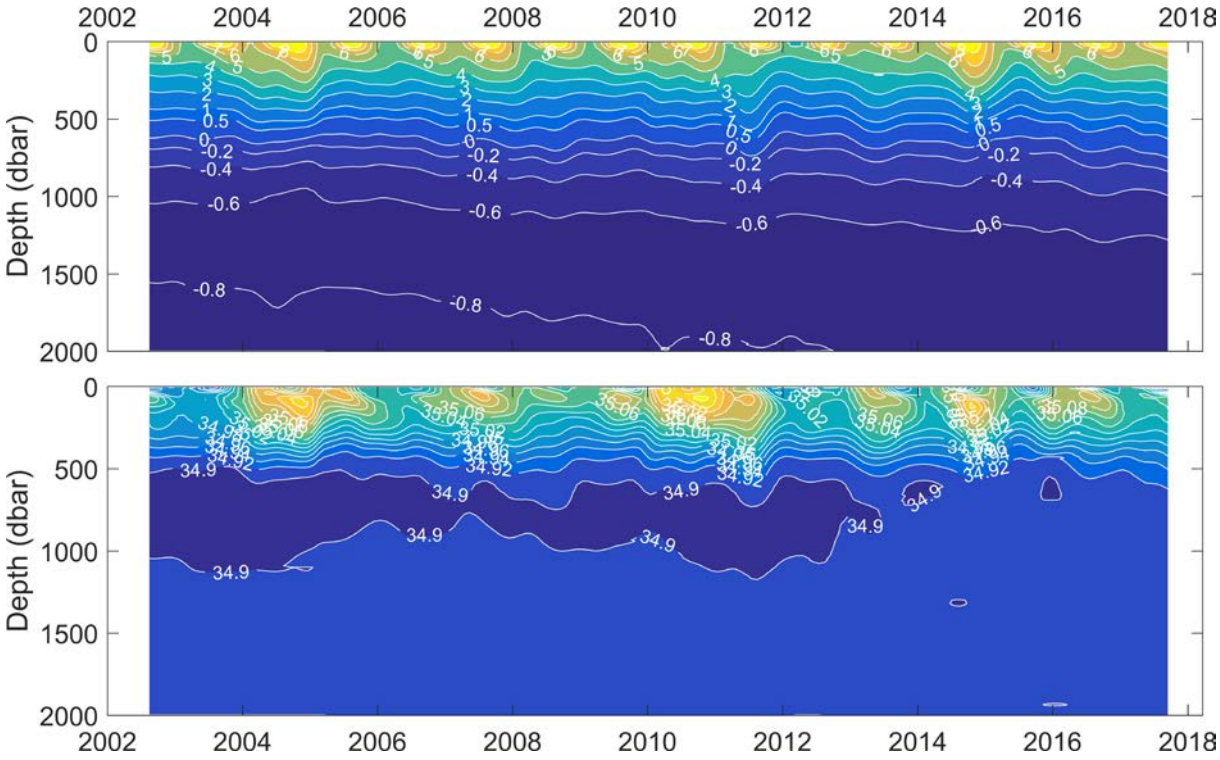

Figure 11. *Temperature and salinity from Argo floats in the Norwegian Basin.*

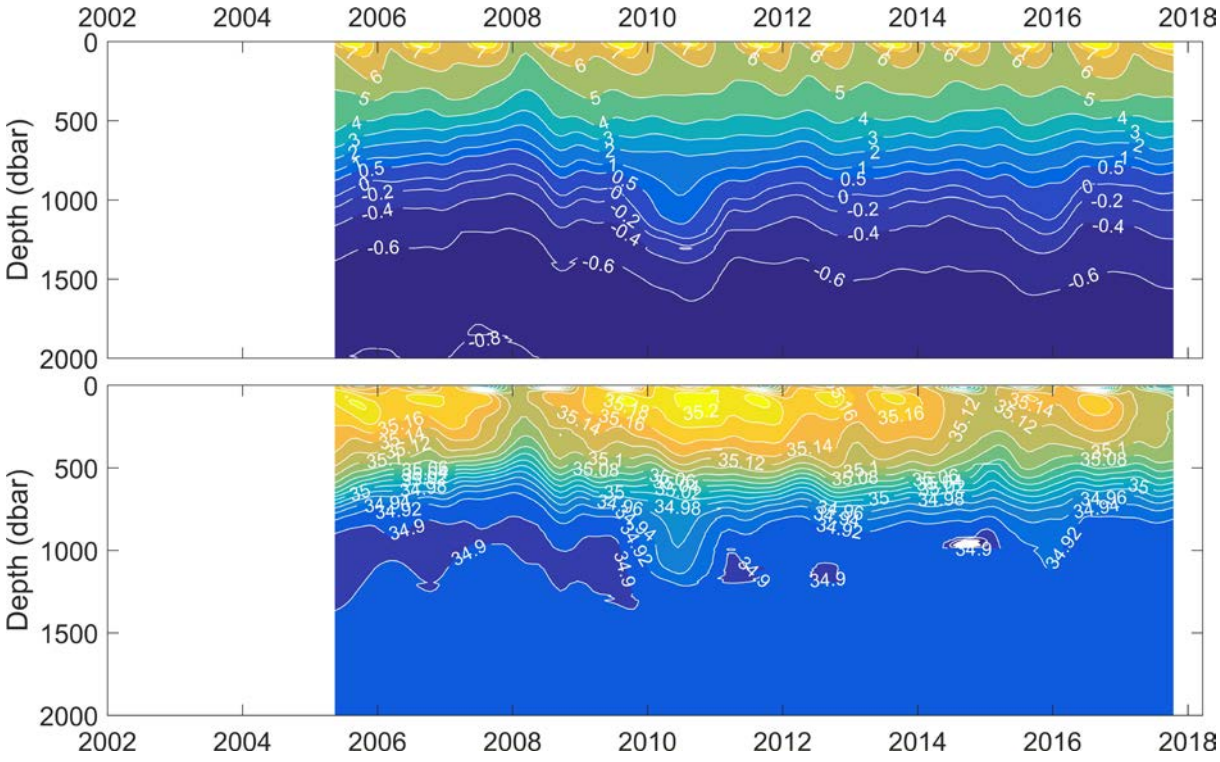

Figure 12. *Temperature and salinity from Argo floats in the Lofoten Basin.*

The Barents Sea

Randi Ingvaldsen

Summary

- The temperature in most the Barents Sea is still higher than the long-term mean, but lower than in 2016. Highest anomalies were observed in the eastern Barents Sea. Just east of Svalbard, temperatures at, or just below, the long-term mean dominated.
- There were small amounts of ice both winter and summer compared to the long-term mean, but more winter sea ice than in 2016.
- The inflow to the Barents Sea showed a maximum in 2015 with annual values of almost 1 Sv above the long-term mean. The inflow reduced to long-term mean values in 2016.

The Barents Sea is a shelf area, receiving inflow of Atlantic water from the west. The inflowing water demonstrates considerable interannual fluctuations in water mass properties, particularly in heat content, which again influence on winter ice conditions. The variability in the physical conditions is monitored in two sections. Fugløya-Bear Island is situated where the inflow of Atlantic water takes place; the Vardø-N section represents the central part of the Barents Sea. In both sections there are regular hydrographic observations, and in addition, current measurements have been carried out in the Fugløya- Bear Island section continuously since August 1997.

The Fugløya-Bear Island Section, which capture all the Atlantic Water entering the Barents Sea from south-west, showed temperatures of 0.4-0.7 °C above the long-term mean during 2017 (Figure 13). This is slightly lower as compared to the two years before.

The volume flux of Atlantic Water flowing into the Barents Sea has been monitored with current measurements in the section Fugløya-Bjørnøya since 1997. The inflow is predominantly barotropic, with large fluctuations in both current speed and lateral structure. In general, the current is wide and slow during summer and fast, with possibly several cores, during winter. The volume flux resembles the velocity field and varies with season due to close coupling with regional atmospheric pressure. Southwesterly wind, which is predominant during winter, accelerates flow of Atlantic Water into the Barents Sea; whereas, weaker and more fluctuating northeasterly wind common during summer, slows the flow. The mean transport of Atlantic Water into the Barents Sea is 2 Sv (Sv = 10^6 m^3s^{-1}) with an average of 2.2 Sv during winter and 1.8 Sv during summer. During years in which the Barents Sea changes from cold to warm marine climate, the seasonal cycle can be inverted. Moreover, an annual event of northerly wind causes a pronounced spring minimum inflow to the western Barents Sea; at times, even an outward flow.

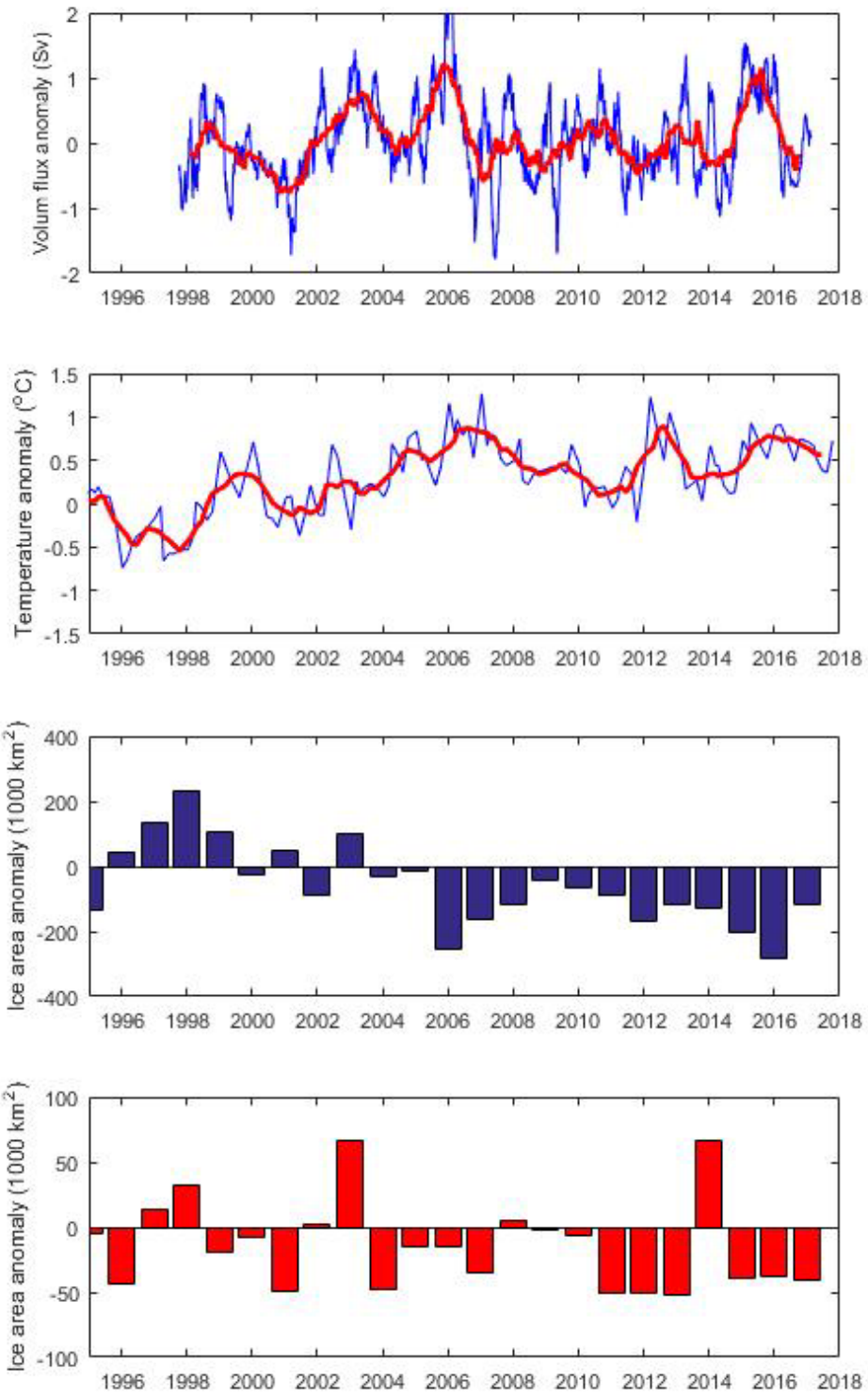

Figure 13. *Upper panel: Volume flux anomalies (in Sv) in the Atlantic Water in the south-western entrance to the Barents Sea. The lines show 3 months (blue) and 1 year (red) moving average. Second panel: Temperature anomalies in the Atlantic Water in the 50-200 m layer. The lines show measured values (blue) and 1 year (red) moving average. Lower panels: Ice area in the Barents Sea (10–60ºE, 72-82ºN) at maximum (April) and minimum (September) ice coverage.*

On average, the Atlantic current brings about 2 Sv of water and 50 TW (relative 0ºC) of heat into the Barents Sea. The volume and heat flux vary with periods of several years, and was significantly lower during 1997–2002 than during 2003–2006. After 2006, the inflow was relatively low for several years before increasing during winter 2014–2015. The year of 2015 had maximum annual inflow when comparing the full time series 1997-2017, with volume and heat fluxes almost 1.5 times higher (~3 Sv/72 TW respectively) then the long-term mean. The inflow decreased again in 2016, making that year close to the long-term mean. The data series presently stops in March 2017, thus no information about the summer, fall and early winter 2017 is yet available.

Hydrographic observations during late summer 2017 show that most of the Barents Sea had temperatures anomalies higher than 0.5ºC in the 50-200 m depth layer, except in the region east of Svalbard (Figure 14). In this region the temperatures were at, or just below, the long-term mean, and as compared to the year before, the temperatures had decreased by 0.5ºC. In the eastern Barents Sea, temperatures 0.5-1ºC above the long-term mean prevails.

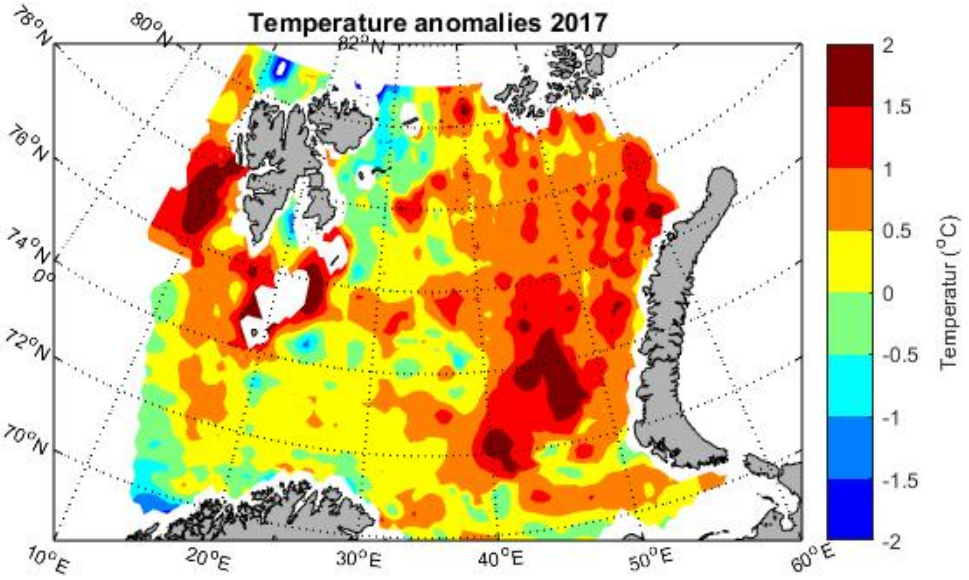

Figure 14. *Temperature anomalies in 50-200 m depth in August-September 2017 relative to the long-term mean (1981-2010).*

The variability in the ice coverage in the Barents Sea is linked to the temperature of the inflowing Atlantic water, the wind field and the import of ice from the Arctic Ocean and the Kara Sea. The ice has a response time on temperature changes in the Atlantic inflow (one-two years), and usually the sea ice distribution in the western Barents Sea respond faster than in the eastern part. There has been a linear negative trend in the ice area, particular in the winter, the last 40 years. The winter of 2016 had record low sea ice cover, likely caused by the record high volume inflow of Atlantic Water in 2015 (Figure 13 and 15). The sea ice cover during winter 2017 were also low, but still with substantially more sea ice at the end of winter as

compared to 2016 (Figure 15). The summer of 2017 was quite similar to the two years before; less sea ice than the long-term mean, but more sea ice than in summer 2001, 2004 and 2011-2013.

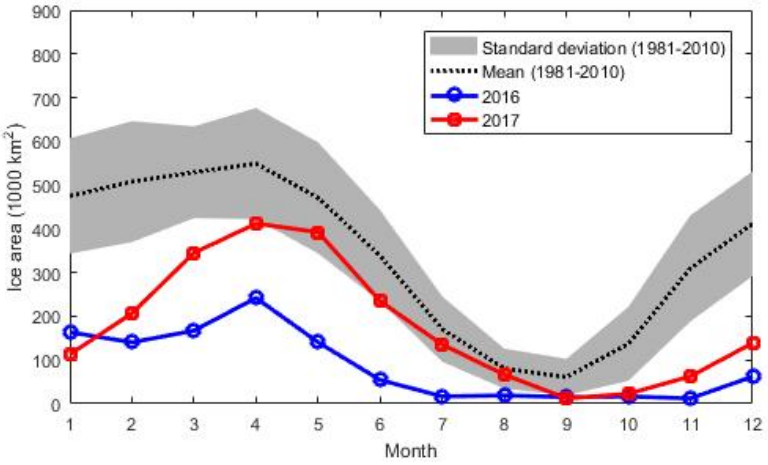

Figure 15. *Seasonal variations in ice cover in the Barents Sea (10–60ºE, 72-82ºN). Long-term mean and standard deviation are calculated based on the period 1981-2010.*

The North Sea

Jon Albretsen, Morten D. Skogen and Solfrid S. Hjøllo

Summary

- In 2016 and 2017, the North Sea and the Skagerrak was warmer than normal throughout both years, and the surface layer was remarkably warm in late summer and autumn.
- The inflow of Atlantic water was slightly below average in 2017, and a mild winter and warm summer gave an increase in the heat content in the North Sea.

Temperature and water masses

The sea surface temperatures in the Skagerrak and the North Sea were warmer than normal (1971-93) throughout 2017. The magnitude of the warm anomaly varied between months and between the northern and southern North Sea. During the first six months of 2017 the sea surface temperature was about 1ºC above normal in the entire North Sea, except in the southern part where the anomaly was higher. Late summer and autumn was particularly warm in the Eastern North Sea and the Skagerrak, with a positive anomaly of about 2ºC in the period September-November. The warming was more moderate in December 2017 with temperatures 0-1ºC above normal.

Source is BSH, Bundesamt für Seeschifffahrt und Hydrographie, http://www.bsh.de/en/Marine_data/Observations/Sea_surface_temperatures/anom.jsp.

The Skagerrak deep-water (~100-200m depth) is mainly characterized by Atlantic Water (AW), and a fixed station approximately 10km off the Torungen lighthouse near Arendal, Norway, is used to indicate the hydrographical variability. The AW temperatures were significantly warmer than the long-term average (reference period is here 1981-2010) during the whole 2017 except in January where the measured temperature indicated normal conditions. While the temperatures in the AW in the Skagerrak were higher than normal in 2016, the values were even higher in 2017 (more than one standard deviation). The salinities in the AW fluctuated around normal conditions with slightly higher values during winter and lower salinities during autumn (Figure 16).

The Norwegian Trench is an elongated depression in the sea floor off the southern coast of Norway reaching from the Norwegian west coast to the Oslofjord in the Skagerrak. Off the Norwegian southwest coast, it is about 270 m deep, and its deepest point is off Arendal where it reaches more than 700 m (close to the central Skagerrak). The Skagerrak basin can then be considered similarly to a fjord basin where stagnating water masses below sill depth are exchanged more or less regularly. Exchange of Skagerrak bottom waters takes place every 1-5 years and usually during March/April. After 1990, 14 exchanges are registered, the last one in March/April 2013 (Figure 17). The Skagerrak bottom water is either replaced by heavier deep AW subducting after flowing southward above the sill in the Norwegian Trench, or by cooled North Sea surface water because of heavy winter cooling. The latter exchange mechanism has been rare during the last 30 years, and a Skagerrak bottom water cooling (along with an increase in oxygen level) has only been registered in 1996 and 2010 during the last three decades. The oxygen level in the Skagerrak basin was close to an overall minimum in 2016, compared with recordings from 1970, and during autumn 2016/winter 2017 a partial increase was recorded. The salinity in the bottom water has remained almost constant, while the temperature has increased to the highest level recorded since 1952. This implies that the bottom water density has decreased, and a new exchange is expected in near future.

Transports and heat content

The ocean circulation model NORWECOM is conducted to calculate transports of inflowing AW through a transect between Utsira, Norway, and the Orkneys. The main AW inflow pathway into the North Sea is from the north following the western slope of the Norwegian Trench. The main proportion of this AW deep water enters the Skagerrak and then circulates anti-clockwise following the direction of the Norwegian Coastal Current. The model results for all months in 2017 indicate that the AW inflow were slightly below the long-term average (reference period is 1985-2010). The net inflow of AW to the North Sea through the English Channel was also low in 2017, implying that the overall supplement of AW to the North Sea and the Skagerrak was relatively low the whole year (Figure 18).

Both seasonal variability and long-term oscillations of the heat content in the North Sea are computed for 1985-2016 from the NORWECOM model simulation. The minimum and maximum heat content will reflect the degree of winter cooling and summer heating of the North Sea, respectively (Figure 19). In 2016, both a mild winter and a warm summer had a large positive impact on the heat content in the North Sea. In 2017, the winter was still mild, while the summer was nearly as warm as in 2016. Due to this warming, the heat content increased, but some of this heat was lost during autumn. The accumulated excess of heat was large in 2016 after a mild winter and an extraordinary warm late summer, but leading to a small shortcoming of heat in 2017 built up during previous years.

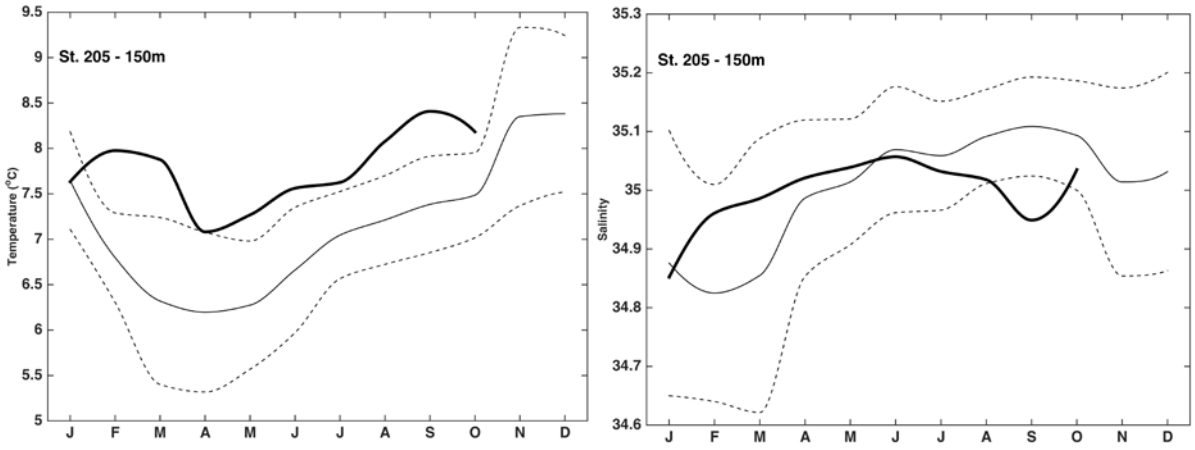

Fig. 16. *Temperature (upper panel) and salinity (lower panel) at 150m depth based on monthly observations in 2017 sampled approx. 10km off Torungen lighthouse near Arendal, representing AW in the Skagerrak. The long-term mean (thin solid line) and the standard deviation (dotted lines) are based on measurements sampled between 1981 and 2010.*

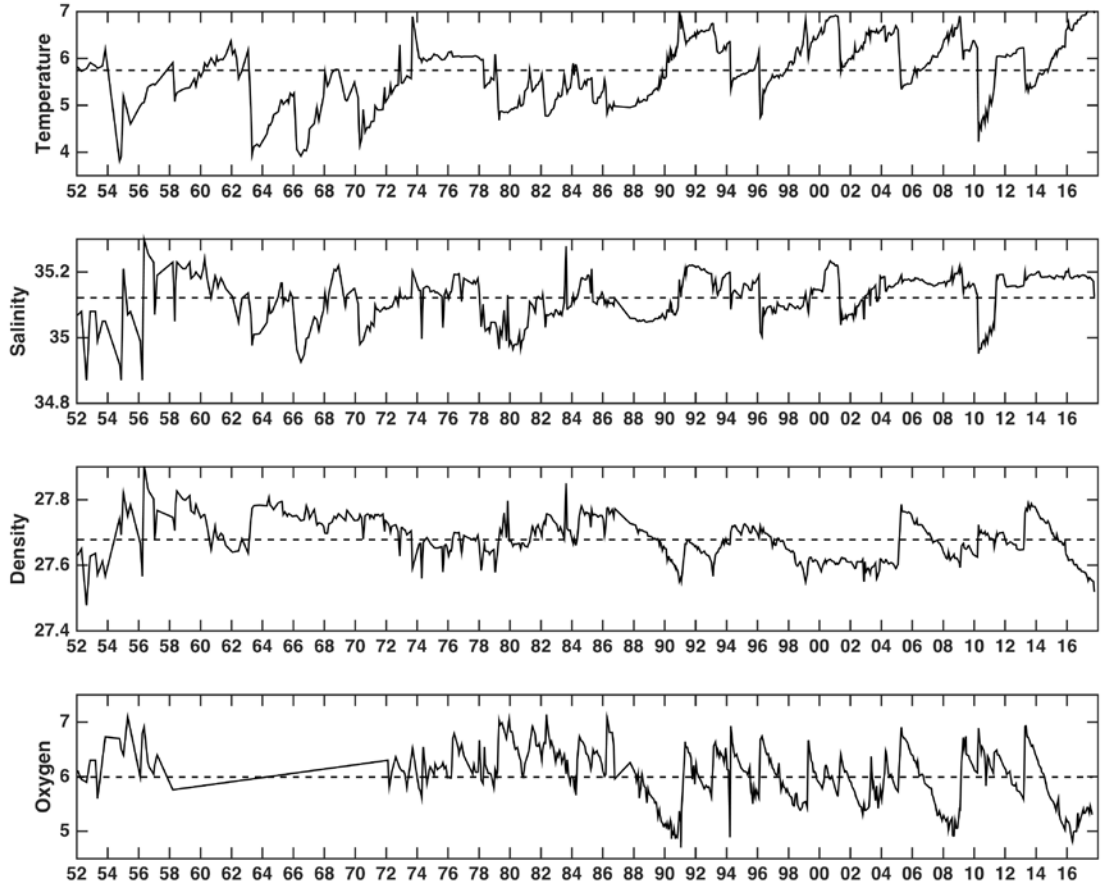

Fig. 17. *Temperature (°C), salinity, density (σ_t in kg/m^3) and oxygen (ml/l) at 600m depth in the Skagerrak Basin from 1952 to 2017. This location depicts the physical environment in the Skagerrak bottom water.*

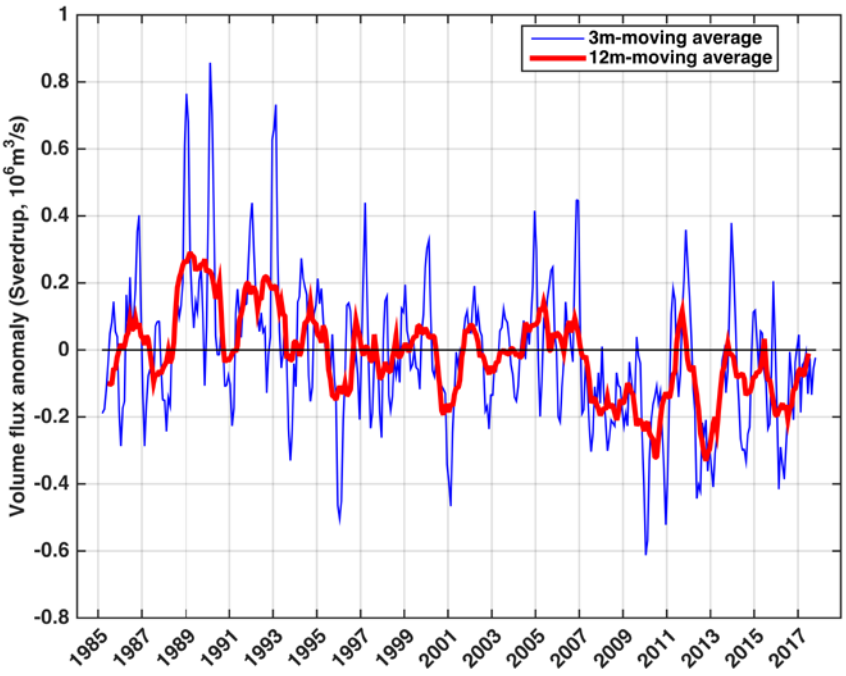

Fig. 18. *Time series (1985-2017) of modelled monthly mean volume transport anomalies of AW into the northern and central North Sea southward between the Orkney Islands and Utsira, Norway. The vertical axis denotes transport anomaly in Sv ($10^6 m^3 s^{-1}$). The anomalies are calculated from the reference period 1985-2010. The blue and red line displays the 3 and 12 months running average, respectively.*

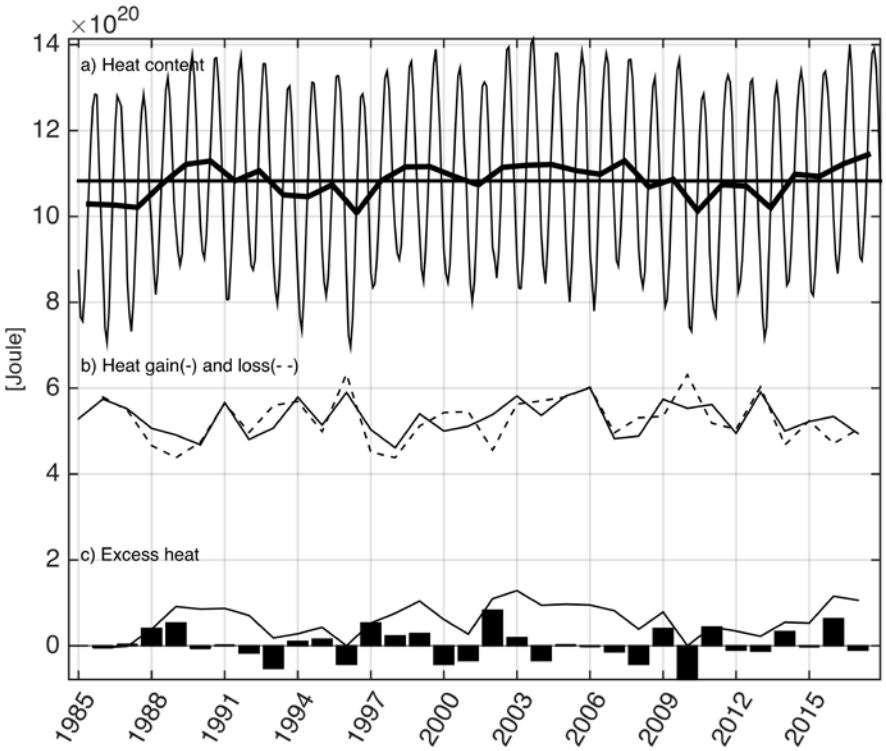

Fig. 19*. a) Modelled North Sea heat content for the period 1985-2017. Monthly (thin line) and annual (thick line) values are shown. b) Heat gain (solid) and loss (dashed line). Heat gain is defined as difference between heat content maximum (in August or September) and minimum (in February or March) for each year. Heat loss is defined as the absolute value of the difference between heat content minimum and maximum the year before. c) Excess heat (bars) and accumulated excess heat (line). Positive values mean a net heat gain, i.e., the winter heat loss is less than the summer heating.*

Hydrographic conditions in the Barents Sea in 2017

A. Karsakov and A. Trofimov

Knipovich Polar Research Institute of Marine Fisheries and Oceanography (PINRO),
6 Academician Knipovich Street, Murmansk, 183038, Russia

The Barents Sea is a shelf sea of the Arctic Ocean. Being a transition area between the North Atlantic and the Arctic Basin, it plays a key role in water exchange between them. Atlantic waters enter the Arctic Basin through the Barents Sea and the Fram Strait (Fig. 1). Variations in volume flux, temperature and salinity of Atlantic waters affect hydrographic conditions in both the Barents Sea and the Arctic Ocean and are related to large-scale atmospheric pressure systems.

The analysis of hydrographic conditions in the Barents Sea is based on the available observations along standard sections and the data from fish stock assessment surveys. The total number of hydrographic stations made by PINRO in 2017 was 921 including 111 stations in the standard sections.

Fig. 1 shows the main Russian standard sections in the Barents Sea the data from which will be discussed further.

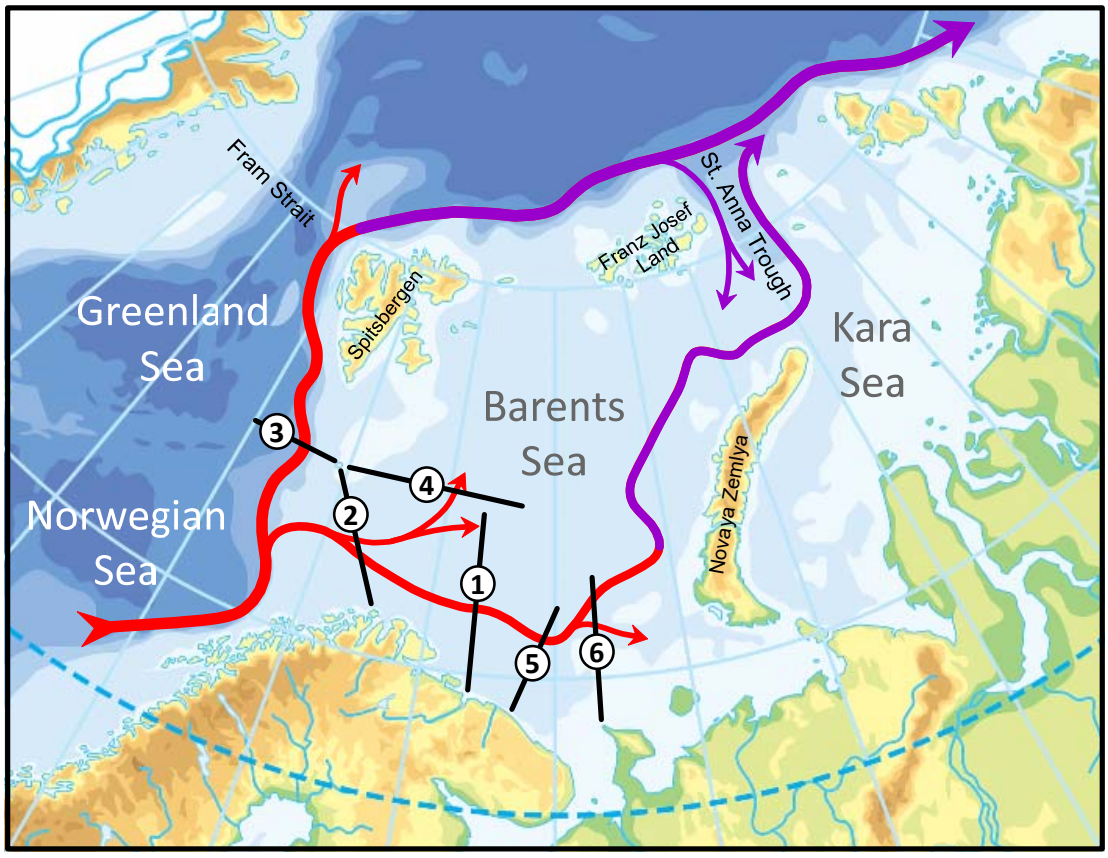

Figure 1. *The main paths of Atlantic waters and the main Russian standard sections in the Barents Sea: Kola (1), North Cape – Bear Island (2), Bear Island – West (3), Bear Island – East (4), Kharlov (5), Kanin (6).*

The observations along these hydrographic sections have been made since the first half of the last century (the Kola Section – since 1900, the North Cape – Bear Island Section – since 1929, the Bear Island – West Section – since 1935, the Bear Island – East Section and the Kanin Section – since 1936). The Kola Section has been occupied more than 1 200 times by now.

Published time series from the main standard sections (Bochkov, 1982; Tereshchenko, 1997, 1999; Karsakov, 2009) were also used in the analysis. Anomalies were calculated using the long-term means for the periods 1951–2010 (Kola Section), 1954–1990 (Kanin Section), 1951–1990 (other standard sections).

Meteorological conditions

In 2017, the winter (December–March) NAO index was 0.89 that was slightly less than in 2016 (1.00). Over the Barents Sea, westerly winds prevailed in January–March 2017 and easterly winds – during the rest of the year. The number of days with winds more than 15 m/s was larger than usual most of the year. It was close to normal only in April, July and October in the western part of the sea, in March, July and October in the central part and in July in the eastern part. In 2017, overall, the storm activity in the central and eastern Barents Sea was a record high since 1981.

Air temperature (http://nomad2.ncep.noaa.gov) averaged over the western (70–76°N, 15–35°E) and eastern (69–77°N, 35–55°E) Barents Sea showed that positive air temperature anomalies prevailed over the sea during most of 2017 (Fig. 2). Higher positive anomalies (>5.0°C) were found in the eastern part in January, February, March and December. Significant negative anomalies (–1.7°C in the west and –1.2°C in the east) were only observed in May (see Fig. 2).

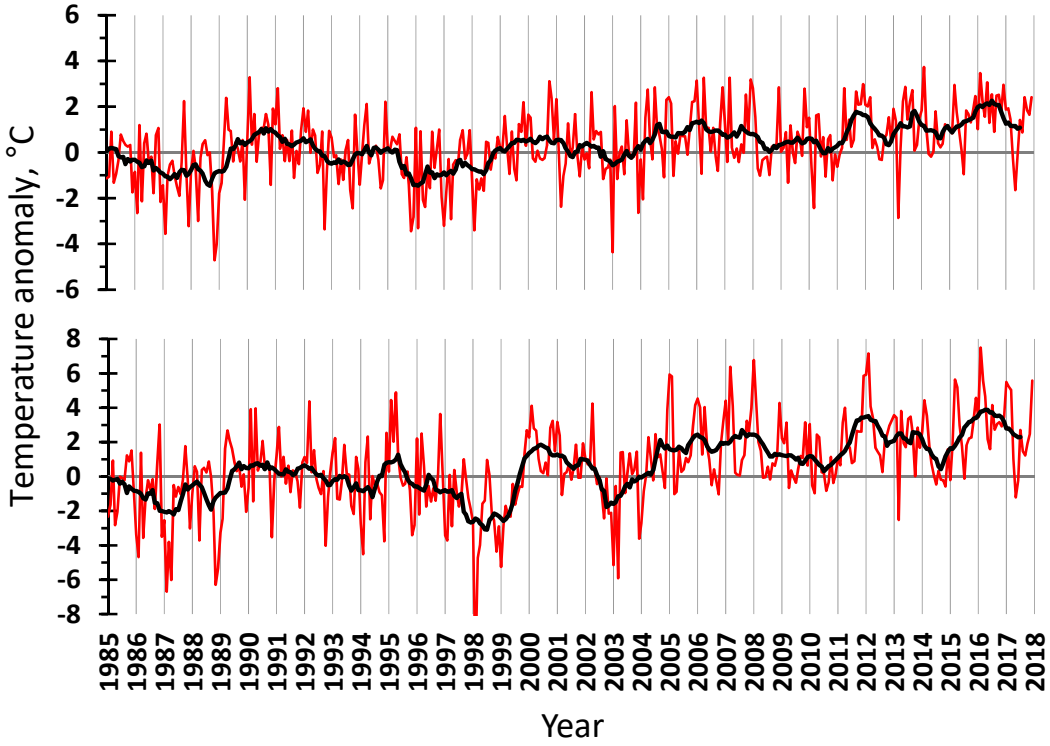

Figure 2. *Air temperature anomalies in the western (upper) and eastern (lower) Barents Sea in 1985–2017. The red line shows monthly values, the black one – 11-month running means.*

Ice conditions

Ice conditions in the Barents Sea in 2017 developed as in low-ice years. In January–March, the ice coverage (expressed as a percentage of the sea area) was 20–23% lower than normal (Fig. 3). However, it was higher than in 2016 from February to the end of the year. The seasonal maximum of ice coverage was, as usual, in April, and it was 17% lower than normal. Ice melting started intensively only in June. In summer, the ice coverage was 6–15% lower than normal but

4–17% higher than in the previous year. In September, ice was only observed between islands of the Franz Josef Land Archipelago and east of the Spitsbergen Archipelago; the ice coverage was 1% that was 6% lower than normal. In autumn, freezing started in the northern Barents Sea in October (more intensively in the third decade); the monthly mean ice coverage was 6% that was 9% lower than normal but 4% higher than in the previous year. In November and December, the ice coverage was 18–23% lower than normal. Overall, the 2017 annual mean ice coverage of the Barents Sea was 15% lower than normal but 7% higher than in 2016.

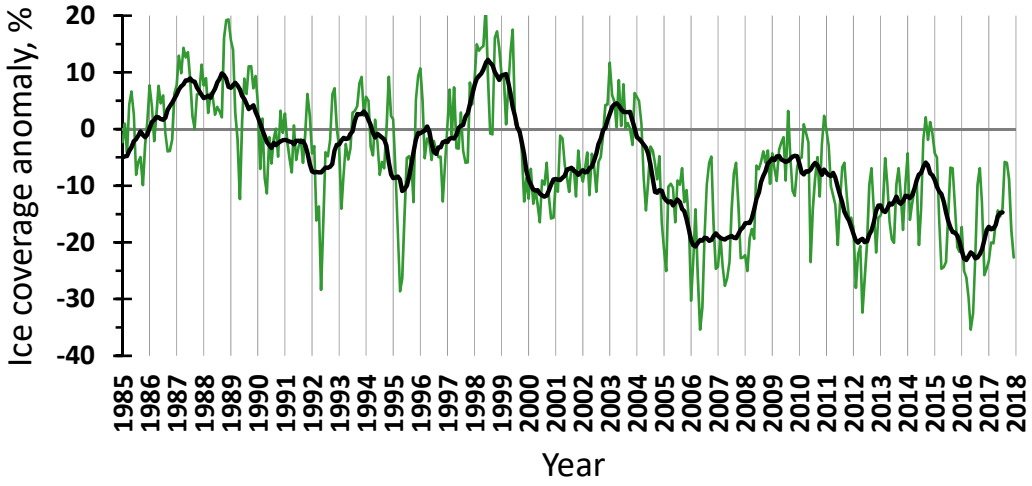

Figure 3. *Ice coverage anomalies in the Barents Sea in 1985–2017. The green line shows monthly values, the black one – 11-month running means (Anon., 2018).*

Hydrographic conditions (standard sections)

In 2017, the Kola Section was occupied seven times that was more than in the previous year. Compared to 2016, when the Kola Section was only occupied in the first five months of the year, in 2017, observations along the section were carried out each month from June to the end of the year. However, despite increasing the number of observations along the Kola Section in 2017, the data gap turned out to be one year (from June 2016 to May 2017 inclusive). That made it impossible to calculate annual mean temperatures and salinities in the section in 2017.

Compared to the first half of 2016, when record high positive temperature anomalies (1.2–1.5°C) were observed in the Kola Section, in the second half of 2017, they decreased significantly (Fig. 4). During most of the observation period in 2017, the Atlantic waters in the 0–200 m layer were 0.8–0.9°C warmer than average. Temperature anomalies in the coastal waters were decreasing from June (0.8°C) to October (0.2°C). Thus, by October, the temperature of the coastal waters was close to average. In November–December, rates of seasonal cooling of waters in the Kola Section were much lower than average (by 0.6°C per month). As a result, by December, positive temperature anomalies in the 0–200 m layer exceeded 1.0°C in all parts of the section that was typical of anomalously warm years (see Fig. 4).

In 2017, the salinity of the coastal and Atlantic waters (the Murman Current) in the Kola Section was 0.05–0.13 lower than normal (see Fig. 4). The salinity of the Atlantic waters in the outer part of the section (the Central branch of the North Cape Current) was close to average.

Besides the Kola Section, some other sections were occupied in the Barents Sea in 2017.

The North Cape – Bear Island Section was sampled in June. The temperature in the North Cape Current (0–200 m) was 0.9°C higher than normal.

There were no observations along the Bear Island – West Section (along 74°30'N) in 2017.

The Bear Island – East Section (along 74°30'N) was sampled in November. The temperature in the 0–200 m layer in the Northern branch of the North Cape Current (74°30'N, 26°50'–31°20'E) was 1.3°C higher than normal.

The Kharlov Section was occupied in May and November. The temperature in the Murman Current (0–200 m) was 1.4–1.6°C higher than normal.

The Kanin Section (along 43°15'E) located in the eastern Barents Sea was sampled in November. The temperature in the 0–200 m layer in the Novaya Zemlya Current (71°00'–71°40'N, 43°15'E) was 1.4°C higher than normal.

Overall, the temperature of the main currents in the Barents Sea in 2017 was higher than normal and typical of warm and anomalously warm years.

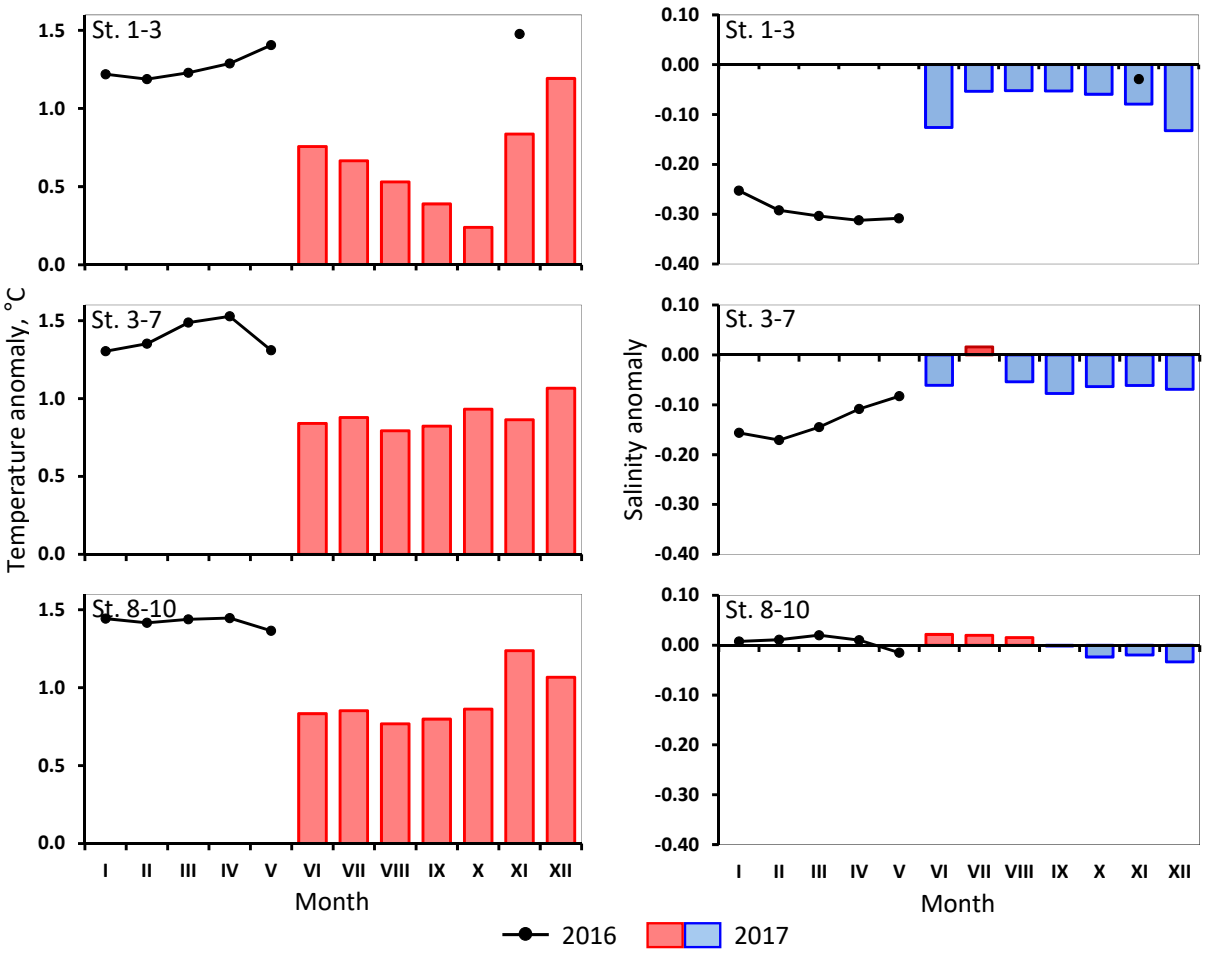

Figure 4. *Temperature (left) and salinity (right) anomalies in the 0–200 m layer in the Kola Section in 2016 and 2017. St. 1–3 – Coastal waters, St. 3–7 – Murman Current, St. 8–10 – Central branch of the North Cape Current (Anon., 2018).*

Hydrographic conditions (surface, 100 m and bottom)

Sea surface temperature (SST) (http://iridl.ldeo.columbia.edu) averaged over the southwestern (71–74°N, 20–40°E) and southeastern (69–73°N, 42–55°E) Barents Sea showed that positive SST anomalies prevailed in both areas during 2017 (Fig. 5). In January–March, they exceeded 1.0°C and were the largest since 1981. In spring and early summer, the anomalies decreased down to 0.5°C in the southwest and down to 0.3°C in the southeast. In July, they increased

abruptly. In July and August, the anomalies in the southwestern part of the sea were the highest since 1981 and in the southeastern part – the largest for 2017. In autumn, the positive anomalies were rather high (0.7–1.5°C).

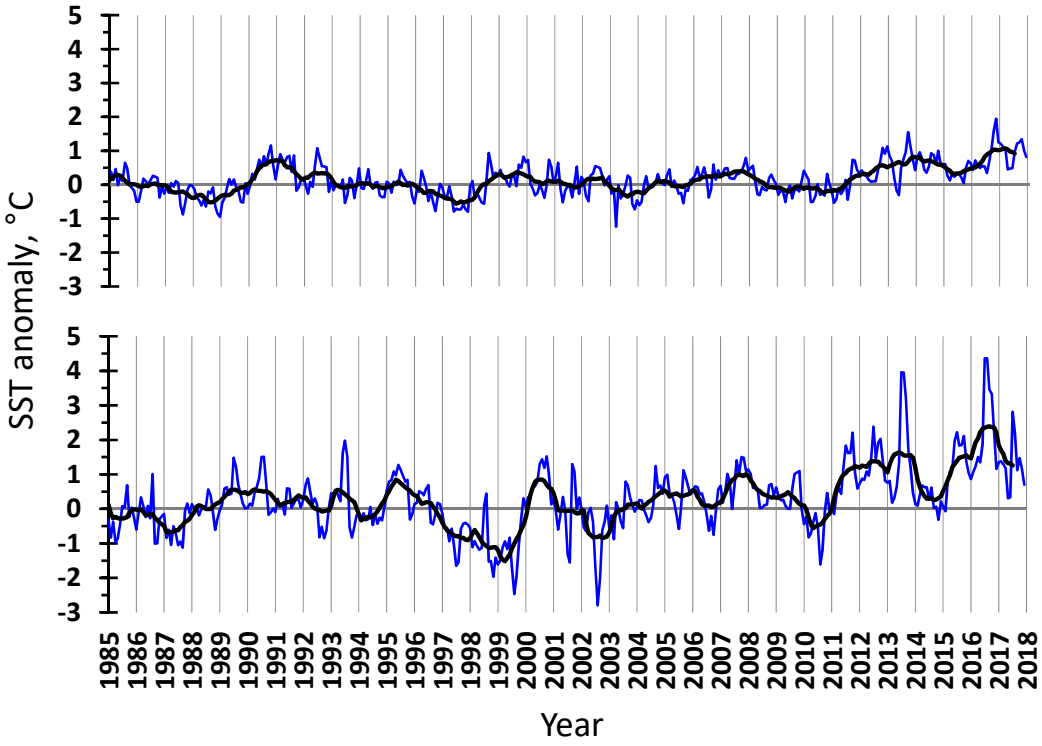

Figure 5. *Sea surface temperature anomalies in the western (upper) and eastern (lower) Barents Sea in 1985–2017. The blue line shows monthly values, the black one – 11-month running means.*

In August–October 2017, the joint Norwegian-Russian ecosystem survey was carried out in the Barents Sea. The surface temperature was on average 1.1°C higher than the long-term mean (1931–2010) in most of the Barents Sea (five sixths of the surveyed area) (Fig. 6). The largest positive anomalies (>2.0°C) were observed west of Bear Island, west and south of the Spitsbergen Archipelago and in the southeastern part of the sea. Negative anomalies took place in the southwestern and northernmost Barents Sea as well as north of the Spitsbergen Archipelago. Compared to 2016, the surface temperature was lower (by 1.0°C on average) in most of the Barents Sea (five sixths of the surveyed area), especially in the northern and eastern parts. The surface waters were on average 0.4°C warmer than in the previous year only in the western Barents Sea, especially in the areas where the largest positive anomalies were found in 2017.

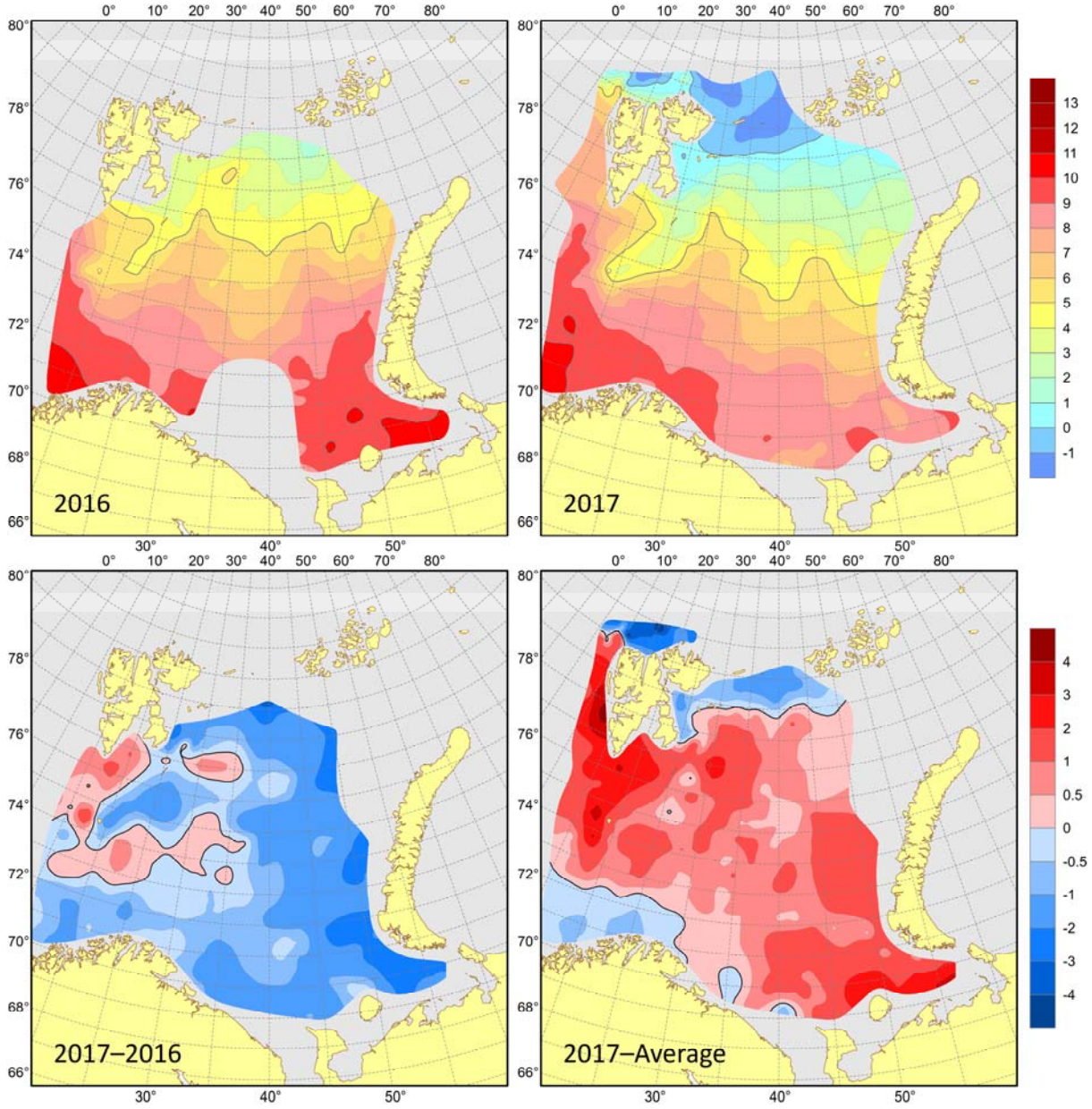

Figure 6. *Surface temperatures (°C) in August–October 2016 (upper left) and 2017 (upper right), their differences between 2017 and 2016 (lower left, °C) and anomalies in August–October 2017 (lower right, °C).*

Arctic waters were mainly found, as usual, in the 50–100 m layer north of 77°N and dominated at 50 m depth. The temperatures at depths of 50 and 100 m were higher than the long-term mean (on average, by 1.0 and 0.8°C respectively) in most of the Barents Sea (Fig. 7). Negative anomalies were mainly found in the northern part of the sea and north of the Spitsbergen Archipelago. Compared to 2016, the 50 m temperature was lower (on average, by 1.1°C) in most of the sea (six sevenths of the surveyed area) and the 100 m temperature was lower (on average, by 0.7°C) almost all over the Barents Sea. Positive differences in 50 m temperature between 2017 and 2016 took place only in some small areas located in the central and western Barents Sea.

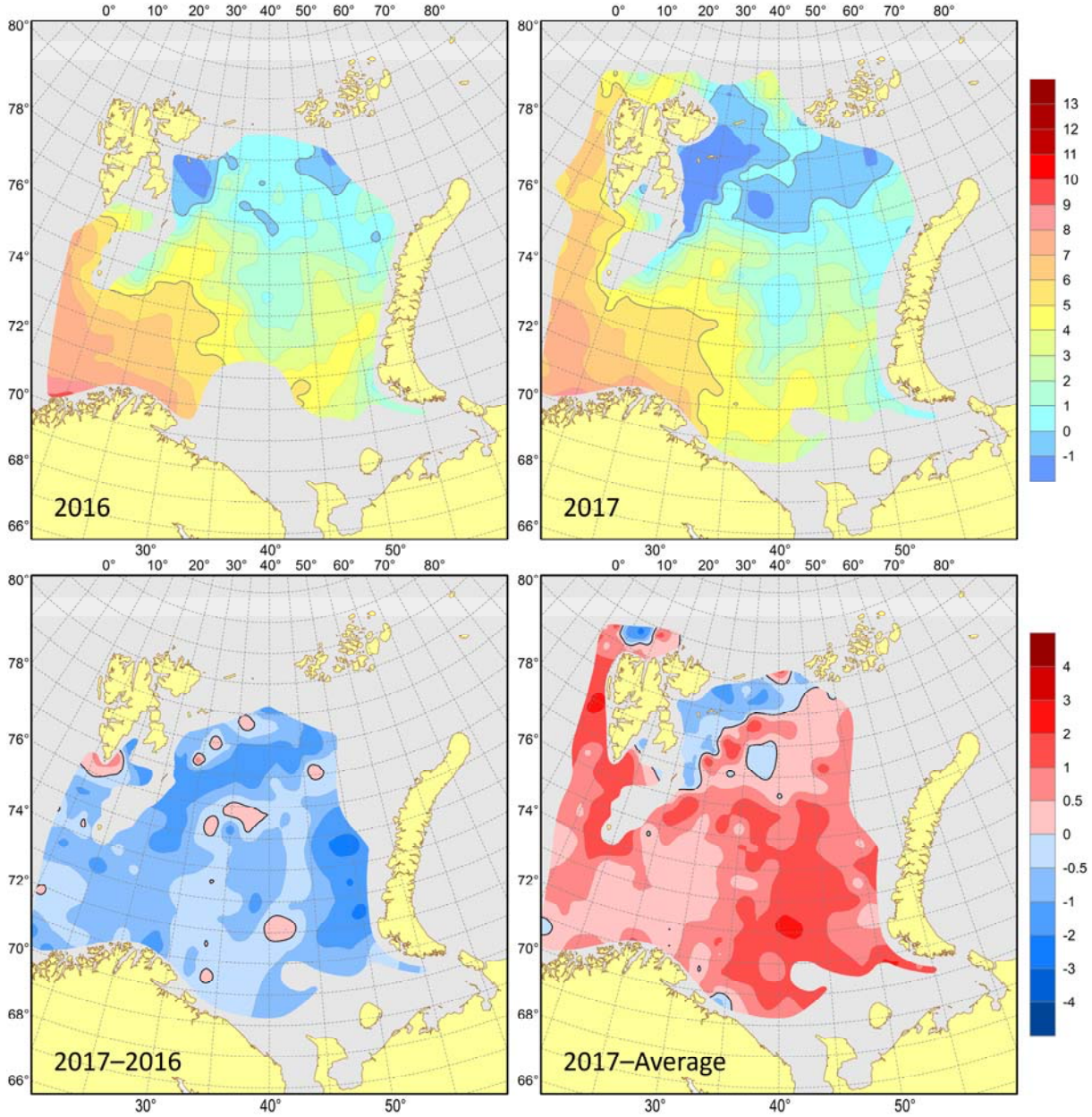

Figure 7. *100 m temperatures (°C) in August–October 2016 (upper left) and 2017 (upper right), their differences between 2017 and 2016 (lower left, °C) and anomalies in August–October 2017 (lower right, °C).*

The bottom temperature was in general 1.1°C above average in most of the Barents Sea (Fig. 8). Negative anomalies (–1.0°C on average) were only observed in the northern sea and north of the Spitsbergen Archipelago. Compared to 2016, the bottom temperature was on average 0.8°C lower in most of the Barents Sea. The bottom waters were slightly warmer (on average, by 0.2°C) than in 2016 only in the Eastern Basin and in a small area east of the Great Bank. In August–October 2017, the area occupied by water with temperatures below zero was larger than in the previous year and it was mainly located east of the Spitsbergen Archipelago. The lowest bottom temperatures (below –1°C) were observed between the Great Bank and the Spitsbergen Archipelago.

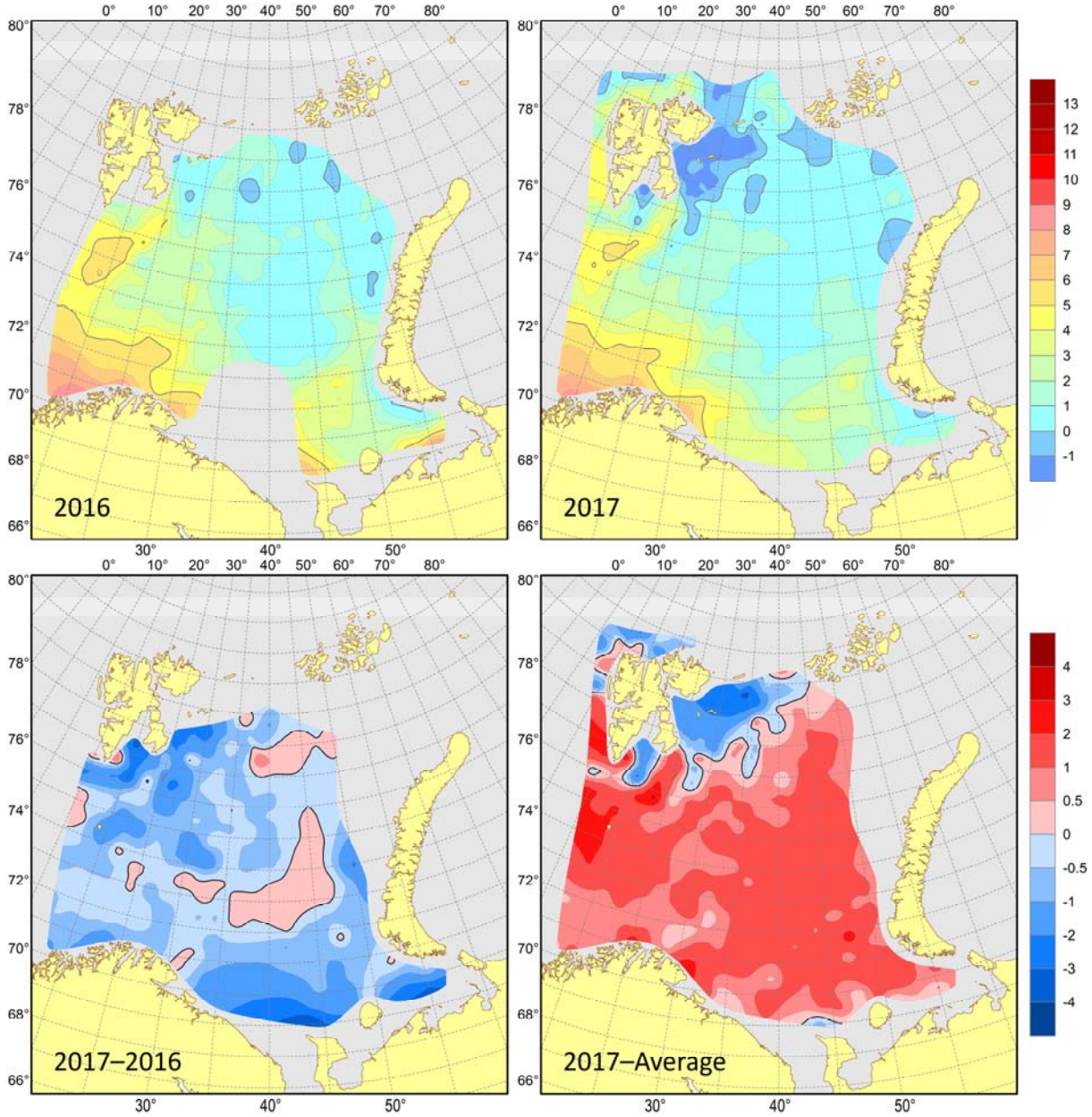

Figure 8. *Bottom temperatures (°C) in August–October 2016 (upper left) and 2017 (upper right), their differences between 2017 and 2016 (lower left, °C) and anomalies in August–October 2017 (lower right, °C).*

In August–October 2017, at 50, 100 m and near the bottom, the area covered by warm water (above 4, 3 and 1°C respectively) was smaller (by 7, 11 and 10% respectively) than in 2016, when it was a record large (Fig. 9). The area covered by cold water (below 0°C) was, on the contrary, larger (by 9, 10 and 4% respectively) in 2017 compared to the previous year, when it was a record small (see Fig. 9). Since 2000, the area covered by cold bottom water was the largest in 2003 and rather small in 2007, 2008, 2012, 2016 and 2017; in 2016, it reached a record low value since 1965 – the year when the joint autumn surveys started.

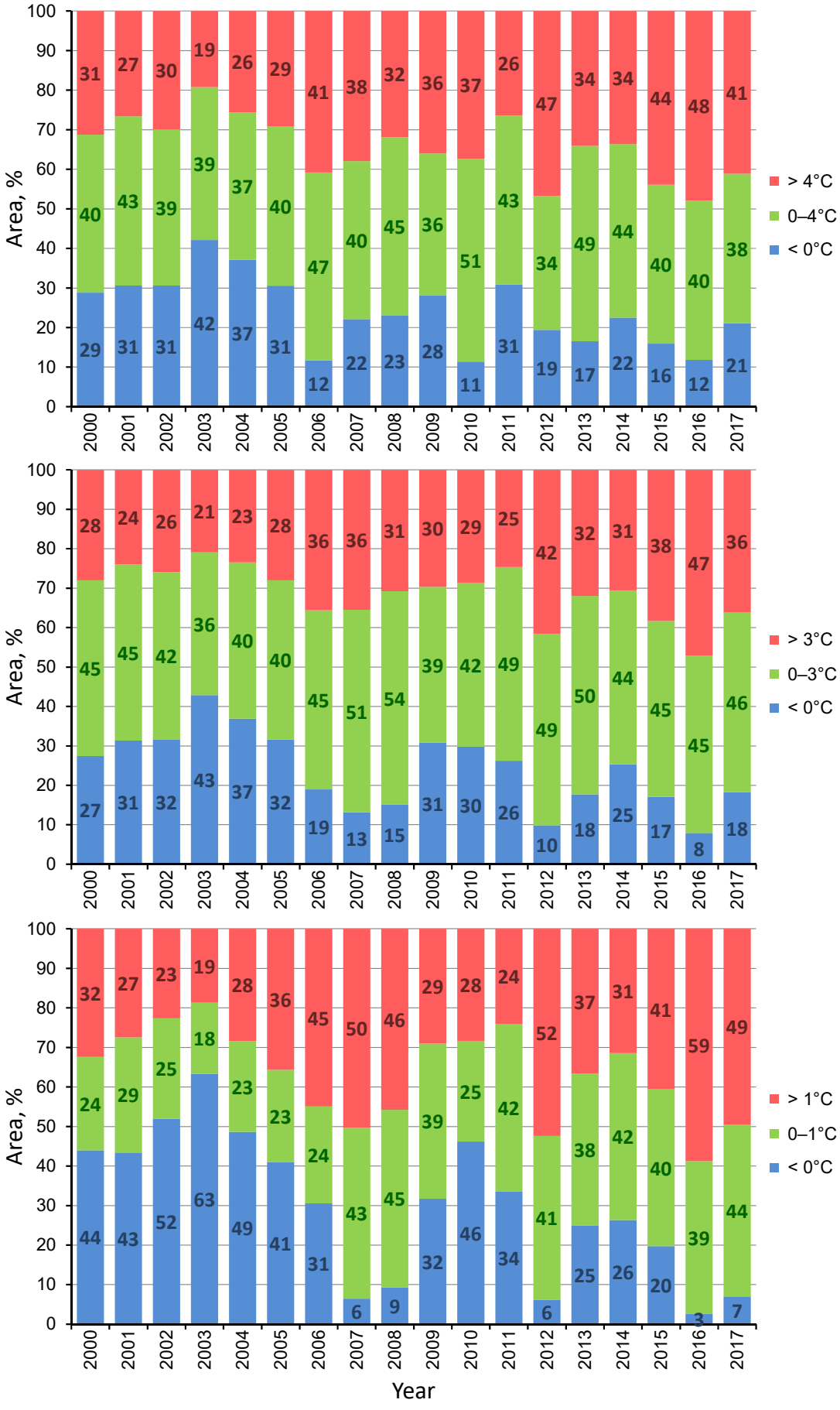

Figure 9. *Areas covered by water with different temperatures at 50 (upper panel), 100 m (middle panel) and near the bottom (lower panel) in the Barents Sea (71–79°N, 25–55°E) in August–September 2000–2017.*

In the past decades, the area of Atlantic and mixed waters has increased, whereas that of Arctic waters has decreased (Fig. 10). In August–October 2017, the area covered by Atlantic waters still remained rather large, though decreased compared to 2016, when it was the largest since 1965. The area covered by Arctic waters was still rather small in 2017, though increased compared to 2016, when it was the smallest since 1965.

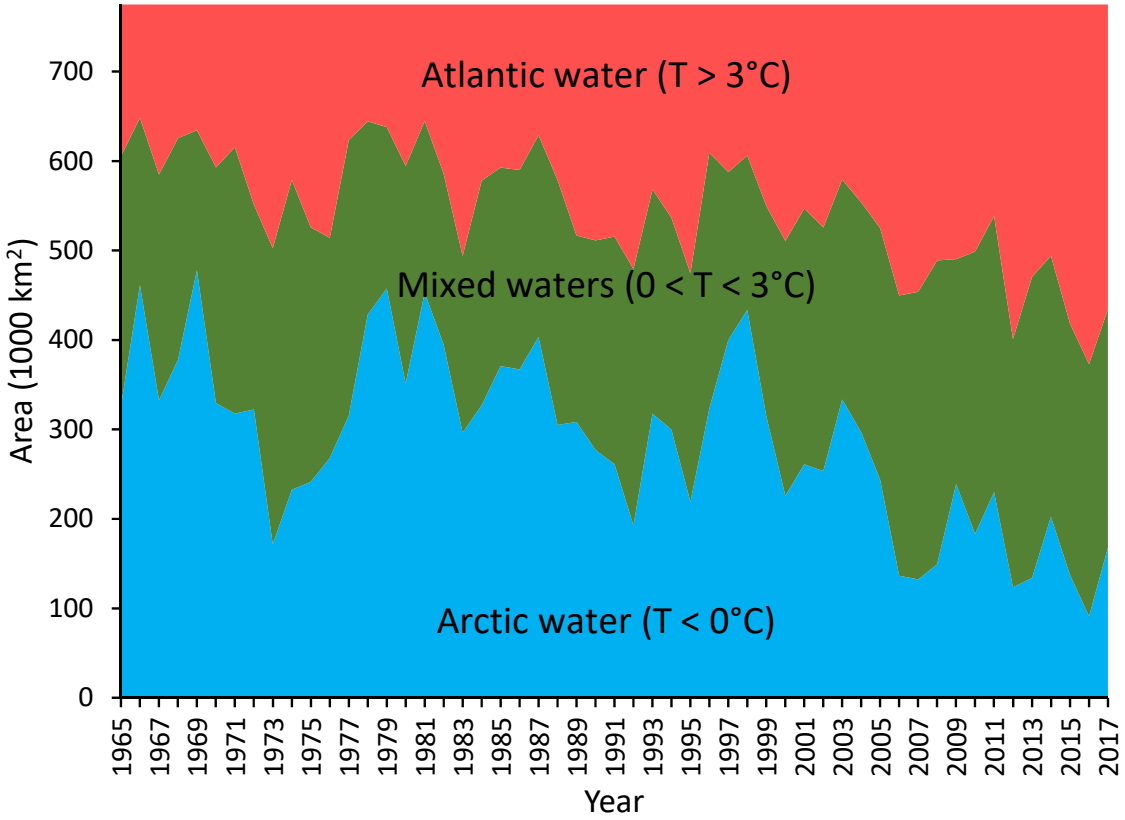

Figure 10. *Area of water masses in the Barents Sea (71–79°N, 25–55°E) in August–September 1965–2017 (based on 50–100 m averaged temperature).*

The surface salinity was on average 0.3 higher than the long-term mean (1931–2010) in most of the Barents Sea (two thirds of the surveyed area) with the largest positive anomalies (>0.8) west of the Spitsbergen Archipelago as well as in the southeastern and northeastern sea (Fig. 11). Negative anomalies (–0.3 on average) were mainly observed in the southern and northern parts of the sea with the largest values north of Kanin Peninsula and north of the Spitsbergen Archipelago. In August–October 2017, the surface waters were on average 0.3 fresher than in 2016 in 75% of the surveyed area with the largest negative differences in the northern (north of 77°N) and south-eastern (along Southern Island of the Novaya Zemlya Archipelago and north of Kanin Peninsula) parts of the Barents Sea. Small positive differences in salinity between 2017 and 2016 (0.1 on average) were found in the central and western parts of the sea as well as north of Kolguev Island.

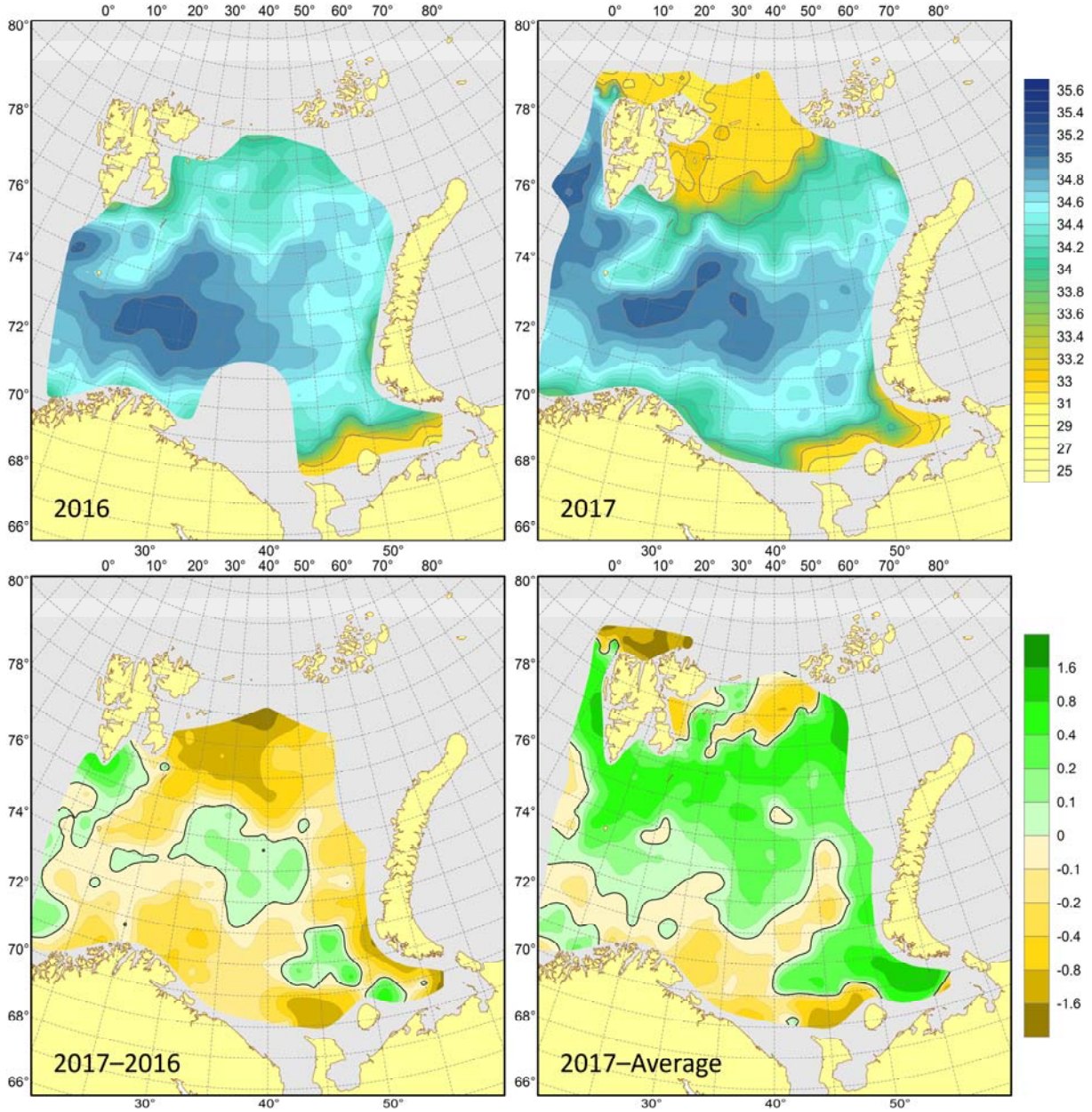

Figure 11. *Surface salinities in August–October 2016 (upper left) and 2017 (upper right), their differences between 2017 and 2016 (lower left) and anomalies in August–October 2017 (lower right).*

The 100 m salinity was close to average in general (Fig. 12). Small negative anomalies (on average –0.1) were mainly observed in the southern Barents Sea and north of the Spitsbergen Archipelago. Small positive anomalies (on average 0.1) were found in the northwestern Barents Sea, especially east of the Spitsbergen Archipelago. Compared to 2016, the 100 m salinity in 2017 was less in most of the Barents Sea (three fourths of the surveyed area). The positive differences in salinity between 2017 and 2016 were mainly found in the northwestern and southeastern parts of the sea, as well as in the coastal waters in the south-westernmost part of the surveyed area.

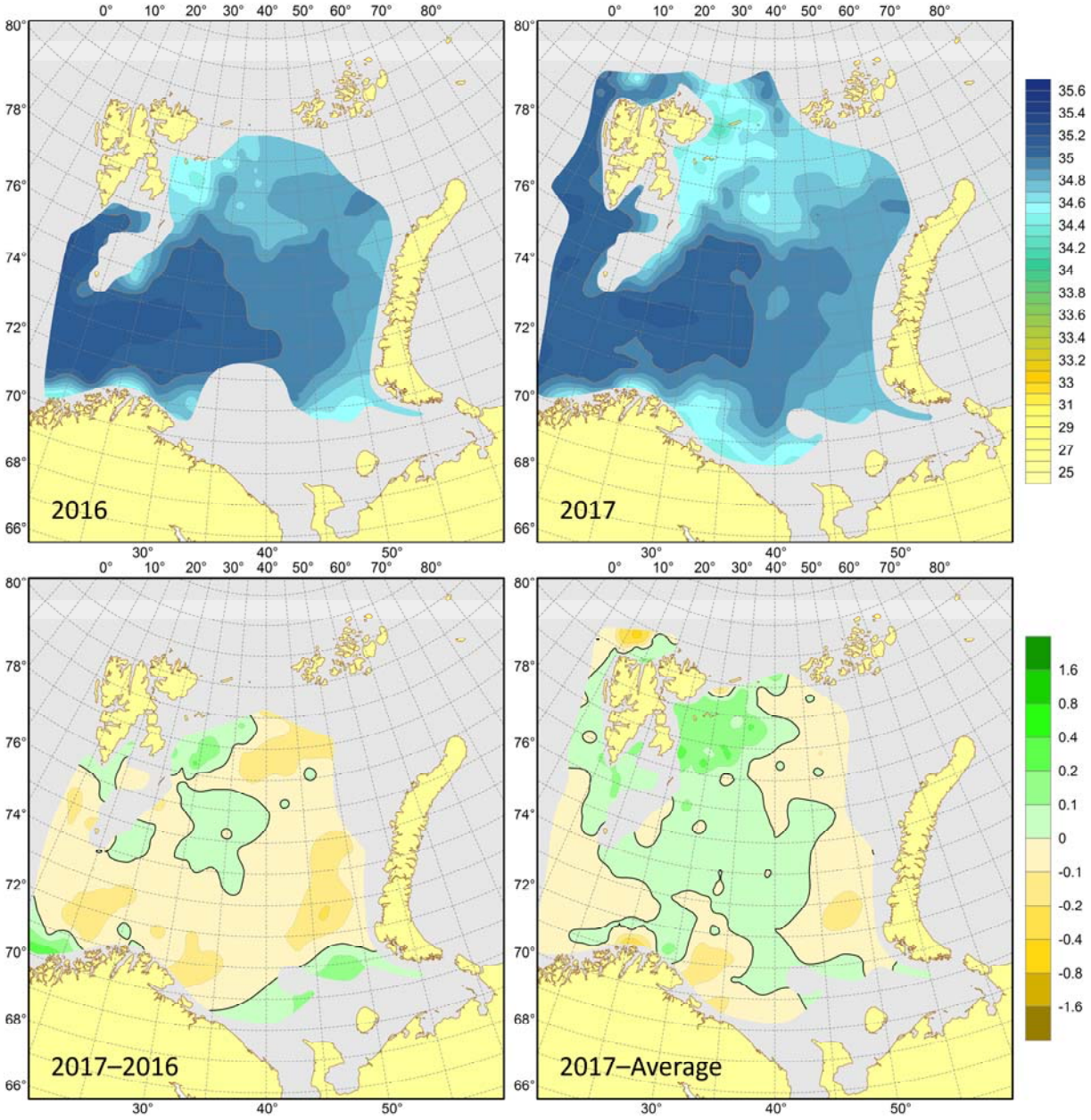

Figure 12. *100 m salinities in August–October 2016 (upper left) and 2017 (upper right), their differences between 2017 and 2016 (lower left) and anomalies in August–October 2017 (lower right).*

The bottom salinity was close to both the average and that in 2016 in most of the Barents Sea (Fig. 13). Significant anomalies were mainly found in shallow waters: negative – in the south-easternmost Barents Sea and east of the Spitsbergen Archipelago, positive – over the Spitsbergen Bank and north of Kolguev Island.

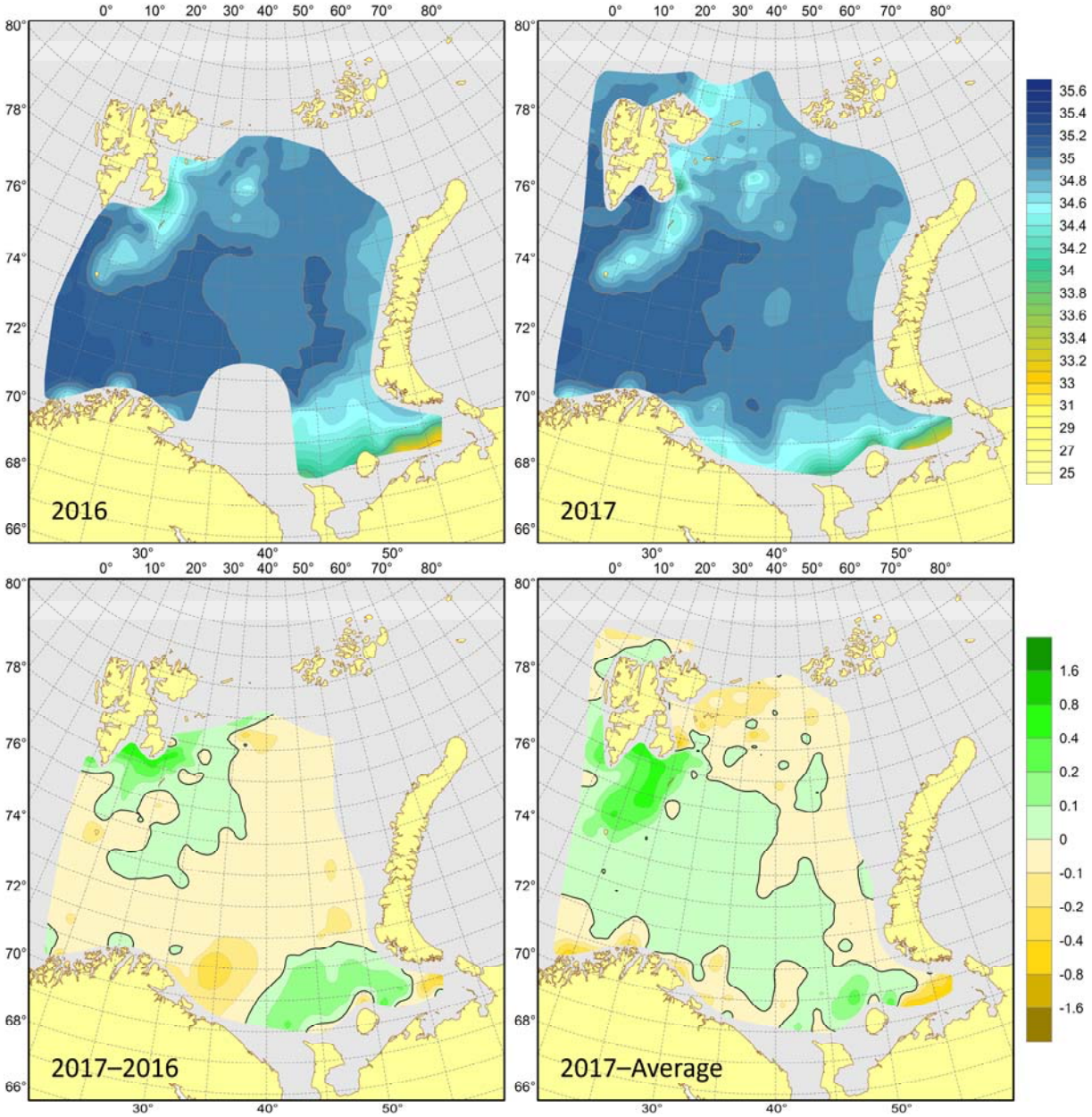

Figure 13. *Bottom salinities in August–October 2016 (upper left) and 2017 (upper right), their differences between 2017 and 2016 (lower left) and anomalies in August–October 2017 (lower right).*

Summary

The air and water temperatures in the Barents Sea in 2017 were still well higher than average and typical of warm and anomalously warm years but lower compared to 2016.

The coastal waters and Atlantic waters in the central part of the Kola Section were fresher than average; the Atlantic water salinity in the outer part of the section was close to average.

In autumn 2017, the area covered by Atlantic waters (>3°C) was still rather large, though it decreased compared to 2016; the areas covered by Arctic and cold bottom waters (<0°C) were still rather small, though they increased compared to 2016.

The ice coverage of the Barents Sea in 2017 was much lower than normal but higher than in 2016; its smallest value (1%) was observed in September, when ice was only found between islands of the Franz Josef Land Archipelago and east of the Spitsbergen Archipelago.

References

Anon., 2018. Status of biological resources in the Barents Sea and North Atlantic for 2018. E.A. Shamray (Ed.). Collected Papers. Murmansk: PINRO Press. (in Russian) in press

Bochkov, Yu.A. 1982. Historic data on water temperature in the 0–200 m layer in the Kola Section in the Barents Sea (1900–1981). Trudy PINRO. 1982. P. 113–122. (in Russian)

Karsakov, A.L. 2009. Oceanographic investigations along the Kola Section in the Barents Sea in 1900–2008. Murmansk: PINRO Press, 2009. 139 pp. (in Russian)

Terescchenko, V.V. 1997. Seasonal and year-to-year variations of water temperature and salinity in the main currents in the Kola Section in the Barents Sea. Murmansk: PINRO Press. 1997. 71 pp. (in Russian)

Tereshchenko, V.V. 1999. Hydrometeorological conditions in the Barents Sea in 1985–1998. Murmansk: PINRO Press. 1999. 176 pp. (in Russian)